5-2011

Development of an On-line Radiation Detection and Measurements Laboratory Course

Derick Kopp
Clemson University, dkopp@clemson.edu

DEVELOPMENT OF AN ON-LINE RADIATION DETECTION & MEASUREMENTS LABORATORY COURSE

A Thesis
Presented to
the Graduate School of
Clemson University

In Partial Fulfillment
of the Requirements for the Degree
Master of Science
Environmental Engineering

---

by
Derick G. Kopp
May 2011

Accepted by:
Timothy A. DeVol, Committee Chair
Brian Powell
Stephen Moysey

ABSTRACT

An on-line radiation detection and measurements lab is being developed with a grant from the U.S. Nuclear Regulatory Commission. The on-line laboratory experiments are designed to provide a realistic laboratory experience and will be offered to students at colleges/universities where such a course is not offered. This thesis presents four web-based experiments: 1) nuclear electronics, 2) gamma-ray spectroscopy with scintillation detectors, 3) gamma-ray attenuation in matter and external dosimetry, and 4) alpha spectroscopy and absorption in matter. The students access the experiments through a broad-band internet connection. Computer-controlled instrumentation developed in National Instruments (NI) LabVIEW™ communicates with the URSA-II (SE International, Inc.) data acquisition system, which controls the detector bias voltage, pulse shaping, amplifier gain, and ADC. Detector and amplifier output pulses can be displayed with other instrumentation developed in LabVIEW™ for the digital oscilloscope (USB-5132, NI). Additional instrumentation developed in LabVIEW™ is used to control the positions of all sources with stepper motor controllers (VXM-1, Velmex, Inc.) and to adjust pressure in the alpha chamber with a digital vacuum regulator (Model 200, J-KEM, Inc.). Unique interactive interfaces are created by integrating all of the necessary instrumentation to conduct each lab. These interfaces provide students with seamless functionality for data acquisition, experimental control, and live data display with real-time updates for each experiment. A webcam is set up to stream the experiment live so the student can observe the physical instruments and receive visual feedback from the system in real time.

DEDICATION

This thesis is dedicated to my wife, Katie, whose ever-present encouragement and undying support sustained me throughout my work. This dedication is but a small token of my appreciation of her understanding and patience through the countless hours that I spent working in the laboratory and studying at the kitchen table.

ACKNOWLEDGMENTS

First and foremost, I would like to thank my advisor, Dr. Tim DeVol, for his investment in my education and his continual guidance, direction, and advice throughout this entire project. His insight and instruction were central to the success of this work; his dedication and his open-door policy were integral to the completion of this work. I would like to thank Dr. DeVol and my other committee members, Dr. Brian Powell and Dr. Stephen Moysey, for their invaluable participation in the revisions of this document. The objectivity of their comments and suggestions helped to produce a much superior document, both grammatically and technically. I would also like to thank those who contributed to my questions on National Instruments Developer Zone. Their comments and instructions accelerated my understanding of LabVIEW™ programming. I would also like to thank Paul Steinmeyer of Radiation Safety Associates for his guidance regarding the development of the URSA-II instrumentation in LabVIEW™.

This research was funded by the United States Nuclear Regulatory Commission (USNRC) Nuclear Education Grant #NRC-38-09-972.

TABLE OF CONTENTS

Page

Table of Contents (Continued)

Page

LIST OF TABLES

LIST OF FIGURES

List of Figures (Continued)

List of Figures (Continued)

Figure Page

List of Figures (Continued)

CHAPTER ONE

INTRODUCTION

1.1 Distance Learning

The advent and accelerated development of the personal computer and the Internet in the last two decades has opened the floodgates for technological applications in education, especially distance learning. Distance learning no longer relies exclusively on the postal system to transport educational material back and forth between teacher and students nor does it leave an individual distance student isolated from other distance students or in-class students. It is now commonplace for individual courses and even entire degrees to be provided on-line with virtual communities consisting of study groups, tutors, and one-on-one time with the professor (Soh and Gupta, 2000). However, as distance learning via Internet has begun to pervade the education community, its efficacy has been questioned and many academic researchers have attempted to respond to these questions. Even more specifically, probing questions are being asked regarding the effectiveness of computerized teaching labs as they become more prevalent in engineering courses because the approach to technological integration can significantly alter the value of engineering education (Magin and Kanapathipillai, 2000; Nickerson, Corter, Esche, & Chassapis, 2007).

Shen, Chung, Chalis, & Cheung (2007) and Nickerson et al. (2007) have demonstrated that distance learning and computerized teaching labs, respectively, can be effective educational methods.

Shen et al. (2007) conducted a 4-year experiment involving 2,071 students at the Hong Kong Polytechnic University determining the effectiveness of a 30-credit on-line masters program compared to a similar program offered in a traditional classroom. Both programs were lecture-based, maintained the same entrance requirements (academic and experience), and offered the same 7 courses. A comparison of the examination results for each program revealed that although the in-class students performed slightly better than the on-line students, the statistics generated by the minor differences provided no evidence regarding the superiority of in-class education over non-traditional education.

Nickerson et al. (2007) undertook the task of developing a model to determine the effectiveness of computerized teaching labs. Three of the six lab experiments of a junior-level Machine Dynamics & Mechanisms course in the Mechanical Engineering department at Stevens Institute of Technology were developed into computer-based experiments, while the other three remained traditional hands-on experiments. After completion of the course, the authors surveyed all 29 students on numerous aspects regarding the experience of the computerized labs versus the traditional labs and compared lab grades from both types of labs. The general consensus of the students was that the computerized labs were as effective as the traditional labs. The authors concluded that both types of labs were equally useful educational tools and reported that the results were positive regarding the further implementation of the computerized labs.

The last decade has seen academic institutions begin to develop the infrastructure necessary to support and successfully implement interactive computerized laboratories with software such as Laboratory Virtual Instrument Engineering Workshop

(LabVIEW™) (Vasquez, 2009), Java (Gao, Yang, Spencer, & Lee, 2005), MATLAB (Kypuros and Connolly, 2007), and Virtual Reality Modeling Language (VRML) (Manseur, 2005). Many academic departments have utilized computerized labs to visualize complex systems, to provide alternative modes of instruction for non-traditional students, and to reduce the costs and space requirements of operating and maintaining physical lab instruments (Powell, Anderson, Van der Spiegel, & Pope, 2002; Li and Liu, 2003; Calvo, Marcus, Orive, & Sarachaga, 2010). A brief perusal of literature demonstrates the use of computerized teaching labs in engineering departments, including mechanical (Knight and McDonald, 1998), earthquake (Elgamal, Fraser, & Pagni, 2002), chemical (Mendes, Marongoni, Meneguelo, Machado, & Bolzan, 2010), and electrical (Chetty and Dabke, 2000).

Interactive computerized laboratories can be computer-based, simulation-based or remote. A computer-based lab is a type of lab that substitutes computerized instrumentation for physical instrumentation in a physical laboratory. A simulation-based lab allows students to control a simulated lab experiment that yields results that are mathematically modeled to represent the expected results. Simulation-based labs are used in in-class education and distance education. A remote lab allows distance students to control and conduct the experiment from a remote location with software controls that are connected to actual instruments.

1.2 Remote Radiation Detection and Measurements Laboratory

1.2.1 Description of Laboratory

The Environmental Engineering and Earth Sciences Department at Clemson University offers a 3-credit undergraduate-/graduate-level laboratory class (EE&S 411/611, respectively) on the fundamentals of radiation detection and measurement. This course features 12 laboratory experiments centered around the major detector categories: gas-filled, semiconductor, and scintillator.

The class is being developed into an on-line class featuring a fully functional remote laboratory that would be offered via broadband to colleges/universities that lack the facilities and licensure to offer such a class. This project was designed to bring the laboratory experience to students who are not able to experience a physical laboratory environment.

Students enrolled in the on-line class will receive electronic resources to guide them through each experiment. Adobe Connect, a computer conferencing program, will enable students to either attend a lecture synchronously (live) or access the lecture asynchronously (recorded). The purpose of the lecture is to introduce the student to the concepts and instruments of each experiment. The primary instructor from Clemson University will lecture to the class prior to conducting each experiment. Blackboard, a course management system from Blackboard, Inc., will be used to host all course information, including instructions to connect to the Clemson network using virtual private network (VPN) software and to conduct each lab. Students will receive a username and password to access the Clemson network and instructions regarding the

proper IP address and password to remotely access the host computer via the Windows Remote Desktop application, available on every Windows-based operating system. Each set of experimental procedures for the remote experiments will be based on the procedures for the associated in-class experiment, but tailored for use in the remote lab.

Each physical experiment is located in the Waste Management, Inc. laboratory building located adjacent to the L.G. Rich Laboratory at the Clemson Advanced Materials Research Center (formerly the Clemson Research Park). The physical experiments are connected to a dedicated host computer, webcam, and a customized LabVIEW™ interface. Students conduct each step of the experiment using controls on the LabVIEW™ interface that communicate with the actual instruments. Students observe the experiment via a streaming video feed provided by webcam.

1.2.2 Motivation Behind the Remote Laboratory Development

This remote laboratory course provides a strong educational tool to academic institutions in order to most efficiently fill the gap in the nuclear industry's dwindling workforce.

The average age of the United States nuclear industry's workforce is relatively high and a significant portion of the workforce is on the verge of retirement. In 2004, over one quarter of the nuclear industry workforce was eligible for retirement within 5 years (ANS, 2004); in 2007, almost half of the employees in the nuclear industry in general were over 47 years old (NEI, 2007). According to 2010 statistics, the average age of National Nuclear Security Administration (NNSA, 2010) employees was 49, 33% of the workforce will reach retirement age within 5 years (NNSA, 2010), and close to 28%

will reach retirement age by 2012 (NNSA, 2010). Only 25% of the employees in the NNSA Science and Engineering department are younger than 40 and retirements in the department looming in the near future threaten to unsettle the department for an unknown length of time (NNSA, 2010). The American Physical Society (APS) reported a great need for nuclear engineers and scientists in a number of fields (APS, 2008) and a Health Physics Society (HPS) report indicated that the rate of health physics graduates was significantly lower than the rate of those retiring from the field based on extrapolated data (HPS, 2004).

Not only faced with a precipitous decline in employee numbers, the nuclear industry is coming upon a renaissance. Even though the nuclear industry has stagnated over the past decades due to a number of circumstances, the viability of increased dependence on nuclear power is quickly becoming a reality. In his May 19, 2010 testimony to U.S. House of Representatives Committee on Science and Technology, Mark Peters emphasized that nuclear power is the answer to a reduction in fossil fuel dependency and long-term environmental protection (Charting the course for American nuclear technology, 2010).

A revitalized hope in nuclear power is demanding an increased number of nuclear employees. In order to train nuclear engineers and technicians, universities and technical colleges need already-developed curriculum to educate an upcoming generation of nuclear employees. Undoubtedly, there is a great need for an educational framework to nurture the development of a younger generation to take the place of an increasingly veteran nuclear industry workforce. Recognizing the low disproportionality of younger

generation nuclear employees, ANS (2004) called for “innovative means of providing educational opportunities to traditional and nontraditional students.” HPS reported the need for “strong, healthy academic programs… to continue to provide a meaningful succession of scientists and engineers” (HPS, 2008).

CHAPTER TWO

LITERATURE REVIEW

2.1 Purpose of Laboratories

Constructivism, one of three fundamental learning theories, posits that learning occurs through interaction with and understanding of one's uncertain and complex environment where experience is integral to critical thinking and intellectual development (Good and Brophy, 1990). As such, constructivist theory closely parallels the objectives of engineering education with the commonality of experiential knowledge (Calvo et al., 2010). Following constructivist theory, laboratory exercises and experiments are integral to engineering education because they replicate real world environments of uncertainty and complexity and challenge students to develop a personal knowledge of the subject through personal experience. In practical terms, opportunities to actively apply lecture-taught concepts increase the utility of engineering education in the real world by augmenting students' knowledge base, aiding in their confidence of the subject area, and developing problem-solving techniques (Calvo et al., 2010; Cooper and Dougherty, 1999; Li & Liu, 2003; Mendes et al., 2010).

2.2 Computerized Teaching Laboratories

A computerized teaching lab is a lab that, in some capacity, utilizes computerized instrumentation. The uses of computerized labs are abundant. Some academic departments have developed computerized labs as alternatives to hands-on labs for

students enrolled in their respective programs (Powell et al., 2002). Others have used computerized labs to supplement standard teaching methods to enhance learning (Gao et al., 2005). While still others have implemented computerized labs in distance education courses that require lab work (Knight & McDonald, 1998; Hall, 2002) and may even be used by collaboraters at multiple universites (Bogdanov et al., 2006). Computerized labs are used in traditional in-class education (Nickerson, et al., 2007) and in distance education (Vasquez, 2009).

The terminology regarding interactive computerized labs varies among authors (Ma and Nickerson, 2006). Some authors (Bhargava, Antonakakis, Cunningham, & Zehnder, 2006) regard any type of computerized lab as a virtual lab and further categorize them as simulation-based, digital, or remote. Others (Nedic, Machotka, & Nafalski, 2003; Ma & Nickerson, 2006; Uran and Safaric, 2009) place virtual labs and remote labs in two separate categories, considering virtual labs to be exclusively simulation-based. Some (Chetty & Dabke, 2000; Li, LeBoef, Basu, & Hampton, 2003) loosely refer to all computerized labs accessed over the Internet as web-based labs, regardless of their nature. Li & Liu (2003) categorize their computerized lab as a digital laboratory.

Regardless of how they are labeled, each type of lab is designed with software controls that represent real instrument controls, which control experiment parameters that, in one way or another, affect the outcome of the experiment. Using these controls, students are able to interact with the experiment in varying degrees, depending on the type of lab and design of the graphical user interface (GUI). A well-developed GUI

designed with realistic controls, such as dials, buttons, and slides, can give students the impression that they are actually turning a dial, pressing a button, or sliding a slide (Nedic et al., 2003).

A summary of the types of computerized teaching labs is provided in Table 2.1.

Table 2.1: Summary of Computerized Teaching Labs

Lab Type	Description/ Definition	Advantages/ Disdavantages
Computer-based lab	A type of lab that substitutes computerized instrumentation for physical instrumentation in a physical laboratory	Advantage: may require less space and/or expensive laboratory equipment Disadvantage: may not enable students to be involved in the rigorous task of setting up entire experiment
Simulation-based lab (also called virtual lab)	A type of lab that replicates actual experiments by mathematically modeling the expected results; used in in-class education and distance education; digital lab is a type of simulation-based lab	Advantage: enables students to interact with systems that would otherwise be impractical to implement in a real laboratory setting Disadvantage: does not convey the inherent difficulties relating to instrument setup, experimental errors, and unexpected results
Remote labs	A type of lab that allows distance students to control physical instruments and acquire and analyze actual data in real-time; students interact with physical laboratory setup; exclusive to distance education	Advantage: allows students who otherwise would not have the opportunity to interact with physical systems to do so Disadvantage: removes tangible dimension of experimentation

2.2.1 Simulation-Based Laboratory

Simulation-based experiments replicate actual experiments by mathematically modeling the expected results (Ma & Nickerson, 2006; Vasquez, 2009). Simulation-based labs are used in traditional in-class education (Cooper & Dougherty, 2000) and distance education (Vasquez, 2009). While conducting the lab, students are able to change parameters and observe the effect to the mathematical model (Depcik and Assanis, 2005). A well-designed simulation-based lab provides students with a firm grasp of reality concerning the experiments (Kucuk and Bingul, 2010). However, a simulation-based lab cannot properly relay the occasional inconsistencies that are present when working with real instrumentation (Vasquez, 2009). In fact, Vasquez (2009) attempted to replicate these inconsistencies in his simulated radiation detection and measurements lab by implementing a random number generator (RNG) to appropriate functions of their mathematical model. However, even an RNG-generated variance still yielded only expected modeled results.

Yarbrough and Gilbert (1999) discussed the integration of a probability and statistics laboratory with simulated civil engineering systems at the University of Texas at Austin. Seven interactive modules were developed that aided the students' understanding of statistical concepts in civil engineering through interaction with and analysis of the simulated systems. Statistical concepts covered were event theory, conditional probability, random variable models, Bernoulli sequence, multiple random variables, statistical interference, and hypothesis testing.

Mendes et al. (2010) documented the development of an "academic software application" called Dsym that introduced distillation dynamics and controls to chemical and food engineering students at Federal University of Santa Catarina in Florianopolis, Brazil. Dysm dynamically simulated a multicomponent distillation tower based on user-defined parameters, which included column specifications (plate number, feed location, weir height, downcomer length, column diameter for stripping and rectifying), component specifications (molecular weight, density, heat of vaporization, bubble point, specific heat of liquid and vapor), initial conditions (temperature, molar composition, flow rate), and feed conditions (feed temperature, feed liquid, vapor molar composition). Numerical, graphical, and tabulated results were displayed and students determined the relationship between individual parameters or groups of parameters and the distillation dynamics.

Cooper & Dougherty (2000) described the development of a training simulator in the chemical engineering department at the University of Connecticut. The simulator was controlled by user-defined parameters, including temperature, pressure, pressure drop, level, flow, density, and concentration that were applied to virtual equipment and processes, including reactors, separators, distillation columns, heat exchangers, and furnaces. Numerical and graphical displays provided students with the tools necessary to analyze chemical engineering processes through application of control theory taught in lecture-based format. A graphical display for the distillation column lab is displayed in Figure 2.1.

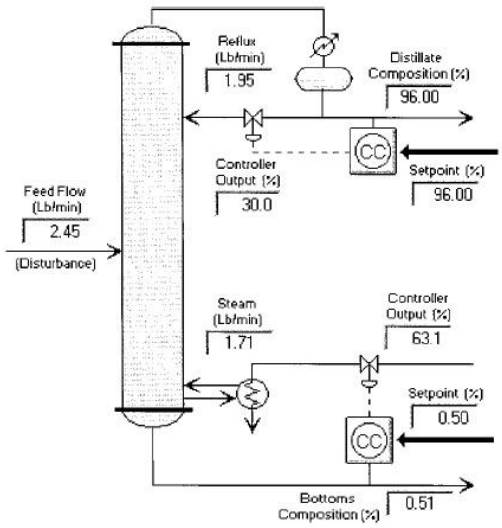

Figure 2.1: Interface for Simulated Distillation Column at the University of Connecticut (Cooper & Dougherty, 2000). [Copyright © 1999 John Wiley. Used with permission.]

Gao et al. (2005) presented the development of Virtual Laboratories for Earthquake Engineering (VLEE) to supplement earthquake engineering education. VLEE simulated structural responses based on user-defined structural and earthquake parameters. Parameters included total mass, natural frequency, damping ratio of the structure, mass ratio of auxiliary mass to structure mass, natural frequency and damping ratio of auxiliary mass and structure mass system, seismic gap, max input amplitude, and input sin wave frequency. Graphical outputs displayed animation of the system, response spectrum, time response, structural displacement, and Bode plot. An example of a graphical output is displayed in Figure 2.2.

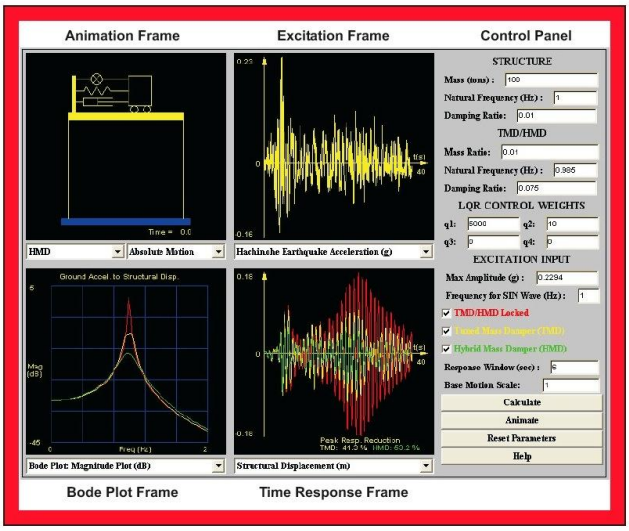

Figure 2.2: Interface to Display Simulated Structural Responses Resulting from Simulated Earthquake Conditions at Earthquake Engineering Research Centers Program (Gao et al., 2005). [Copyright © 2005 Wiley Periodicals, Inc. Used with permission.]

Li & Liu (2003), who developed Interactive Groundwater (IGW), an award-winning education software package at Michigan State University, called their lab a digital laboratory. A digital laboratory is a type of simulation-based lab that enables students to apply actual data to a simulated environment, using mathematical modeling to generate and interpret the results. IGW allowed students to assemble and visualize simulated complex groundwater systems using data from actual groundwater and aquifer systems. Data were gathered from physical systems and stored in digital libraries, which were made available to students through an interactive GUI, displayed in Figure 2.3. The computational, statistical, and graphical libraries from which the modeling software drew to formulate the simulations were Flow and Transport Solver library, Sparse Matrix Solver (SMS) library, Geostatisitcal Software library (GSLIB), Olectra Chart Library, and Inova GIS Library. The set of modeling software used to generate the final model

included Real-Time and Grid Independent Conceptual modeling, Real-Time Flow and Reactive Transport Modeling, Real-Time Hierarchical Modeling, Real-Time Cross Sectional Modeling with Approximate “Lateral” Influx, Real-Time Stochastic Modeling, and Real-Time Model Analysis. Using the GUI, students interfaced with the solvers and the modeling logic to develop a concrete understanding of the interactions of the modeled systems.

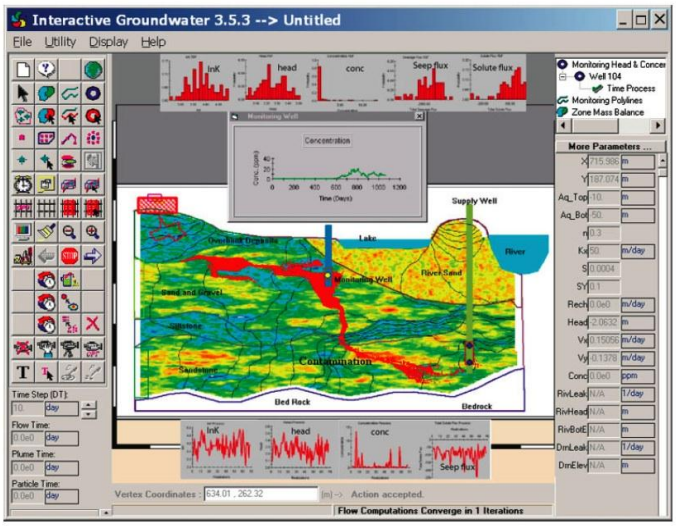

Figure 2.3: A Graphical User Interface (GUI) Developed for Interactive Groundwater (IGW) (Li & Liu, 2003). [Copyright © 2004 Wiley Periodicals, Inc. Used with permission.]

2.2.2 Remote Laboratory

Remote labs allow distance students to remotely control physical instruments, enabling acquisition and evaluation of actual data (Swain et al., 2003). Remote labs increase scheduling flexibility by maximizing the potential of the lab usage while continuing to promote interactive learning with actual experiments (Calvo et al., 2010).

Students have access to the actual instruments via an Internet connection by connecting to a server and host computer that is connected to the instruments in the physical lab (Nickerson et al., 2007). The set of software controls designed to control the actual instrument can be programmed in one of several computer languages to communicate with the actual instrument controls via a Data Acquisition Card (Elgamal et al., 2002) or serial port (Neitzel and Lenzi, 2000; Orabi, 2002). Some remote labs are even equipped with live streaming video feed from a camera located in the physical lab (Scanlon, Colwell, Cooper, and Di Paolo, 2004).

Swain et al. (2003) documented the collaboration of faculty and students from South Carolina State University with Pisgah Astronomical Research Institute (PARI) to develop a remote astronomy laboratory. Access to the PARI server was determined by comparison of the USERID and password combination entered on the login screen to a database of valid USERID and password combinations. A LabVIEW™ interface was developed to remotely access the PARI server and to facilitate the remote control of the SMILEY radio telescope to acquire live data using a real-time engine. The LabVIEW™ interface was converted to a fully functional web-based interface and was hosted at a dedicated IP address. The main display at the web address allowed students to navigate the experiment by providing options to login to the PARI server, calculate the dish coordinates, position the dish, and acquire data. Logic and algorithms developed by a NASA/PARI team facilitated the remote positioning of the dish by controlling the electric motors and circuitry and were not discussed in detail. The coordinate calculations calculated values for azimuth and altitude based upon local sidereal time, right ascension,

and declination as defined by user-input. Values for azimuth and altitude of the object were also exported as text files.

2.3 LabVIEW™

National Instruments LabVIEW™ is a programming environment that utilizes a graphically-based programming language, G, that is easily developed for applications in instrument control, data acquisition, and data analysis. All LabVIEW™ code is developed and written in the block diagram. Programming functions are represented by icons and are connected by wires that represent flow of data between the functions. Icons are selected from programming palettes and placed on the block diagram. The palettes are divided into structure, numeric, Boolean, string, comparison, array and cluster, time and dialog, File I/O, Instrument I/O, Data Acquisition, and Communication. The Structure functions determine the logical flow of data and include sequence structures that set the order and timing of consecutive events, case structures that are identical to 'If…Then' arguments, and For loop and While loop structures that are conditional arguments. Numeric, Boolean, string, comparison, array and cluster, and time and dialog functions manipulate and modify the acquired data. The file I/O, instrument I/O, data acquisition, and communication functions control instrument communication and data acquisition, analysis, and storage. Instrumentation controls and displays are located on the front panel, a user interface that is easily designed for multiple applications. Like the block diagram functions, instrumentation controls and displays are selected from palettes and placed on the front panel. Front panel control and display palettes include numeric,

Boolean, string and table, list and ring, array and cluster, graphs and charts, and path and refnum. For each item of instrumentation placed on the front panel, a representative icon is placed on the block diagram and properly incorporated into the programming code (Bitter, Mohiuddin, and Nawrocki, 2001).

LabVIEW™ has enjoyed popularity with computer-controlled instrumentation development in both educational and industrial applications and has accelerated the availability of remote lab development (Nedic et al., 2003). The following examples from published literature are presented here to demonstrate the diverse and extensive use of LabVIEW™ in academic applications for development of computer-controlled instrumentation for control of actual instruments.

Orabi (2002) described the integration of LabVIEW™ in a materials testing laboratory at the University of New Haven. An interface, displayed in Figure 2.4, was developed with LabVIEW™ to communicate with a Tinius Olsen Lo-Torq Bench Model Testing Machine. The interface enabled students to define experimental parameters, such as time interval, length, and diameter of material, and to view data from the experiment. The interface provided numerical and graphical data, which aided in the students' understanding of shear stress, shear strain, and the relationship between applied torque and angle of twist. The experimental values determined for the mechanical properties of aluminum produced in the lab agreed with published values.

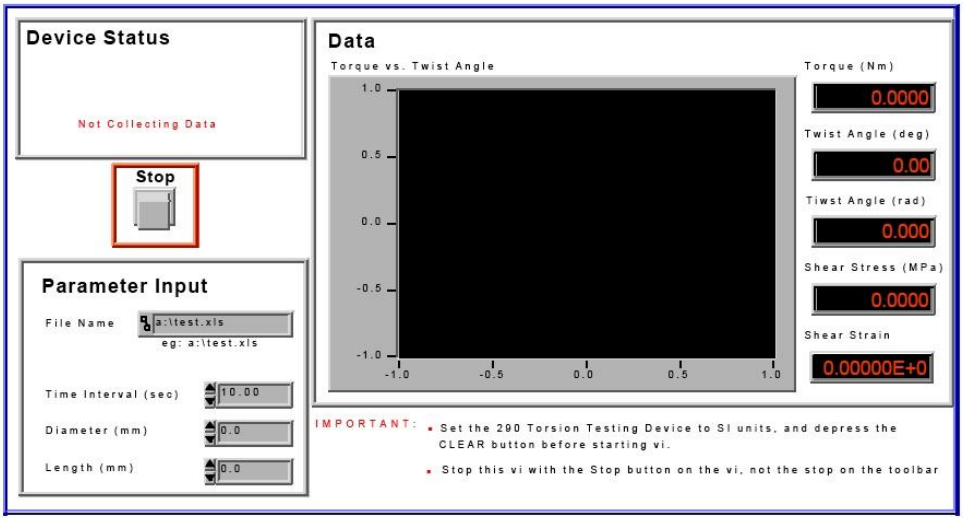

Figure 2.4: LabVIEW™ Interface for Materials Testing Laboratory at the University of New Haven (Orabi 2002.) [Copyright © 2002 American Society of Engineering Education. Used with permission.]

Kiritsis, Huang, and Ayrapetyan (2003) documented the integration of LabVIEW™ in a vibration experiment in the mechanical engineering department at McNeese State University. A cantilever was created by mounting an aluminum beam onto a vibration exciter. The vibration exciter was driven by a power amplifier that oscillated as determined by the sine wave output of a function generator. Two linear variable differential transformers measured the oscillation of the input motion and of the resulting motion of the free end of the cantilever. A strain gauge measured the strain at the position of application and an accelerometer measured the acceleration of the free end of the beam. The sensors were connected to a 4-channel sensor input module that communicated with LabVIEW™. The LabVIEW™ interface, displayed in Figure 2.5, allowed students to determine the number of samples and sample rate during acquisition. All data acquisition and analysis was conducted with the LabVIEW™ interface, which

displayed both numerical and graphical results of the acceleration, velocity, and displacement.

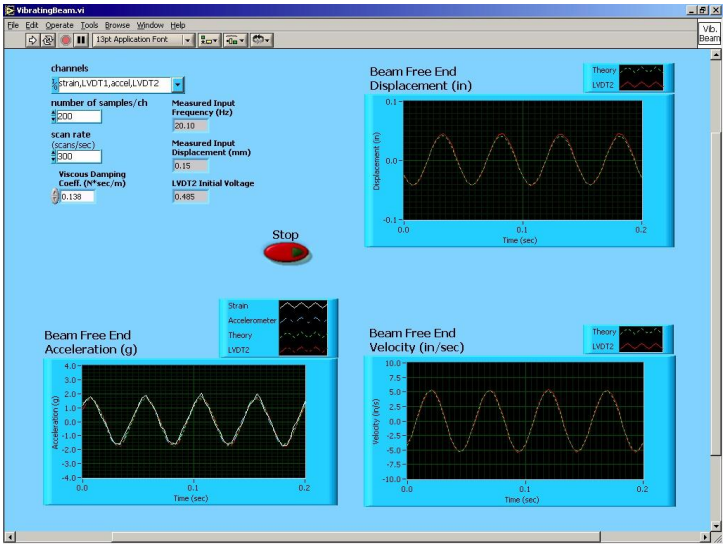

Figure 2.5: LabVIEW™ Interface for Vibration Experiments at McNeese State University (Kiritsis et al., 2003). [Copyright © 2003 American Society for Engineering Education. Used with permission.]

Globig (2003) developed an interdisciplinary engineering course with LabVIEW™ at the University of Dayton for students majoring in computer engineering technology, mechanical engineering technology, manufacturing engineering technology, and electronic engineering technology. This course familiarized these students with various types of simple data acquisition systems utilized in engineering fields not directly related to their specific majors. The students began by developing their own LabVIEW™ interfaces for simulated experiments and progressed to developing more complex interfaces for actual experiments in a group setting. All real data acquisition was conducted with LabVIEW™-developed instrumentation that interfaced with National

Instrument's DAQ Signal Accessory. Using a linear displacement potentiometer, students determined the maximum displacement and displacement constant for a displacement transducer and the linearity, repeatability, and overall accuracy of the displacement transducer and a force/torque transducer. In another lab, students verified the experimental values for stress and strain by building a bridge amplifier, mounting strain gauges to a beam, properly connecting the equipment, and acquiring the appropriate data. In a later lab, students developed oscilloscope instrumentation, displayed in Figure 2.6, which was used to determine amplitude, frequency, and input voltage and to display the signal generated from the DAQ Signal Accessory. Using a motor and the DAQ Signal Accessory for another lab, students calculated the rotational velocity, deceleration, frictional torque, power consumed by friction, and motor efficiency. Students also built a vibrating cantilever with an aluminum beam and a vibrator and determined resonance frequency as a function of cantilever length by acquiring data from an accelerometer mounted on the free end of the cantilever.

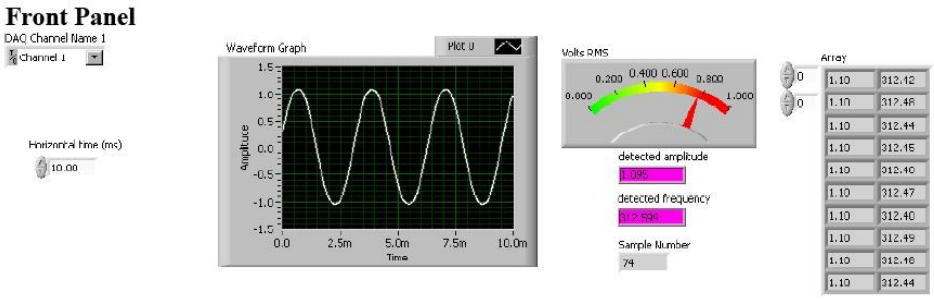

Figure 2.6: Oscilloscope Instrumentation Developed with LabVIEW™ at the University of Dayton (Globig, 2003). [Copyright © 2003 American Society for Engineering Education. Used with permission.]

Abu-Mulaweh (2009) described the development of a LabVIEW™-monitored and –controlled heat pump system for use in a thermodynamics lab in the mechanical engineering department at Purdue University at Fort Wayne. A laboratory computer running LabVIEW™ controlled the data acquisiton system via a data acquisition bus installed in the pump that communicated with an external data acquisition system via LabVIEW™.

Arthur and Sexton (2003) described the incorporation of LabVIEW™-developed instrumentation to upgrade the energy laboratory in Virginia Military Institute's mechanical engineering department. Old pressure gauges, thermometers, and analog rotameters from a small-scale steam turbine power plant were replaced with pressure transducers and thermocouples. Signals from these and other data acquisition sensors were connected to National Instruments analog-to-digital I/O cards, which communicated with LabVIEW™. The digitized signals were monitored with a LabVIEW™-developed interface, which displayed turbine inlet steam pressure and temperature, condenser temperature, condensate temperature, condenser cooling water inlet and outlet temperatures, the electric generator voltage, and current supplied to the electrical load. Similarly, an old inclined liquid manometer and thermometer from a small-scale water cooling tower were replaced with pressure transducers and thermocouples. Using the same data acquisition setup as the small power plant lab, a separate LabVIEW™ interface was developed to monitor the digitized signals for the cooling tower lab. The interface displayed tower inlet and outlet dry bulb and wet bulb air temperatures, water inlet and outlet temperatures, and air pressure drop through the tower.

Zhao (2006) described the use of LabVIEW™ in a freshman engineering course at Indiana University Purdue University Fort Wayne. Students set up acquisition systems and acquired data from multiple labs with the various LabVIEW™ interfaces. Labs included measurements of linear dimensions with linear variable differential transformers, temperatures with thermocouples, and displacement of a cantilever beam with laser displacement sensor. Students controlled experimental parameters, such as number of samples, sample rate, and length of sample. The interface for the cantilever beam experiment is displayed in Figure 2.7.

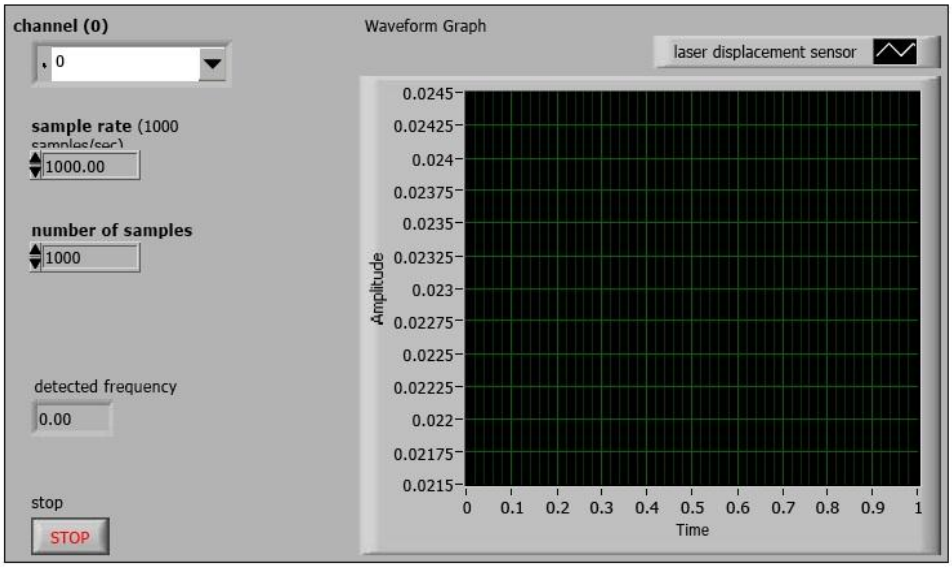

Figure 2.7: LabVIEW™ Interface for Cantilever Beam Experiment at Indiana University Purdue University Fort Wayne (Zhao, 2006)

Knight & MacDonald (1998) described the integral use of LabVIEW™ in the modernization of a mechanical engineering laboratory and the development of a new mechanical engineering laboratory class at the University of Tennessee at Chattanooga.

For each lab that utilized LabVIEW™ for data acquisition, analysis, and presentation, the data acquisition system comprised a unique LabVIEW™ interface that was developed and integrated with a National Instruments data acquisition board. The LabVIEW™-based labs were a refrigeration trainer lab that used a heat pump-air conditioning trainer, a heat conduction lab that used a thermal conduction system, an internal combustion engine mass and energy balance lab that used a 1.1-liter internal combustion (IC) engine, a materials testing lab that used a 5' long steel beam, a linear vibrations lab that used a vibrations apparatus, a rotational balancing lab that used a static and dynamic balancing apparatus, and a kinematics lab that analyzed the piston and crank motion of a lawnmower engine. The labs used a variety of sensors, including thermocouples, pressure sensors, linear variability differential transformers, accelerometers, turbine meters, anemometers, and other necessary flow meters to acquire all necessary data.

2.4 Computerized Radiation Detection and Measurement Teaching Labs

Over the last two decades, only two computerized teaching labs have been developed for radiation detection and measurement courses. The first was at the University of Florida in 1993 and the second was at Oregon State University in 2009.

Ellis & He (1993) developed a computer-based laboratory at the University of Florida's Nuclear Engineering Sciences department for the purpose of integrating computers into their analog radiation detection instrumentation. Fourteen lab experiments were successfully computerized with LabVIEW™, allowing for real-time instrument control and data acquisition and analysis. The lab experiments introduced fundamentals

such as Geiger-Mueller detectors, proportional counters, gamma-ray spectroscopy with scintillator and High Purity Germanium (HPGe), and charged-particle spectroscopy with semiconductor. To provide computerized instrumentation, interfaces were developed for a range of nuclear instruments, including single-channel analyzer (SCA), multi-channel analyzer (MCA), and digital oscilloscope. Communication between computer and instruments was mediated via IEEE-488 (GPIB) and control bus network. HyperCard, a hypermedia system developed for Macintosh, provided the interactivity of the user interfaces and was used to present experimental procedures, to conduct experiments by accessing LabVIEW™ interfaces, and to transfer acquired data to digital storage for further analysis. WordPerfect and Cricket Graph operated concurrently to generate instructional output regarding acquired data immediately following the conclusion of the experiment. The students accessed the interface for each lab by selecting the desired lab from a Table of Contents menu.

Vasquez (2009) developed "virtual detection equipment" at Oregon State University, which was designed to introduce distance students to the fundamentals of instrumentation by conducting simulated experiments similar to those typically offered in a traditional upper-level radiation detection course. Analog detectors, such as Geiger Muller (GM) tube and proportional counter, and analog equipment, such as signal splitter, pre-amplifier, amplifier, oscilloscope, dual counter/timer, SCA, and MCA were mathematically modeled. In addition, the activity of radioactive sources was also modeled with user-defined decay variables. Gamma-ray spectra were not modeled; real

spectra from select gamma-ray isotopes were acquired for the development of this lab and stored digitally.

For each of the gas-flow detectors, pulse data from ^{137}Cs and ^{60}Co was acquired with an oscilloscope, converted to digital data, and stored in an Excel spreadsheet as V(t) vs. t data. Empirical modeling equations were developed for pulse height, count rate, alpha and beta plateaus, dead time, and radioactivity as functions of student-defined parameters. The LabVIEW™ interface for each detector included NIM bin-style controls that allowed students to change parameters, such as high voltage, gain, acquistion time, and source-detector geometry. Conducting the gas-flow detector labs involved recalling the stored V(t) vs. t data and modeling it according to students' selection of the available parameters to produce modeled results representing actual results that would be expected from physical detectors. The LabVIEW™ interface developed to conduct the proportional counter lab is displayed in Figure 2.8.

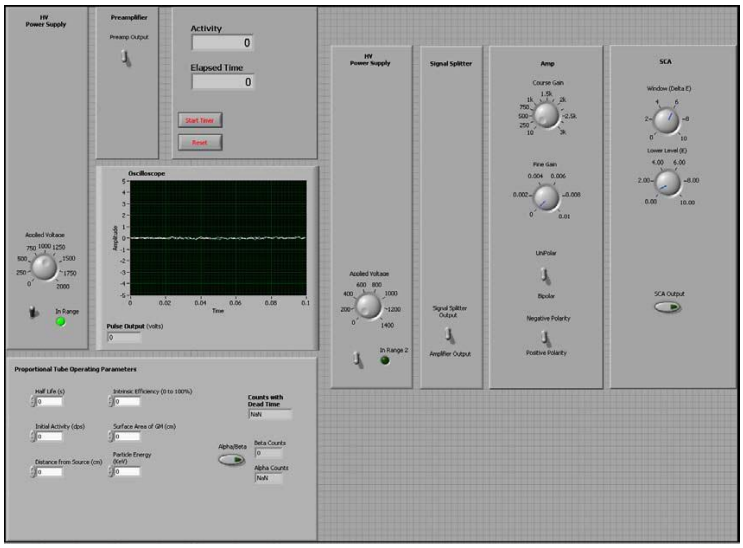

Figure 2.8: Virtual Detection Equipment for Proportional Counter Lab at Oregon State University (Vasquez, 2009). [Copyright © 2009 David C. Vasquez. Used with permission. All rights reserved.]

Each virtual instrument was modeled to produce the same effect on the stored pulse data that the corresponding analog instrument would have had on actual real-time data. The virtual signal splitter was created by acquiring pulses from a real signal splitter, converting the pulses to digital data, storing the pulses as a V(t) vs. t plot in Excel, and developing a 'signal-splitter formula' to model the signal splitting effect on raw pulses. The virtual pre-amplifier had no user-definable parameters and simply functioned to amplify and shape the proportional detector pulse. The virtual amplifier allowed the user to select polarity and to set coarse gain and fine gain parameters, which modified the signal input. The virtual SCA allowed students to define a lower level discriminator (LLD) and an upper level discriminator (ULD) with LLD and energy window dials. The SCA displayed a graph of modeled pulses that fell between the LLD and the ULD. The virtual MCA was essentially a sequence of SCA's programmed in series, and displayed a

spectrum of all modeled pulses. The Dual Counter/Timer regulated the acquisition time of each counting period.

If students chose not to recall the digital pulse data stored in Excel for the GM tube lab, they determined their own count rate by defining initial activity, decay constant, and decay time. Using these parameters, data were modeled to conduct the experiment based on the standard decay equation presented in [Eq. 2.1]:

$$A(t) = A_0 e^{-\lambda t} \qquad \text{[Eq. 2.1]}$$

where A_0 is initial activity, λ is the decay constant, and t is length of decay. For the proprotional counter lab, students were required to create their own isotope by determining count rate and selecting particle type and energy.

For the scintillator lab, ^{137}Cs and ^{60}Co spectra were acquired with NaI(Tl) with Gamma Vision software and saved in a database. The LabVIEW™ interface allowed students to recall a graphic of the selected spectrum from the database. The graphic highlighted characteristics of gamma-ray spectroscopy, including Compton edge, full energy peak(s), and backscatter. The interface for the scintillator lab is displayed in Figure 2.9.

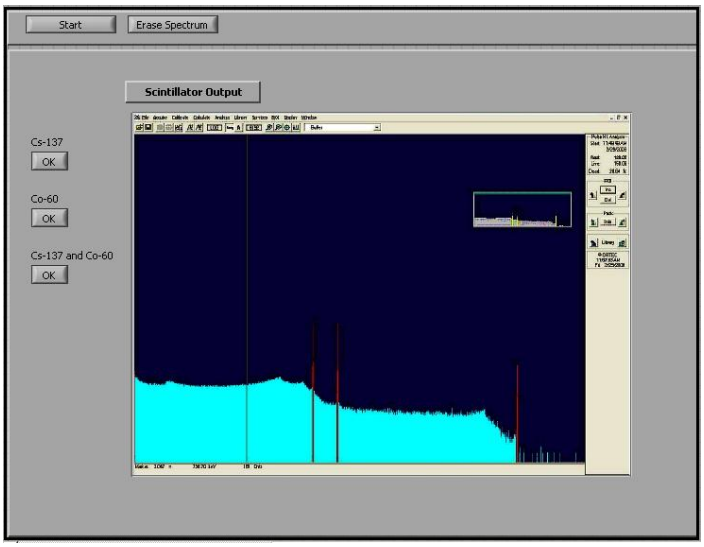

Figure 2.9: Interface to Recall and Display Gamma-ray Spectra for Scintillator Lab at Oregon State University (Vasquez, 2009). [Copyright © 2009 David C. Vasquez. Used with permission. All rights reserved.]

2.5 Need for Computerized Teaching Labs

Many academic institutions have found it increasingly difficult to provide a traditional laboratory experience for students (Li et al., 2003), yet engineering employers presume that engineering graduates entering the workforce have benefited from hands-on experience during their education (Nedic et al., 2003). Issues facing the development or modernization of hands-on labs include limited funding for equipment and equipment maintenance, space, access, lack of faculty involvement, and safety resources. Safety includes radiological and general laboratory concerns. Financial pressures limit the ability to purchase updated equipment (Abu-Mulaweh, 2009) and to support laboratory-related faculty and staff (Uran & Safaric, 2009). The demand that physical laboratories put on space is liable to increase the operational costs (Ma & Nickerson, 2006) and restricts the ability to integrate lab experiments with lecture-taught material (Bhargava et

al., 2006). Access to physical labs poses great difficulty to non-traditional students, part-time students, and students with disabilities (Calvo et al., 2010). Outdated laboratory equipment combined with limited funds to replace the equipment have led to faculty disinterest regarding the development and support of physical laboratories, including the lack of expertise and/or certification to instruct in the lab (Knight & McDonald, 1998). Some institutions are not prepared or equipped to deal with the required safety measures necessary to operate certain equipment or conduct certain experiments (Huang, Su, Samant, and Khan, 2001). Computerized labs allow for an efficient use of time and resources (Elgamal et al., 2002). In general, computerized labs are cost-effective (Shin, 2002), space saving (Powell et al., 2002), and easily accessible (Budhu, 2001; Nedic et al., 2003). Simulation-based labs, specifically, also relieve institutions of safety concerns (Manseur, 2005; Yao, Li, & Liu, 2007).

2.6 Assessment of Computerized Teaching Labs

Computerized labs have been utilized to successfully demonstrate the agreement between theory and practice (Cooper & Dougherty, 2000; Kiritsis, Huang, & Ayrapetyan, 2003) and increase students' learning potential of course material (Budhu, 2001). Whelan (1997) reported an extremely encouraging reaction to the computerized lab at Dublin City University, although the author admitted the small group of enrolled students was exceptionally hard-working. After implementing and conducting computerized labs at their respective institutions, Hall, Jr. (2002), Nickerson et al. (2007), and Scanlon et al. (2004) concluded that computerized labs were as useful of an educational tool as hands-

on labs and reported that the results were positive regarding the further implementation of the computerized labs. Additionally, Cockrum & Koutras (2001) concurred concerning the operational functionality of computerized lab exercises.

Vasquez (2009) asserted that students are somewhat disadvantaged in a simulated lab by not experiencing a physical lab environment and may not understand the difficulties relating to instrument error and unexpected results when only working with simulated instruments. Toader (2005) identified potential technical issues of Internet-mediated labs, including system failure or network corruption of the host computer or server. Although Nedic et al. (2003) claimed that simulation-based labs are inadequate alternatives to hands-on labs and even contended that physical lab experiences cannot be properly substituted by any means, the authors recognized the distinct benefit of adaptability and convenience of computerized lab experiences and stated that there are many variables regarding the effectiveness of computerized labs. Their final conclusion was students should be exposed to a balance of hands-on, simulation-based, and remote labs during their engineering education.

Simulation-based labs and remote labs are both prevalent in engineering education. Simulation-based labs enable student interaction with systems that would otherwise be impractical to implement in a real laboratory setting. Remote labs allow students to remotely interact with real equipment and to acquire and to evaluate real data when such a laboratory is practical and efficient to set up. Neither simulation-based labs nor remote labs can fully convey the practicalities of working with real systems to students, but a remote lab most closely duplicates that of a real laboratory atmosphere

when the traditional lab setting is not feasible. Many engineering departments at universities across the nation have successfully used LabVIEW™ in a wide range of applications to interface with real equipment and to conduct real data acquisition and analysis.

No remote laboratories currently exist for radiation detection and measurement courses that can be offered to distance students. Ellis & He (1993) developed a computerized teaching lab for the in-class traditional students at the University of Florida. More recently, Vasquez (2009) developed a simulation-based lab for students in enrolled in a distance education radiation detection and measurements course. For these reasons, the laboratory course presented in this thesis is designed using the LabVIEW™ programming environment to provide a remote radiation detection and measurements laboratory course for distance students.

CHAPTER THREE

RESEARCH OBJECTIVES AND TASKS

3.1 Research Objective

The overarching objective that extends beyond the scope of the specific tasks presented in this thesis is to create a remotely accessible laboratory course consisting of 12 experiments. This course will be offered to students who don't have the opportunity to be involved in a physical lab environment because of lack of expensive laboratory equipment, lack of licensing for handling of radioactive materials, and/or lack of qualified faculty at their academic institution. This on-line lab will be coupled with on-line lectures to give the distance students as realistic an experience as possible. The reason for the on-line lab as documented here is to allow the students to interact with physical counting systems, to actively engage in experimental setup, and to acquire and analyze actual data in real-time.

3.2 Tasks

This specific project contributes to the development of the remote laboratory by achieving the following tasks:

(1) Develop computer-controlled interfaces for six physical instruments (Universal Radiation Spectrum Analyzer II (URSA-II), oscilloscope, BiSlide™, rotary table, pressure transducer, rotating shaft),

(2) Create unique seamless interfaces for each of the following experiments: (i) Nuclear Electronics, (ii) Gamma-ray Spectroscopy with Scintillation Detectors, (iii) Gamma-ray Attenuation & External Dosimetry, and (iv) Alpha Spectroscopy and Absorption in Air.

(3) Create interchangeable code for the motor controllers that will enable an accelerated completion of the interfaces for the remaining eight lab experiments, and

(4) Adapt experimental procedures from those already written for the physical lab to guide distance students through each step of the remote experiments, detailing the specific use of the web-based computer interfaces.

CHAPTER FOUR

MATERIALS AND METHODS

4.1 URSA-II

URSA-II (SE International), displayed in Figure 4.1, is a modern data acquisition system, which provides the bias voltage, signal shaping and amplification, and analog-to-digital conversion of the data for each of the labs. URSA-II provides all multi-channel analysis of the data and almost exclusively all electronics parameters for each of the labs. URSA-II can be configured to process radiation pulses to display a spectrum consisting of 256, 512, 1024, 2048, or 4096 channels. Positive voltage is provided via internal bias voltage from 0 V to 2000 V at up to 0.5 mA. Shaping time is adjustable from 0.25μs to10 μs. Coarse and fine gain yields an overall gain range of less than x1 to x250. All parameters are software controlled. URSA-II has two detector inputs. One input is the standard series "C" connector for detectors with a conjoined high voltage and signal cable. The other input is for detectors with separate high voltage (SHV connector) and signal (BNC connecter) cables. URSA-II is powered by 12V DC power supply or by six "AA" NiMH rechargeable batteries, which are automatically recharged by the 12V DC power source. URSA-II connects to the host computer using a standard RS232 serial port or USB port in conjunction with an RS232-to-USB adapter.

Figure 4.1: URSA-II (www.radpro.com)

4.2 LabVIEW™

National Instruments LabVIEW™ is a platform on which to develop remote instrumentation to control physical instruments and is comprised of two integral parts that create an intuitive environment for development: front panel and block diagram. The front panel is the interactive interface that consists of controls and indicators that allows the user to control the instrument in real time and receive feedback from the instrument in real time. When developing an interface, controls such as buttons, knobs, and switches are selected from formatting palettes and placed onto the front panel at the desired location and orientation. Similarly, indicators such as graphs, numerical displays, and LED lights are selected from the appropriate palettes and placed on the front panel. An example of a front panel is displayed in Figure 4.2.

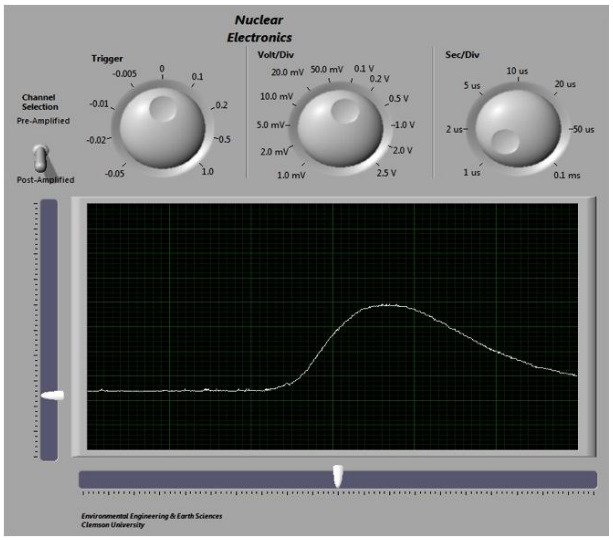

Figure 4.2: LabVIEW™ Front Panel

The block diagram contains all of the programming that relays commands from the front panel to the physical instruments and vice versa. All initialization of serial ports and USB ports and manipulation of data are included in the block diagram. Programming in LabVIEW™ uses an icon-based programming language, G. Wires, which represent the flow of data, connect the icons, which represent operator functions. The block diagram resembles an intricate flow diagram. An example of a block diagram is displayed in Figure 4.3.

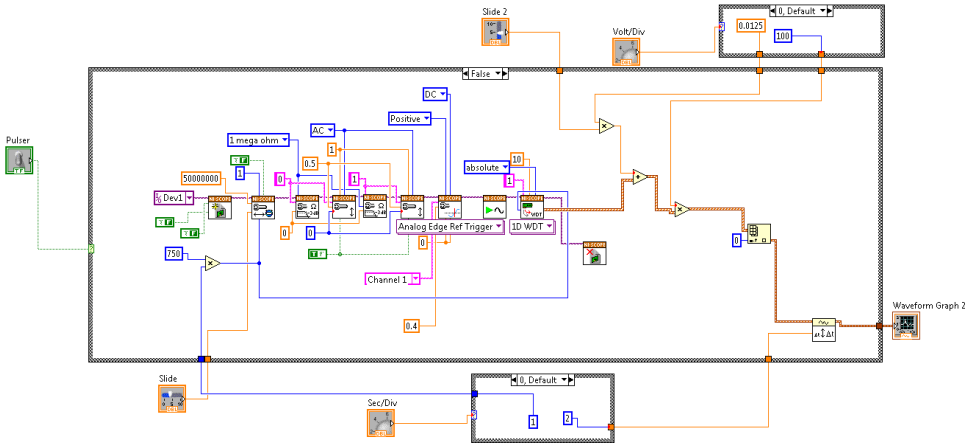

Figure 4.3: LabVIEW™ Block Diagram

Each experiment is centered around a National Instruments LabVIEW™ interface (front panel) which consists of two sections. The first section of the interface allows students to control instrument parameters and experimental setup. For example, using the controls on the front panel, the students can adjust applied voltage, amplifier gain, polarity, etc. on the URSA-II. This section is enclosed by the dotted lines in Figure 4.4. The second section of the interface allows students to acquire and process data and observe the outputs from the instruments. Once all necessary instrument parameters have been selected and setup has been completed, the students can acquire data and observe the graphical and numerical displays. Graphical displays include differential pulse height spectrum from URSA-II and signal display from the digital oscilloscope. Numerical displays include counting information such as total number of counts, count rate, time expired, and current vacuum chamber pressure. This section is enclosed by the solid lines in Figure 4.4.

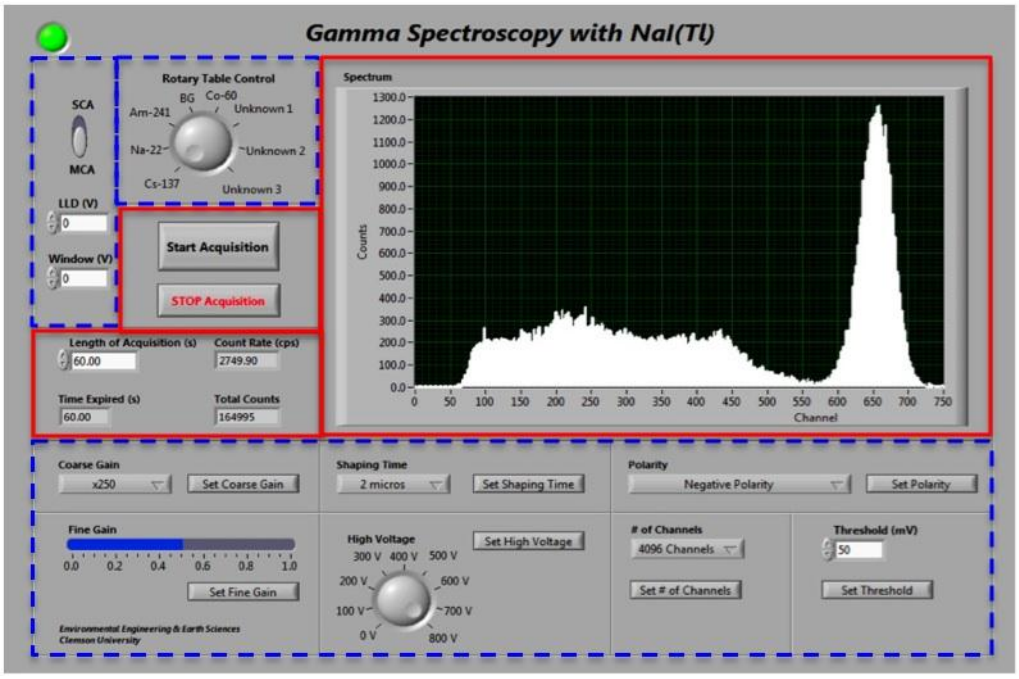

Figure 4.4: Description of LabVIEW™ Interface Sections. The dotted lines enclose the controls for electronics parameters and experimental setup. The solid lines enclose the controls and displays for data acquisition.

Upon completion of an acquisition, a standard Windows 'Save As' dialog box prompts the students to save the acquired data. This data is exported to Microsoft® Excel and saved as 2-D data; one column represents channel number and the other column represents the corresponding number of counts. Students can graph this data and use Excel algorithms to determine peak channel number, net peak area, and full-width-half-maximum (FWHM).

Each interface is typically comprised of instrumentation for multiple pieces of equipment. For example, the interface for the alpha spectroscopy lab includes instrumentation for URSA-II, motor controller, and digital vacuum regulator. Instrumentation for each individual instrument was developed separately and then

combined and integrated to provide seamless functionality to multiple instruments in one interface. The interface for each instrument is designed to duplicate the original instrument controls and software as closely as possible while providing maximum utility to students.

4.3 Motor Controller

The stepper motor controller (VXM-1, Velmex, Inc.), displayed in Figure 4.5, is a high-performance, programmable, 2-phase, unipolar device that governs the action of each motor-driven assembly. Various motor-driven assemblies are responsible for all source handling by positioning the appropriate sources in relation to the respective stationary detectors. The motor-driven assemblies used are a rotary table, a slide actuator, and a rotating shaft. The inclusion of the motor-driven assemblies to control experimental setup introduces an important dimension to the remote laboratory. It allows for the handling of multiple sources for a single experiment without requiring the presence of a lab assistant at Clemson and provides an active role for the students in experimental setup.

The stepper motor controller interfaces with the computer via RS-232 serial port. The motor controller can operate a motor between 1 and 6,000 steps/sec and maintain constant speed within 0.1% variation. The motor controller communicates with a motor via a 6-pin motor cable connector and a 4-pin limit cable connector.

Figure 4.5: Velmex VXM-1 Stepper Motor Controller (www.velmex.com)

4.4 Motor

One of the standard motors that accompanies the motor controller is a Vexta PK245-01AA, displayed in Figure 4.6. With no gearhead, the motor has a basic step angle of 1.8° and a step accuracy of 0.05°. However, the motor controller operates in half-step mode, lowering the basic step angle and step accuracy to 0.9° and 0.0025°, respectively. This translates to 400 steps per revolution with an accuracy of 1/144,000 of a rotation.

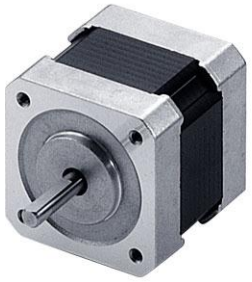

Figure 4.6: Vexta PK245-01AA Motor (www.orientalmotor.com)

4.5 Digital Vacuum Regulator

A digital vacuum regulator (Model 200, J-KEM, Inc.), displayed in Figure 4.7, is a pressure regulating system that allows the students to control the pressure level in the vacuum chamber in the alpha spectroscopy lab. The DVR is controlled by a pressure transducer that regulates pressure by automatically operating a valve that separates the vacuum source from the system being evacuated and can regulate the pressure to within 1 torr of the desired pressure. A needle valve (DVR-PNV, J-KEM, Inc.) stabilizes the pressure fluctuations inherently introduced by the DVR. A vacuum pump (DuoSeal 1399B-01, Welch) provides evacuation to the system. The vacuum pump is a single stage belt-driven pump. It features thermal overload protection and operates at 750 RPM to achieve a low ultimate pressure of 0.02 torr. The volumetric rate of free air displacement is 35 L/min. The motor is a ½ horsepower motor.

Figure 4.7: J-KEM Model 200 Digital Vacuum Regulator (www.jkem.com)

4.6 Digital Oscilloscope

The digital oscilloscope (USB-5132, National Instruments), displayed in Figure 4.8, is a bus-powered USB digitizer/USB oscilloscope that is used primarily with the nuclear electronics lab. The digital oscilloscope provides all of the basic functions of a standard laboratory oscilloscope and was developed by National Instruments to work directly with LabVIEW™. The oscilloscope communicates with the computer via USB port and has two BNC connector I/O ports. It has a sample rate range of 762 S/s up to 50 MS/s and can sample simultaneously on both channels. It has a timebase frequency of 50 MHz, which is accurate at ±50 ppm. It has a peak-to-peak (V_{pk-pk}) amplitude range of 0.04 V to 40 V.

Figure 4.8: NI USB-5132 Digital Oscilloscope (www.ni.com)

4.7 Rotary Table

The rotary table (B4836TS, Velmex, Inc.) is a motor-driven assembly driven by a Vexta PK266-03A-P1 motor with a 4.9″ circular platform. A gearbox provides a gear ratio of 36:1, which produces a basic step angle of 0.025° per step. The rotary table has

an accuracy of 0.03° and repeatability of 3 ten-thousandths of a degree. With a maximum input of 600 RPM, the table can rotate at 16.7 RPM, or 100° per second. The assembly has a typical backlash of 200 arc-seconds. The rotary table uses a worm and gear design with a central ball bearing. The horizontal load capacity is 200 lbs. The rotary table is displayed in Figure 4.9.

Figure 4.9: Velmex B4800TS Series Rotary Table (www.velmex.com)

4.8 BiSlide™

The BiSlide™ (MB10-1800-M10-33, Velmex, Inc.) is a 15 foot-long slide actuator driven by a Vexta 296B2A-SG10 motor. The assembly consists of a motor and gearbox mounted perpendicular to the traverse. The basic step angle of the motor is 0.18° per step and the gearbox provides a ratio of 10:1. The output of the gearbox is directly coupled to a stainless steel pulley that drives a steel reinforced timing belt. The timing belt advances 4 tenths of an inch per motor rotation and has a straight-line accuracy of 7 ten-thousandths of an inch per 10 inches of travel and a repeatability of 2 ten-thousandths

of an inch. A 4.6″ x 3.1″ carriage is clamped to the belt and provides a versatile platform for linear translation. The BiSlide™ is displayed in Figure 4.10.

Figure 4.10: Velmex Belt Drive BiSlide™ (www.velmex.com)

4.9 Host Computer

The host computer is connected to the Clemson University network, which operates on a dedicated T1 line. The computer has a static IP address, which easily facilitates remote connection. Currently, one computer hosts all four of the labs. Although this computer can communicate with and operate all of the instruments for all of the labs, hardware limitations restrict it from doing so simultaneously. Each lab requires a unique hardware configuration, which must be set prior to conducting the lab.

CHAPTER FIVE

RESULTS & DISCUSSION

The following sections describe each of the four labs developed for the remote lab in the following order: (1) Nuclear Electronics, (2) Gamma-ray Spectroscopy with Scintillation Detectors, (3) Gamma-ray Attenuation and External Dosimetry, and (4) Alpha Spectroscopy and Absorption in Air. Each section contains theory required to conduct each lab, description of the user interface developed for student interaction with the physical lab setup, summary of the experiment & objectives, and experimental setup. The description of each user interface explains the purpose and the function of each control and display. The procedures for each lab are included in Appendices D – G, respectively.

5.1 Nuclear Electronics Lab

5.1.1 Theory

The purpose of nuclear electronics is to create electronic signals from interactions between radiation and the detector that can be processed and counted to determine energy and activity of the source.

Two types of cables are utilized in nuclear electronics. A high voltage cable with SHV or MHV connectors provides high voltage, or detector bias, from a high voltage power supply to a detector. Detector bias is necessary for proper operation of the detectors to generate a transmittable signal. Signal cables, typically with BNC

connectors, transport the electronic signal between Nuclear Instrument Modules (NIMs) and instruments. These modules are produced according to a specified standard for electronics systems in radiation detection and measurement. The modules typically used in nuclear electronics include tail pulse generator (TPG), preamplifier, amplifier, high voltage, SCA, counter/timer, and MCA.

A TPG is used to simulate radiation pulses. Both the shape (timebase) and amplitude of the simulated pulse can be adjusted with the TPG. The primary function of a preamplifier is to couple the detector to the amplifier. The preamplifier increases the power of the signal from the detector so that the signal can be transmitted over long cables. The preamplified pulse is bipolar and generally tails off. An amplifier is utilized to increase the gain and shape the pulse amplitude from the preamplifier. The amplifier can properly shape the pulse in order to reduce pulse pile-up. Pulse pile-up occurs when two or more pulses are spaced too close together such that the pulses "pile up" and cannot be analyzed as separate pulses. Pulse shaping reduces pulse pile-up by minimizing the total width of the pulses to accommodate high count rates. An amplified and shaped pulse is unipolar or bipolar and has greater amplitude than the preamplified pulse.

Oscilloscopes display radiation pulses (voltage vs. time) and allow measurement of pulse height (amplitude) and pulse width (timebase) of any signal pulse. Oscilloscopes also enable triggering. Internal triggering allows the observer to analyze a signal only above a certain voltage which is determined by the trigger level.

An SCA enables the analysis of a pre-defined range of pulse amplitudes from all of the energies produced by the detector. The SCA uses two independent discrimination

levels to produce a logic pulse when the signal (linear) pulse amplitude falls between the two discrimination levels. The two independent discrimination levels are determined by setting a lower-level discriminator (LLD) and either explicitly setting an upper-level discriminator (ULD) or implicitly determining a ULD by setting an energy window, where the ULD is equivalent to the LLD + energy window. A counter/timer works in conjunction with an SCA to determine the number of counts that are detected within the energy window during a pre-determined amount of time.

The method most often used to display signal amplitude is a histogram known as the differential pulse height distribution. The abscissa of this distribution is a linear pulse amplitude scale from 0 to, for example, 4096 (2^{12}) channels. The ordinate is the number of counts within each channel.

An MCA is used to analyze the differential pulse height spectrum. An integral part of the MCA is the analog-to-digital converter (ADC) which converts the signal pulse amplitude to a digital number that is proportional to the amplitude of the pulse. An MCA functions as multiple stacked SCAs; each energy window of the MCA is a channel. The digital number produced by the ADC is the channel that represents the energy of the radiation pulse. For every pulse detected by the detector, the MCA increments the number of counts in the associated channel, thereby generating a differential pulse height spectrum that graphically describes the radiation interactions in the detector material. ORTEC Maestro-32 and Canberra Genie™ 2000 are examples of MCA software packages expedites the analysis and archiving of the differential pulse height spectra.

5.1.2 Web-based Computer Interface

The web-based computer interface that was developed to conduct the Nuclear Electronics lab is displayed in Figure 5.1. The integration of instrumentation for two individual instruments into one seamless interface can be observed in this figure. The left half of the interface contains the controls and display for the digital oscilloscope while the right half of the interface contains the controls and display for the nuclear spectroscopy software operated and controlled by URSA-II.

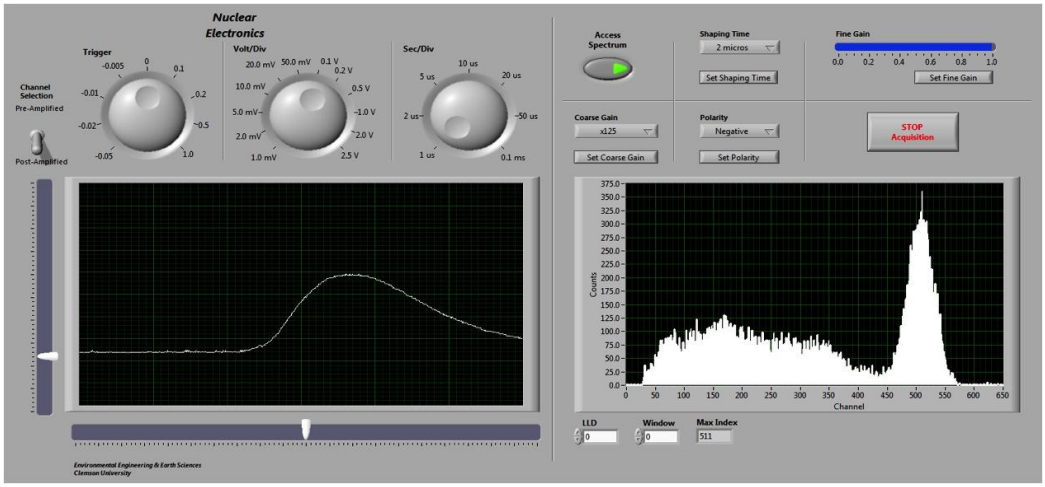

Figure 5.1: Interface for Nuclear Electronics Lab

The computer-controlled instrumentation for the digital oscilloscope has been developed to be almost completely interchangeable with actual instrumentation for a physical oscilloscope. Operating the digital oscilloscope will require a minimal learning curve, at most, for students who are familiar with standard oscilloscope instrumentation and will provide valuable realistic experience to students who are not yet familiar with oscilloscope instrumentation.

The toggle switch, positioned at the top left of the oscilloscope instrumentation, allows the students to select which of the two input channels is displayed. One channel displays the signal directly before amplification and shaping while the other channel displays the signal directly after amplification and shaping. The knobs positioned above the display control trigger level, voltage amplitude, and time base, respectively, from left to right. Signal placement on the display is controlled by the sliding indicators on the horizontal and vertical bars that extend the length of the abscissa and ordinate, respectively. The display is a standard real-time oscilloscope display with time displayed on the abscissa and pulse amplitude displayed on the ordinate.

The computer-controlled instrumentation developed for the URSA-II with LabVIEW™ provides the students with complete command of all electronics and timing controls necessary for nuclear spectroscopy and delivers informative displays for a complete understanding of the MCA results. Through experience with the URSA-II interface, students will gain first-hand knowledge of and familiarity with standard MCA software.

Beginning at the top left of URSA-II controls and continuing clock-wise, the controls enable the students to turn the spectroscopy software on and automatically begin collecting the spectrum, set shaping time, set fine gain, end the acquisition, set polarity, and set coarse gain. Beneath the spectrum display, students set an energy range of interest by determining the LLD and Window. Prior to performing the actual experimentation, the students are instructed to use these controls to set all of the necessary parameters for

operating URSA-II. Because this is an introductory lab, not all URSA-II controls are included in this interface; the remaining controls are pre-programmed.

This interface provides numerical and graphical displays in real-time. The graphical display is a standard differential pulse height spectrum with Channel Number displayed on the abscissa and number of counts per channel displayed on the ordinate. As each spectrum is acquired, students observe the live in-growth of the spectrum with a 20 Hz refresh rate. Students control the zoom function of the graph to focus on important spectral features both during and after the acquisition. The only numerical display on this interface is Max Index so that students can determine the correlation between coarse gain/fine gain settings and peak channel number. A green indicator at the top left of the interface informs the students that the URSA-II is properly communicating with LabVIEW; a red indicator prompts the students to contact appropriate personnel at Clemson University to attend to the problem.

5.1.3 Summary of Experiment & Objectives

The objectives of this experiment are (1) to become familiar with the operating characteristics of basic nuclear pulse counting instrumentation, (2) to become familiar with the use and operation of the digital oscilloscope, (3) to become familiar with National Instruments LabVIEW™, and (4) to become familiar with nuclear spectroscopy software packages.

The students are introduced to the functions of the various electronics of nuclear spectroscopy by observing and comparing characteristics of the pre-amplified and amplified pulses. These characteristics include pulse height, polarity, and frequency. As

the students view and manipulate these pulses on the oscilloscope, they become familiar with the oscilloscope and its controls. The students acquire a spectrum of the tail pulse generator pulse at multiple amplifications and verify the linearity between amplification and the peak channel number. The detailed procedures for the Nuclear Electronics Lab as presented to the students are included in Appendix D and demonstrate, in part, the completion of Objective #4.

5.1.4 Experimental Setup

The equipment and instruments used in this lab are summarized in Table 5.1.

Table 5.1: Equipment and Instruments Used in Nuclear Electronics Lab

Name	Model
Digital Data Acquisition System	URSA-II
Digital Oscilloscope	NI USB-5132
Preamplifier	ORTEC 113
Tail Pulse Generator	ORTEC 480

The URSA-II used in this lab is modified by the manufacturer to provide pre-amplified and post-amplified and shaped signals to the digital oscilloscope. Since URSA-II does not contain a pre-amplifier, the “pre-amplified” pulse is simply the radiation pulse immediately prior to amplification. The URSA-II outputs installed for the modification are LEMO ports. A LEMO to BNC adapter cable is used to connect the outputs to the digital oscilloscope inputs. The modified URSA-II is displayed in Figure 5.2.

Figure 5.2: Manufacturer-modified URSA-II

5.2 Gamma-ray Spectroscopy with Scintillation Detectors Lab

5.2.1 Theory

An inorganic scintillator is a crystalline material that emits light immediately following energy absorption. Since gamma rays do not create direct ionization of materials through which they travel, detection of gamma-ray photons requires gamma-ray interactions in which the gamma ray transfers all or part of its energy to electrons in the absorbing material. Prior to interaction with the gamma rays, the electrons are bound at lattice sites and reside in the valence band, a discrete energy level in the crystal lattice. The absorption of energy can excite the electrons of the valence band to the conduction band, another discrete energy level where electrons migrate within the crystal. In a pure crystal, electrons cannot dwell in the gap of energies between the valence and conduction band, called the forbidden gap. The de-excitation of an electron from the conduction band across the forbidden gap to the valence band in a pure crystal is an inefficient process and, most likely, the photon emitted would not be in the visible range. Therefore, an impurity, called an activator, is added to the pure crystal. The activator alters the lattice sites of the crystal and creates energy states in the forbidden gap. In a crystal with an

activator, electrons that undergo interactions with gamma rays are excited from the valence band to an activator excited state in the forbidden gap. Almost instantaneously, another electron de-excites from an excited state to an activator ground state in the forbidden gap, resulting in the emission of visible light. The intensity of light emitted is proportional to the original energy of the incident gamma ray. The light photons are absorbed by a photocathode of a photomultiplier tube (PMT) and converted back to an electron. The photoelectron is subsequently multiplied in the dynode structure of the PMT, creating an electrical signal for each detected gamma ray that once amplified and shaped is quantified with the MCA software. The resultant differential pulse height spectrum is used to infer energy deposition in the detector.

Spectroscopy is the analysis of energy deposition and subsequent identification and quantification of radionuclides. Certain distinct features of gamma-ray interactions generate spectral features unique to gamma-ray spectra. There are three distinct gamma-ray interactions that contribute to the shape of the spectrum. These interactions are presented in order of increasing energy.

The first gamma-ray interaction is photoelectric absorption. The probability of photoelectric absorption is proportional to $Z^{4-5} \Big/ E_{\gamma}^{3.5}$, where Z is the atomic number of the absorbing material and E_{γ} is the energy of the gamma ray (Knoll, 2000). Because it is desirable for all interactions to end with photoelectric absorption, detector materials with high atomic numbers are preferred. Photoelectric absorption occurs when the incident gamma ray transfers all of its energy to an inner shell electron. The energy of this photoelectron, E_{e^-}, is equivalent to the energy of the incident gamma-ray photon, hv,

minus the binding energy of the electron in its original electron shell, E_b. The binding energy is the energy required to remove the electron from its current electron shell. The equation that governs the energy of the photoelectron is given in Eq. 5.1 (Knoll, 2000):

$$E_{e^-} = h\nu - E_b \qquad \text{[Eq. 5.1]}$$

As the photoelectron is removed from its original electron shell, a void is created in the shell that must be filled. Another electron in a higher electron shell fills the void and, in the process, emits energy equal to the difference in binding energies. When this energy is emitted via electromagnetic radiation, it is called a *characteristic X-ray*. If, instead, this energy is transferred to yet another electron, which is ejected from the atom, this is called an *Auger electron*. The summation of the energy of the photoelectron and the energy emitted by the characteristic X-ray or Auger electron is equivalent to the total energy of the incident gamma ray. The deposition of the photoelectron energy and the binding energy occurs almost simultaneously such that the detector detects the equivalent to the total gamma-ray energy. This results in a feature of the spectrum called the full energy peak.

The second gamma-ray interaction is Compton scattering. The probability of Compton scattering is proportional to Z/E (Knoll, 2000). In Compton scattering, the incident gamma ray collides with a "free electron" or a weakly bound electron, transferring only part of its energy to that electron. Compton scattering results in an energetic electron, called a *recoil electron*, and a scattered gamma-ray photon. The

distribution of energies between the energy of the recoil electron, E_{e^-}, and the energy of the scattered gamma ray, $h\nu'$, is dependent on the scattering angle of the gamma ray, θ. The equations to determine the energies of the scattered gamma-ray photon and the recoil electron are given in Eqs. 5.2 & 5.3, respectively:

$$h\nu' = \frac{h\nu}{1 + \left(\frac{h\nu}{m_0 c^2}\right)(1 - \cos\theta)} \qquad \text{[Eq. 5.2]}$$

$$E_{e^-} = h\nu - h\nu' = h\nu\left(\frac{\left(\frac{h\nu}{m_0 c^2}\right)(1 - \cos\theta)}{1 + \left(\frac{h\nu}{m_0 c^2}\right)(1 - \cos\theta)}\right) \qquad \text{[Eq. 5.3]}$$

where m_0c^2 is the rest mass energy of the electron (511 keV) (Knoll, 2000). Two characteristics of Compton scattering are visible in the differential pulse height spectrum. The first characteristic is the *Compton continuum.* Theoretically, all scattering angles can occur and a continuum of energies, called the Compton continuum, that spans all theoretical energies of the recoil electron will be visible in the spectrum. The maximum energy transferred to the recoil electron occurs when $\theta=\pi$, which occurs when the incident gamma ray scatters directly backwards. This backscattering results in the *Compton edge*, the second characteristic of Compton scattering. The Compton edge is a semi-abrupt edge at the uppermost energy of the Compton continuum. The energy of the Compton edge is given by Eq. 5.4 (Knoll, 2000):

$$E_{e^-}\Big|_{\theta=\pi} = h\nu\left(\frac{\frac{2h\nu}{m_o c^2}}{1+\frac{2h\nu}{m_o c^2}}\right) \qquad \text{[Eq. 5.4]}$$

The energy difference between the full energy peak and the Compton edge is given by Eq. 5.5 and is equivalent to the minimum possible energy of the scattered gamma ray (Knoll, 2000):

$$h\nu'\big|_{\theta=0} = h\nu - E_{e^-}\Big|_{\theta=\pi} = \frac{h\nu}{1+\frac{2h\nu}{m_0 c^2}} \qquad \text{[Eq. 5.5]}$$

The third gamma-ray interaction is pair production. The probability of pair production is proportional to $Z^2 \times E$ for $E \geq 1.02$ MeV (Knoll, 2000). Pair production occurs when the incident gamma-ray photon disappears in the electric field close to the protons of the nuclei of the detector material or other charged body and creates an electron-positron pair in its place. An energy of $2m_0c^2$ (1.02 MeV) is required to create an electron-positron pair. When an incident gamma ray that is involved in pair production has an energy that exceeds 1.02 MeV, the excess energy is shared between the positron and the electron. The energy of the electron-positron pair is given by Eq. 5.6 (Knoll, 2000):

$$E_{e^-} + E_{e^+} = h\nu - 2m_0c^2 \qquad \text{[Eq. 5.6]}$$

Once created, the unstable positron dissipates its energy and quickly combines with another electron. This positron and electron mutually annihilate and two *annihilation photons*, each with energy of m_0c^2, appear in their place. If both annihilation photons further interact in the scintillating material, the net effect is a contribution to the full energy peak. Two characteristics of the gamma-ray spectrum unique to pair production arise from pair production interactions in the detector material. If only one annihilation photon interacts in the detector material and the other escapes the detector without further interaction, a peak is visible at $h\nu - m_0c^2$, and is called a *single escape peak*. If both annihilation photons escape the detector without further interaction, a peak is visible at $h\nu - 2m_0c^2$, and is called a *double escape peak*.

Interactions of gamma rays with the surrounding material of the detector cause three distinct characteristics in spectra from gamma-ray emitting isotopes. If the incident gamma ray undergoes photoelectric absorption in the surrounding material and the characteristic X-ray of that surrounding material is detected (undergoes photoelectric absorption in the detector), a characteristic X-ray peak is produced equivalent to the energy of the X-ray photon. When incident gamma rays undergo Compton scattering in the surrounding material with $\theta > 110°$, the energies of these scattered photons that are detected are very similar and a *Backscatter peak* occurs at approximately $\theta = \pi$ (Eq. 5.2). If pair production occurs in the surrounding material and one of the annihilation photons is detected, a peak called an *annihilation peak* will be visible at 0.511 MeV.

Full energy peaks of a spectrum from a source with multiple known gamma-ray energies are used to calibrate the energy response of the counting system. A good scintillating material has a linear energy response over a wide range of energies. Identification of unknown isotopes that emit gamma rays is accomplished by identifying the energy of its full energy peak based on the energy calibration of known isotopes and determining which isotope emits a gamma ray with that (those) energy(ies).

Detection efficiency for scintillating materials is dependent on the energy of the incident gamma ray. Generally, low-energy gamma rays have a higher probability of detection than high-energy gamma rays. High-energy gamma rays have the ability to pass straight through the detector material without transferring any energy to any of the absorbing material's electrons.

Two types of detection efficiencies can be calculated with the aid of multiple calibrated monoenergetic sources. Absolute peak detection efficiency, $\varepsilon_{abs,peak}$, is dependent on detector properties and the geometry of the counting system. $\varepsilon_{abs,peak}$ is defined as the number of counts in the full energy peak recorded by the detector divided by the number of quanta emitted by the source and is calculated by Eq. 5.7:

$$\varepsilon_{abs,peak} = \frac{counts_{fullenergy}}{A \times f \times t} \qquad \text{[Eq. 5.7]}$$

where $counts_{fullenergy}$ is the total number of counts in the full energy peak, A is the source activity (Bq), f is the branching ratio, and t is the length of acquisition in seconds (Knoll, 2000). Intrinsic peak detection efficiency, $\varepsilon_{int,peak}$, quantifies efficiency of the detection

mechanism alone and is defined as the number of counts in the full energy peak recorded by the detector divided by the number of quanta incident on the detector and is calculated by Eq. 5.8:

$$\varepsilon_{\text{int},peak} = \varepsilon_{abs,peak} \times \frac{4\pi}{\Omega} \qquad \text{[Eq. 5.8]}$$

where Ω is the solid angle, which accounts for the source-detector geometry (Knoll, 2000). However, when determining detection efficiency for a given experimental setup, it is difficult to obtain a curve that properly reflects the energy dependent detection efficiency –absolute or intrinsic— because of the poor energy resolution of scintillating materials.

Energy resolution quantifies the response function of a detector. Good energy resolution corresponds to a precise response function; poor energy resolution corresponds to an imprecise response function. Scintillating materials have relatively poor energy resolution because the energy resolution is dependent on many variables, such as scintillation efficiency (how well the excited electrons convert their energy to photons of light), light collection efficiency (how well the scintillation light is collected on the PMT), and quantum efficiency (how well the PMT creates electrical signals from the photons of light). Therefore, an alternative method to experimentally determining the efficiency calibration of a given counting system and geometry for small-scale lab experiments is to use published efficiency calibrations that have been tabulated for many source-detector geometries (Knoll, 2000).

Different scintillating materials have different properties. Properties that vary between materials used for scintillation detectors are detection efficiency and scintillation efficiency. As eluded to earlier, detection efficiency is dependent on the atomic number of the detector material. Scintillation efficiency is inversely proportional to energy resolution. Other factors, such as cost of the material, determine the availability of different sizes of detectors. Some scintillating material is also slightly radioactive, which contributes to poor resolution in the range of energies close to the energy of the material's radioactivity.

5.2.2 Web-based Computer Interface

The web-based computer interface for Gamma-ray Spectroscopy with Scintillation Detectors is displayed in Figure 5.3. This interface integrates the control for the motor controller that operates the rotary table and all the controls and displays for nuclear spectroscopy.

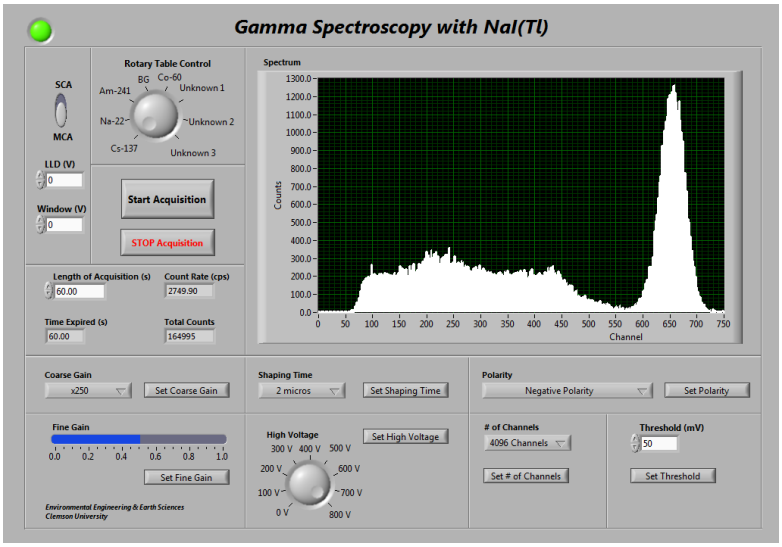

Figure 5.3: Interface for Gamma-ray Spectroscopy with Scintillation Detector Lab

The large knob located towards the top left of the interface controls the motion of the rotary table. The computer-controlled instrumentation for the rotary table in this lab provides students with the control of the source placement. The selection tool for the rotary table was chosen to resemble the rotary table so that students rotate the knob as if they were directly rotating the rotary table themselves. The programming for the rotating assemblies was developed to non-sequentially advance the assemblies through the smallest angle possible to any of the desired positions based on students' selection. Once students rotate the knob, the rotary table responds by rotating to the desired position. A webcam streams images that provide visual feedback in real-time and enable students to confirm that the device has responded correctly.

The remaining controls and displays on the interface are to control URSA-II and display the spectrum and acquisition statistics. This interface includes all of the controls included in the nuclear electronics lab plus additional controls, allowing the students to

control all of the electronics. To the left of the large knob is the switch to acquire data in SCA mode or MCA mode. In SCA mode, the appropriate LLD and Energy Window can be determined. Beneath the rotary table control knob are two buttons to begin and end an acquisition. The button to end the acquisition is pressed when it is desired to stop the acquisition before the user-defined length of acquisition has been reached. Beneath the 'STOP Acquisition' button are the controls and display for counting time and statistics. The students enter the desired length of acquisition. During the acquisition, counts rate, total counts, and expired time are updated in 0.05-second intervals. The bottom half of the interface are the controls for electronics parameters. In clock-wise order beginning with the top left of these controls is coarse gain, shaping time, polarity, threshold, number of channels, high voltage, and fine gain.

5.2.3 Summary of Experiment & Objectives

The objectives of this lab are (1) to identify gamma-ray interaction mechanisms using a NaI(Tl) detector, (2) to perform an energy and efficiency calibration of the gamma-ray detector, (3) to identify an unknown source by gamma-ray spectroscopy, and (4) to quantify differences in detection efficiency and energy resolution between detectors of two different scintillation materials.

To conduct the gamma-ray spectroscopy lab, the students acquire a background spectrum and spectra from multiple known and unknown gamma-ray isotopes with URSA-II. After conducting an energy calibration using the energies of the known isotopes, they identify the unknown isotopes based on the energy calibration and quantify the unknown isotope based on standard NaI(Tl) efficiency curves. They also locate the

characteristics of gamma-ray spectroscopy on multiple spectra. These characteristics include Compton edge, Compton continuum, characteristic X-ray, and backscatter peak. Students also acquire a spectrum with a 1.5″ x 1.5″ $LaBr_3$(Ce), which is placed in the same position as the 2″ x 2″ NaI(Tl) detector by personnel at Clemson University at the students' request as instructed by the procedures. Students observe and comment on the differences between spectra acquired with NaI(Tl) and $LaBr_3$(Ce) detectors. The detailed procedures for the Gamma-ray Spectroscopy with Scintillation Detector Lab as presented to the students are included in Appendix E and demonstrate, in part, the completion of Objective #4.

5.2.4 Experimental Setup

The equipment and instruments used in this lab are summarized in Table 5.2.

Table 5.2: Equipment and Instruments Used in Gamma-ray Spectroscopy with Scintillation Detectors

Name	Model
Digital Data Acquisition System	URSA-II
Motor Controller	VXM-1
Motor	Vexta PK266-03A-P1
Rotary Table	Velmex B3648TS
2″ x 2″ NaI(Tl) Detector	Bicron 2M2/2
1.5″ x 1.5″ $LaBr_3$(Ce) Detector	SGC BrilLanCe 380
7 Gamma-ray Sources[1]	--

1. See Table 5.3

A 17″ diameter clear plastic plate machined at Clemson University is mounted on the central rotating mechanism of the rotary table. 1″ diameter depressions were etched at 45° increments around the circumference of the circular plate. Seven sealed 1″ diameter

gamma-ray sources are placed in the depressions. One of the depressions is left blank for background acquisition. The seven gamma-ray sources are listed in Table 5.3.

Table 5.3: Gamma-ray Sources and Activities Used in Gamma-ray Spectroscopy with Scintillation Detectors

Source	Activity
^{137}Cs	1 μCi (Jun 2003)
^{241}Am	1 μCi (July 1967)
^{60}Co	1 μCi (Jun 2003)
^{22}Na	1 μCi (Jun 2003)
Unknown #1 (^{57}Co)	1 μCi (July 2010)
Unknown #2 (^{152}Eu)	1 μCi (Aug 1995)
Unknown #3 (^{40}K)	10 nCi (Jan 1970)

The 2″ x 2″ NaI(Tl) detector is positioned horizontally beneath the circular plate such that the centers of the gamma-ray sources pass directly over the center of the NaI(Tl) crystal. For spectra acquisitions with the 1.5″ x 1.5″ $LaBr_3$(Ce) detector, the 2″ x 2″ NaI(Tl) detector must be removed and the 1.5″ x 1.5″ $LaBr_3$(Ce) detector set in its place by a lab assistant at Clemson University. A still image of the top view of the rotary table setup with the 2″ x 2″ NaI(Tl) detector as seen with the webcam is displayed in Figure 5.4. ^{137}Cs is in the counting position.

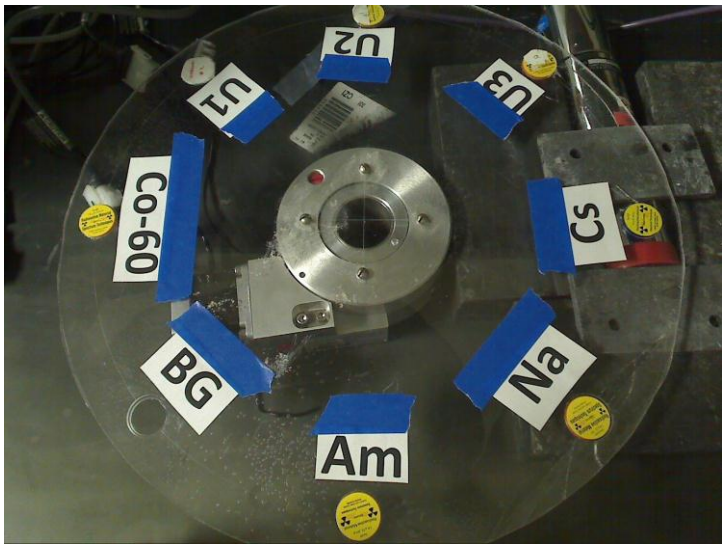

Figure 5.4: Rotary Table Setup for Gamma-ray Spectroscopy with Scintillation Detector Lab

5.3 Gamma-ray Attenuation and External Dosimetry Lab

5.3.1 Theory

Gamma rays undergo discrete (non-continuous) interactions in matter. These interactions result in the attenuation of the intensity of the gamma rays. The rate of attenuation per unit length of material, the *linear attenuation coefficient*, is material-dependent. The intensity, *I*, of a gamma ray that has traveled through a linear distance *x* of absorber material with linear attenuation coefficient μ is determined by Eq. 5.9:

$$I = I_0 e^{-\mu x} \qquad \text{[Eq. 5.9]}$$

where I_0 is the original intensity of the gamma ray before attenuation (Knoll, 2000). Attenuation coefficients have been tabulated for many materials. Attenuation coefficients

are experimentally determined by acquiring a series of spectra from a collimated source with increasing absorber thickness, plotting the curve of intensity of full energy peak vs. thickness of absorber, and determining the coefficient μ in Eq. 5.9 according to the exponential curve of intensity vs. absorber thickness. A *mass attenuation coefficient* can be calculated by dividing the linear attenuation coefficient by the density of the absorber material. The *half-value layer* or *half-value thickness* is the thickness of a material required to reduce the original intensity of a gamma-ray beam by a factor of two.

Gamma rays can only indirectly ionize material through interactions with the absorber material; they do not create direct ionization. Gamma-ray radiation can only be attenuated by increasingly thicker absorber materials; it cannot be completely absorbed. This phenomenon is observed by acquiring a series of spectra from a single collimated source with increasing absorber thickness and then analyzing the energy of the full energy peak in subsequent spectra. With constant source-detector distance, the full energy peak of a monoenergetic source will remain at the same energy, regardless of the decreasing intensity of the full energy peak with increasing absorber thicknesses.

The equation used to calculate dose rates is given by Eq. 5.10:

$$\dot{D}(Sv/hr) = 5.76 \times 10^{-7} \frac{Sv/hr}{MeV/g \times s} * \sum_i \left(\phi_P * \frac{\mu}{\rho_i} * E_i \right) \qquad \text{[Eq. 5.10]}$$

where ϕ_P^0 is the flux at some point $P\left(\frac{1}{cm^2 \times s}\right)$, μ/ρ is the absorbed energy coefficient of tissue $\left(\frac{cm^2}{mg}\right)$, and E is the corresponding energy (MeV) (Cember and Johnson, 2009).

The flux at a point P can be approximated experimentally by Eq. 5.11:

$$\phi_P^0\left(\frac{1}{cm^2 * s}\right) = \frac{CR}{A} * \frac{1}{\varepsilon_{\text{int},peak}} \qquad \text{[Eq. 5.11]}$$

where CR is the count rate acquired from the spectra (*cps)* and A is the cross-sectional area of the detector (cm^2), and , $\varepsilon_{int,peak}$ was defined in Section 5.2.1 (Faw and Shultis, 1999).

The equation for theoretical flux at a point P from a point source is given by Eq. 5.12:

$$\phi_P^0\left(\frac{1}{cm^2 * s}\right) = \frac{\dot{S}}{4\pi r^2} e^{-\mu x} \qquad \text{[Eq. 5.12]}$$

where $\dot{S}$ is the emission rate (*1/s*) and r is the source-detector distance (cm^2) (Faw & Shultis, 1999).

A line source is essentially an infinite number of point sources in succession. Therefore, Eq. 5.12 is modified to accommodate a succession of point sources in order to calculate theoretical flux for a line source. For the geometry in which the detector is

located at a distance *h* above the center of the line source, theoretical flux is calculated by Eq. 5.13:

$$\phi_P^0\left(\frac{1}{cm^2 * s}\right) = \frac{2 * \dot{S}_l}{4\pi h}\left[F(\theta,\mu t)\right] \qquad \text{[Eq. 5.13]}$$

where $\dot{S}_l$ is the emission rate per unit length $\left(\frac{1}{cm \times s}\right)$, θ is the angle created between *h* and the distance between point *P* and the end of the line source (rad), and the values of the Secant Integral, $F(\theta,\mu t)$, are tabulated for given pairs of θ and μt (Faw & Shultis, 1999).

5.3.2 Web-based Computer Interface

The web-based computer interface for Gamma-ray Attenuation and External Dosimetry lab is split into two interfaces. The interface for the gamma-ray attenuation procedures, displayed in Figure 5.5, is similar to the one developed for Gamma-ray Spectroscopy, but does not include the SCA controls. URSA-II controls and displays are identical to and located in the same position as the Gamma-ray Spectroscopy lab interface.

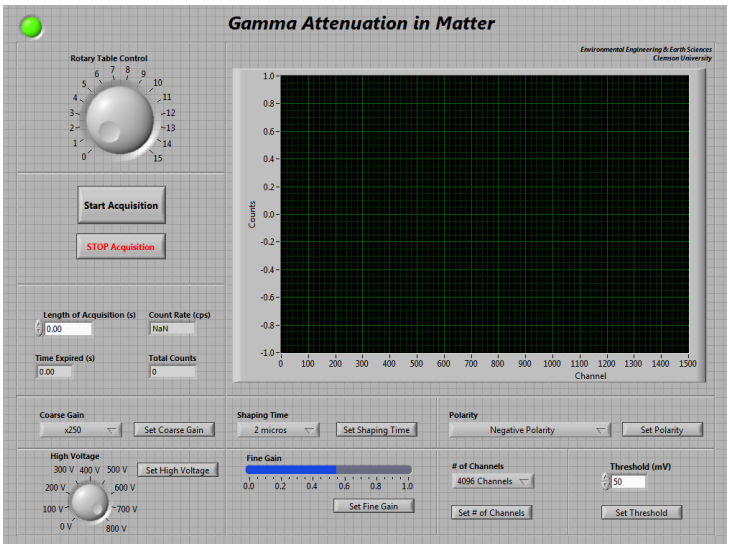

Figure 5.5: Interface for Gamma-ray Attenuation Procedures for Gamma-ray Attenuation and External Dosimetry Lab

In the interface for the external dosimetry lab, Figure 5.6, the slide control located at the top of the interface operates the motion of the BiSlide™. Because of the length of the BiSlide™ and the slow speed at which the carriage travels, the Reset BiSlide™ button located to the left of the BiSlide™ control allows students to cancel the current motion of the BiSlide™ and reset the destination of the carriage once a new selection has been made. This allows the students to remedy the situation if an incorrect selection was made without having to wait for the BiSlide™ to complete its motion before another selection could be made.

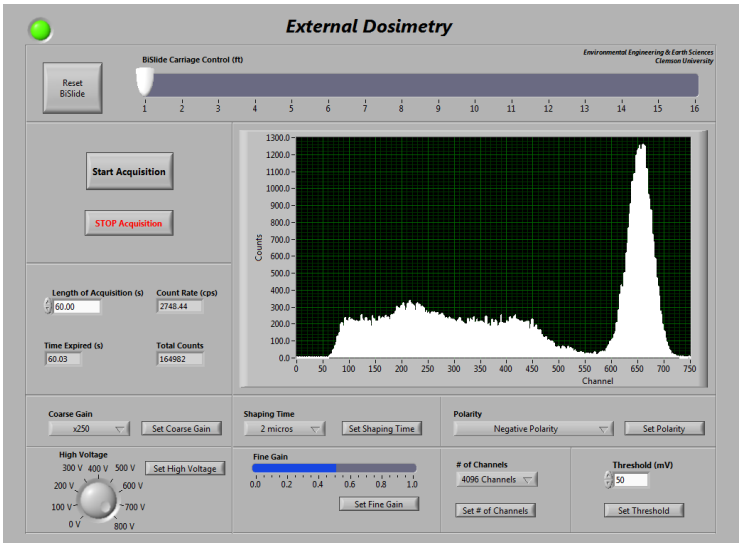

Figure 5.6: Interface for External Dosimetry Procedures for Gamma-ray Attenuation and External Dosimetry Lab

5.3.3 Summary of Experiment & Objectives

The objectives of this lab are (1) to determine the attenuation coefficient for gamma rays in aluminum and lead, (2) to demonstrate that gamma rays undergo attenuation not energy absorption in material, (3) to verify the functional relationship between dose and distance for a point source, and (4) to verify the functional relationship between dose and distance for a line source.

To conduct the gamma-ray attenuation portion of the lab, the students will collect a series of spectra with URSA-II with 15 different absorber thicknesses placed in-between a collimated source and the detector. They will analyze these spectra to determine the attenuation coefficient of aluminum and lead and observe that gamma rays are only attenuated, not absorbed.

To conduct the external dosimetry portion of the lab, the students will collect a

series of spectra at 1-ft. increments between 0 ft. and 15 ft. for a point source and a line source. Upon analysis of these spectra, they will determine the correlation between dose and distance for both source geometries. At present, it is necessary for the instructor at Clemson University to manually replace the point source with the line source; this process has not yet been automated. The procedures for the Gamma-ray Attenuation and External Dosimetry Lab as presented to the students is included in Appendix F and demonstrate, in part, the completion of Objective #4.

5.3.4 Experimental Setup

This lab utilizes two motor-driven assemblies and setups. The first setup is used to conduct the gamma-ray attenuation procedures and the second setup is used to conduct the external dosimetry procedures.

The equipment and instruments used for the gamma-ray attenuation portion of the lab are summarized in Table 5.4.

Table 5.4 Equipment and Instruments Used for Gamma-ray Attenuation Procedures of Gamma-ray Attenuation and External Dosimetry Lab

Name	Model
Digital Data Acquisition System	URSA-II
Motor Controller	Velmex VXM-1
Motor	Vexta PK266-03A-P1
Rotary Table	Velmex B4836TS
2″ x 2″ NaI(Tl) Detector	Bicron 2M2/2
5 μCi ^{57}Co	calibrated Jan 2005
15 Absorber Thicknesses[1]	--

1. See Table 5.5

The rotary table is the same rotary table and 17″ diameter circular plate used for the gamma-ray spectroscopy with scintillation detector lab with absorber thicknesses placed on the table instead of gamma-ray sources. The absorber thicknesses used are listed in Table 5.5.

Table 5.5: Absorber Thicknesses Used for Gamma-ray Attenuation

Absorber Thicknesses (mg/cm^2)[1]	Absorber Material
549.2	Al
619.6	Al
687.5	Al
858.7	Al
960.5	Al
974.4	Pb
1082.4	Al
1224.7	Al
1373.4	Al
1498.3	Al
1602.3	Al
1824.2	Pb
2650.6	Pb
4450.8	Pb
7193.6	Pb

1. Absorber Set Model AB-23 from Atomic Accessories, Inc.

The collimated source is placed beneath the rotary table, centered directly beneath the stationary detector, which is suspended vertically above the rotary table. The source used is the 1″ diameter sealed ^{137}Cs source used in the gamma-ray spectroscopy with scintillation detector lab. The setup for the gamma-ray attenuation portion of the lab is displayed in Figure 5.7.

Figure 5.7: Rotary Table Setup for Gamma-ray Attenuation Procedures for Gamma-ray Attenuation and External Dosimetry Lab

The equipment and instruments used for the external dosimetry portion of the lab are summarized in Table 5.6.

Table 5.6 Equipment and Instruments Used for External Dosimetry Procedures of Gamma-ray Attenuation and External Dosimetry Lab

Name	Model
Digital Data Acquisition System	URSA-II
Motor Controller	Velmex VXM-1
Motor	Vexta 296B2A-SG10
Slide Actuator (BiSlide™)	Velmex MB10-1800-M10-33
2″ x 2″ NaI(Tl) Detector	Bicron 2M2/2
0.1 Ci ^{137}Cs point source	calibrated July 1986
876 Bq/cm ^{137}Cs line source	calibrated Feb 1977

The BiSlide™ is mounted on the wall. The source is placed on the carriage of the BiSlide™ and URSA-II and the detector are mounted on the end of the BiSlide™. Markers on the BiSlide™ denote distance in feet. This setup is displayed in Figure 5.8.

Figure 5.8: BiSlide™ Setup for External Dosimetry Procedures for Gamma-ray Attenuation and External Dosimetry Lab

5.4 Alpha Spectroscopy and Absorption in Air

5.4.1 Theory

Alpha particles are heavy charged particles which consist of two protons and two neutrons. Since alpha particles are heavy charged particles, they directly ionize the absorbing materials. In semiconductors, electron-hole pairs are created along the path taken by the alpha particle. It is the creation of these electron-hole pairs that generate the electrical signal from the detector. Unlike gamma rays that may pass through an absorber material without any interaction, alpha particles travel only a very short distance in absorber materials before complete absorption occurs. Unlike the multiple spectral features produced by gamma-ray interactions, alpha spectroscopy generally has only one spectral feature—the full energy peak. Energy calibration for alpha spectroscopy is conducted in the same manner as energy calibration for gamma-ray spectroscopy. Detection efficiency calibration for alpha spectroscopy is very simple because it is energy independent—unlike that for gamma rays. If an alpha particle travels through the medium separating the alpha source and enters the active region of a detector, it will be detected

100% of the time. The most significant consideration when comparing detection efficiency calibration of alpha radiation and gamma-ray radiation is that alpha particles may be absorbed in the medium separating the source and the detector but the ε_{int} is 100%.

Alpha particles are the least penetrating of the most common types of radiation. While the energy of an alpha particle decreases as it travels through an absorber, the number of alpha particles does not decrease until the particles have traveled a distance sufficient for the alpha particle to lose all of its energy. This perpendicular distance into a material is known as *range,* which is proportional to its energy as indicated in Eq 5.14 for energies between 2MeV and 8 MeV:

$$R_{air} = 0.322E^{3/2} \qquad \text{[Eq. 5.14]}$$

where R_{air} is the range in air (*cm*) and E is the energy of the alpha particle (*MeV*) (Cember & Johnson, 2009). At a path length greater than the range, the number of alpha particles that travel beyond that distance in the absorber is zero. An alpha particle's range in air is dependent on the density thickness of air, which is determined by temperature and pressure. Range in air can be experimentally determined by varying source-detector distance, temperature, or pressure while the other variables remain constant. If temperature and source-detector distance are held constant, the total number of counts in the full energy peak will remain relatively constant for varied increasing pressures until the density thickness of air exceeds the range of the alpha particles. Using Eq. 5.15, range

for ambient pressure and temperature can be determined from experimental range, pressure, and temperature. Assuming that air is an ideal gas, the ratio of air density is simply the ratio of pressures. The ratio of range, R, is proportional to the inverse ratio of air density, ρ (Knoll, 2000):

$$\frac{R_{ambient}}{R_{pressurized}} = \frac{\rho_{pressurized}}{\rho_{ambient}} \qquad \text{[Eq. 5.15]}$$

5.4.2 Web-based Computer Interface

The web-based computer interface for Alpha Spectroscopy and Absorption in Air lab is displayed in Figure 5.9. All URSA-II controls and displays are identical to the previous two interfaces.

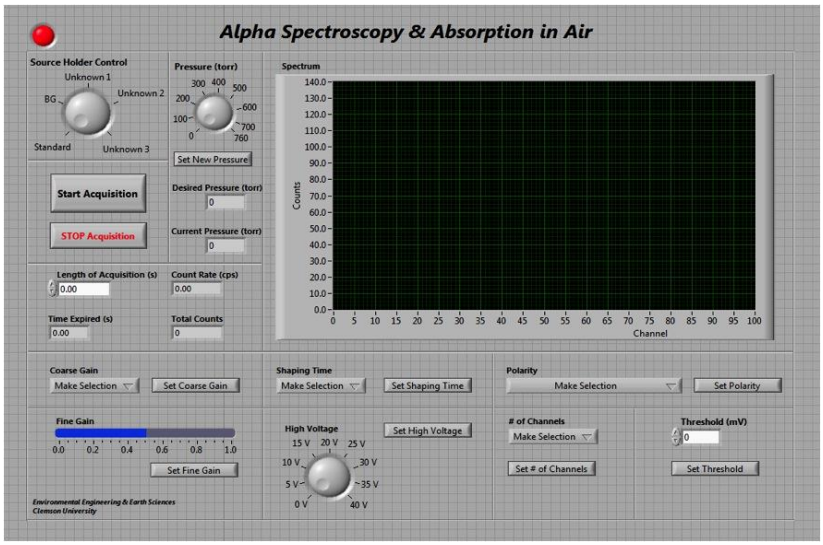

Figure 5.9: Interface for Alpha Spectroscopy and Absorption in Air Lab

5.4.3 Summary of Experiment & Objectives

The knob to control the source holder is located in the top left corner of the interface. The knob to select the desired pressure of the digital vacuum regulator and the displays for the current and desired pressure are located to the right of the source holder knob.

The computer-controlled instrumentation for the DVR allows students to indirectly control the evacuation level of the vacuum chamber by controlling the pressure level of the chamber. The students adjust the pressure of the chamber by rotating a knob to the desired pressure and selecting 'Set New Pressure'. The pressure levels are selected in increments of 1 torr. A numerical display updates the current pressure in real-time at a rate of 20 times per second so that students can confirm when the chamber has been evacuated to the desired level. The current pressure is displayed in increments of 0.1 torr. The DVR only facilitates evacuation of a system; it does not purge an evacuated system. Purging of the system requires personnel at Clemson University to manually purge the vacuum chamber. An inefficient option to return the system to ambient pressure is to allow the chamber to slowly leak until it is in equilibrium with ambient pressure. Further discussion on this is presented in Section 6.2, "Future Work".

5.4.4 Summary of Experiment & Objectives

The objectives of this experiment are (1) to learn how to calibrate an alpha spectrometer for energy and efficiency, (2) to measure the range of alpha particles in air, (3) to investigate the loss of alpha particle energy as it travels through different density thicknesses of air, and (4) to identify and quantify unknown sources.

The students acquire spectra of known alpha standards at a given pressure level to calculate energy and efficiency calibrations with known energies and activities. The calibrations are used to identify and quantify, respectively, unknown nuclides from spectra acquired under the same experimental conditions as the standards were acquired. The students also acquire a series of spectra for multiple unknown sources at incremental pressure levels to observe the energy loss of alpha particles, calculate the range of alpha particles in air for multiple energies, and identify the unknown sources based on the range of the alpha particle. The detailed procedures for the Alpha Spectroscopy and Absorption in Air lab as presented to the students are included in Appendix G and demonstrate, in part, the completion of Objective #4.

5.4.5 Experimental Setup

The equipment and instruments used in this lab are summarized in Table 5.7.

Table 5.7 Equipment and Instruments Used for Alpha Spectroscopy and Absorption in Air Lab

Name	Model
Digital Data Acquisition System	URSA-II
Motor Controller	Velmex VXM-1
Motor	Vexta PK245-01AA
PIPS Detector in Vacuum Chamber	Canberra 7400A
Preamplifier	Canberra 2004DM
Digital Vacuum Regulator	J-KEM Model 200
Needle Valve	J-KEM DVR-PNV
Pulser	ORTEC 480
Vacuum Pump	Welch DuoSeal 1399B-01
Alpha Source Holder	--
Alpha Sources[1]	--

1. See Table 5.8

The source holder for the vacuum chamber is designed for precise and repeatable positioning of up to eight sources. A 2.4″ tall octagon was machined at Clemson University with 1″ square edges. 1″ diameter alpha sources are secured to the edges. This source holder is suspended in the vacuum chamber by connection to a rigid shaft that penetrates the rear wall of the vacuum chamber and connects to the shaft of the motor with a coupling. An oil seal is fitted to the rear wall of the vacuum chamber at the penetration site to maintain the integrity of the vacuum chamber. Although the octagon will not need to be taken out of the vacuum chamber on a regular basis, the shaft can be easily disconnected from the coupling to replace or exchange the alpha sources. The alpha sources used in this lab are summarized in Table 5.8. A front view of the alpha source holder placed inside of the vacuum chamber is displayed in Figure 5.10. The schematic of the evacuation system is displayed in Figure 5.11.

Table 5.8: Alpha Sources and Activities Used in Alpha Spectroscopy and Absorption in Air Lab

Alpha Source	Activity
Unknown #1 (^{238}Pu)	6.102 x 10^2 Bq (July 1978)
Unknown #2 (^{148}Gd)	5.432 x 10^2 Bq (Aug 1979)
Unknown #3 (^{239}Po)	2.88 x 10^2 Bq (Aug 1999)
Mixed Alpha Standard	specified on calibration sheet (see Appendix I)

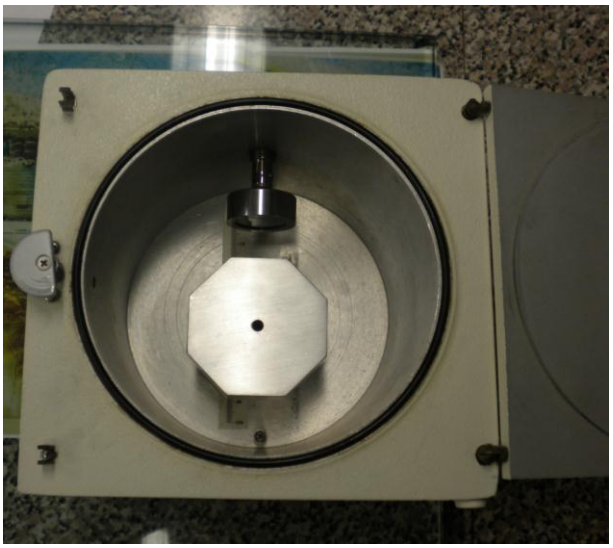

Figure 5.10: Alpha Source Holder in Vacuum Chamber

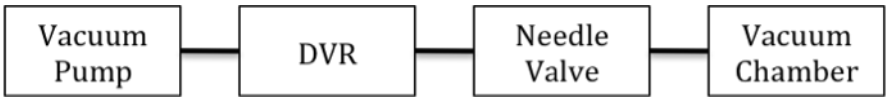

Figure 5.11: Schematic of Evacuation System for Alpha Spectroscopy and Absorption in Air

5.5 Determining the Efficacy of this Remote Lab

The efficacy of this lab must be determined in the context of its target audience. This lab course is intended to be completed over the course of an entire semester. It is an alternative to accelerated lab courses that are conducted in short summer sessions or during multiple weekends of a semester. For students at Clemson University, it is not intended to replace the current traditional hands-on lab. Therefore, the advantages and disadvantages of this lab course must be compared to an accelerated hands-on lab course

and/or a simulated course, not the semester-long traditional lab course already offered at Clemson University.

This thesis assembles the hardware, software, and procedures toward a remote lab, but, at the conclusion of this thesis, it is not completely developed. An in-depth exhaustive study regarding the efficacy of this remote lab may be completed at a later time and is not included in this work. Such a study is time intensive and requires many students to complete this course to yield a statistically significant number of samples.

5.6 Advantages of this Remote Lab

When compared to a summer session lab course, this remote lab enables students to conduct all the required labs over an entire semester-length course instead of distributing the work over a much shorter period of time. Students are able to spend an entire week preparing each lab report instead of a couple of days. When compared to a multiple-weekend course, students are able to evenly distribute their coursework instead of unevenly distributing the work over short periods of time and conducting multiple labs over the course of a single weekend. Students can prepare lab reports in the week following each lab while the information is still fresh in their memory instead of having to return to their respective schools and preparing multiple lab reports for labs over a period of weeks.

When compared to simulation-based labs, this lab provides a laboratory atmosphere that most closely duplicates that of a real laboratory atmosphere; the goal is for it to be the next best thing to being there. By offering students the opportunity to

actively engage in experimental setup and to observe and to interact with real components of each counting setup, students receive an appreciation of real laboratory systems that simulated experiments fail to deliver. Even simulated systems that have introduced mathematical fluctuations into the results fail to portray a real sense of the difficulties and inconsistencies when dealing with real systems and actual data (Vasquez, 2009). Anido, Llamas, and Fernandez (2001) concluded that if the practical skills learned by using the equipment are high, then remote labs are more effective than simulation-based labs.

5.7 Methods to Combat Disadvantages of this Remote Lab

Although experimentation is a major part of each lab, instrument setup and student interaction and collaboration are also vitally important. However, students in this remote lab will not be able to physically set up and troubleshoot the instrumental setup for each lab and interact directly with other students. To combat these disadvantages, measures will be taken to educate the students regarding the physical setup of each lab and provide student-to-student interaction.

A kit that contains cables with BNC and SHV connectors will be sent to students upon enrollment in the course. Instructions included in the kit will guide the students in observing and understanding the physical differences between BNC and high voltage connectors. Students will be required to physically connect the BNC and SHV connectors with the corresponding cables.

See additional suggestions in Section 6.2, “Future Work”.

CHAPTER SIX

CONCLUSION

6.1 Significance of Work

This on-line class meets the needs of the nuclear workforce by introducing university students nationwide to the field and possibly attracting these students to pursue a career in health physics or radiochemistry. The availability and ease of access that this non-traditional class offers students can open a significant educational opportunity that some may not have otherwise. The fundamentals covered in the class are applicable to all areas of nuclear science and technology. This will increase the base number of students who will be interested in taking the course. Students with various majors such as geochemistry, physics, and chemistry could choose to take the proposed course as a technical elective. Non-nuclear science majors can also benefit from the proposed course by bringing nuclear expertise to their respective fields.

With the weight of educating an increased number of students in nuclear engineering and science programs on their shoulders, universities can quickly and cost-effectively respond by approving this on-line course for transfer credit. This eases the strain that would be associated by having to develop a course of this nature. The time and costs associated with acquisition and maintenance of required facilities, instruments, and licensing will be alleviated for universities that endorse this remote laboratory.

6.2 Future Work

Future work for this project includes integrating computer-controlled instrumentation for each of the remaining eight labs, developing the interface and infrastructure to operate and support the remote-access lab, and performing rigorous system tests to ensure that the remote labs are free from detectable signs of error.

Integrating computer-controlled instrumentation for the remaining labs involves determining the set of instruments necessary for each lab and developing a seamless interface in LabVIEW™ that allows for control of all necessary instruments within one computer window for each laboratory experiment.

Developing an interface to facilitate the schedule regulation of the remote class involves the creation of a web-based module with which students can sign up for segments of time for each particular lab. This system will ensure that no two students or groups of students can access the same experiment simultaneously. Developing an infrastructure to support the remote class and allow students to access the individual labs involves converting each LabVIEW™ interface to a web-hosted interface at a dedicated IP address. The web-hosted interface will be a mirror image of the LabVIEW™ interface, but will reduce the bandwidth footprint required to conduct the lab remotely. Once students have received approval to conduct a certain experiment at a given time via the scheduling interface, instructions will be provided regarding accessing the web-hosted interface to conduct the actual lab.

Rigorous system tests will concentrate on testing the integrity of programming for each of the instruments. Tests may include high-count rate acquisitions for extended

periods of time, attempting to operate multiple instruments simultaneously, adjusting electronics parameters during an acquisition, and duplicating common operational errors.

Due to the hardware limitations of the workstation in the lab at Clemson University, the current mode of operation for this course is to set up one lab for a given week and progress through the semester one lab at a time in order of assignment. In the future, twelve workstations will be set up in the lab at Clemson University and each remote lab will have a dedicated workstation. At that time, all labs will be available simultaneously throughout both semesters and multiple summer sessions.

Procedures for Clemson University personnel will be developed to restart and test each piece of equipment in the case of power failure. It is possible that at other times, including power failure, the zero position for motor controllers will have to be reset. Procedures will be developed to determine the status of the motor controller, and if necessary, to rectify the situation. Procedures will also be developed to reinstate Internet connectivity to the host computer in the case of network failure.

The following tasks are specific tasks that will increase the automation of the labs and remove any need for aid from personnel at Clemson University to help remote students conduct the labs.

For the alpha spectroscopy lab, an automated solenoid valve will be inserted in the line between the DVR and the vacuum chamber. Computer-controlled instrumentation will be developed for the valve and a switch included on the interface that will allow students to close and open the valve. This will give the students complete control over the evacuation and purging of the system, respectively.

For the gamma-ray spectroscopy lab, the experimental setup will be altered to permanently include the 1.5″ x 1.5″ $LaBr_3$(Ce) detector and a corresponding URSA-II. This will alleviate the burden of a Clemson University lab assistant having to substitute the 1.5″ x 1.5″ $LaBr_3$(Ce) detector for the 2″ x 2″ NaI(Tl). detector during experimentation. The detectors will be placed opposite of each other and the interface will include a switch to choose the detector with which to acquire spectra. The switch will control the URSA-II with which the host computer communicates. All URSA-II controls and displays will be the same for both URSA-II's. However, a second rotary control knob will be developed for the 1.5″ x 1.5″ $LaBr_3$(Ce) since the position of the sources will be different with respect to the detector.

Two specific tasks to increase the pedagogical value of this course are yet to be developed. First, an electronic puzzle will be developed in a LabVIEW™ interface that will be presented to the students prior to the beginning of each lab. This puzzle will require the students to place each instrument in the correct order with the correct cables in the counting system. The students will not be able to proceed to experimentation until they have correctly positioned and connected each instrument. Second, a system will be developed and implemented that will enable individual students from multiple colleges and universities to interact with each other and discuss the concepts and procedures and collaborate in a group setting. This system may be based on the idea of an open Skype™ "channel".

Functionality testing of the computerized instrumentation will be conducted before the remote lab is offered to students. Testing will ensure that all technical aspects

of the remote lab were developed correctly and operate according to design. Some of this testing will be conducted by collaborators at Savannah River National Lab (SRNL) and South Carolina State University (SCSU), who will follow the written procedures and evaluate the lab accordingly. Testing will also be conducted in EE&S 610, an introductory course to environmental radiation protection, as portions of the remote lab will be implemented as demonstrations throughout the course.

The efficacy of this remote laboratory course should be determined by tests conducted by the Science and Engineering Education department at Clemson University. Testing will involve surveying and interviewing students who take this remote laboratory course, once it is completed, and students who take an accelerated laboratory course during a summer session or during multiple-weekend visits to a host university. The surveys and interviews will be conducted by professional educators and will determine students' overall retention and pedagogical aptitude of the course.

APPENDICES

Appendix A

URSA-II Programming Guide

Tips for Understanding URSA-II Programming Guide

- A notated block diagram of URSA-II programming is located on the CD accompanying this thesis. The file is called 'Block Diagram Example.vi'.
- Preliminary steps that are necessary prior to acquisition (found in sequence steps 0 & 1 of the primary sequence structure) are explained in detail in the notated block diagram. Instructions found in this guide expound on steps (found in sequence step 2 of the primary sequence structure) that are only labeled in the notated block diagram.
- Wires that "disappear" behind other structures or icons can easily be located and followed by clicking on the visible part of the wire. The entire wire, including the hidden portions, will be highlighted.
- Context Help is an invaluable tool for understanding the functions of certain icons and their role in the grand scheme of URSA-II programming. Context Help can be accessed by clicking on Help → Show Context Help or pressing Ctrl + H. When the mouse hovers over an icon, Context Help displays a summary of the icon's function and a detailed diagram of its inputs and outputs.
- A hexadecimal-to-ASCII conversion table can be found at www.asciitable.com.
- A complete two-value hexadecimal-to-decimal conversion table can be found at www.ascii.cl/conversion.htm.

Introduction: Format of URSA-II Data

During acquisition, data is sent to the serial port in 3-byte packets, separated by a forward slash. These packets are in the form

/FF/ab/cd

where each byte contains two hexadecimal values that combine to form one hexadecimal number. *FF* represents a decimal number of *255* (*F* converts to a decimal value of *15*; 15*16+15*1=255) and simply functions to identify the beginning of the 3-byte packet. The second value of the second byte and both values of the third byte are combined to form a hexadecimal number, ordered *bcd*. When converted to decimal format, this number represents the channel number of the detected pulse.

The first value of the second byte, *a*, represents the number by which to increment the associated channel number. The number of pulses that are detected during "dead time" are recorded on a hardware counter such that *a*=initial pulse + number of pulses registered on the hardware counter.

Overview of LabVIEW™ Acquisition of URSA-II Data

During live acquisition, URSA-II data continuously streams to a buffer. When LabVIEW™ queries the buffer, all data in the buffer is transferred to LabVIEW™ in 1-D string format that looks similar to:

FF/14/A5/FF/22/5E/FF/17/4G…

Although each byte consists of two hexadecimal values, LabVIEW™ interprets each byte of the 1-D string as one hexadecimal number that cannot be separated into its two individual values. (For these instructions, a number is made up of individual values; i.e. the number *24* is made up of two values: *2* and *4*.) And although URSA-II streams pure hexadecimal numbers to the serial port, LabVIEW™ interprets and presents hexadecimal numbers between 20 and 7F as ASCII characters. For example, a 3-byte packet streamed from URSA-II as */FF/13/7E* would be presented by LabVIEW™ as */FF/13/~* because the hexadecimal number *7E* corresponds to the ASCII character ~. Note that there is no place on the interface where the streamed data is presented by LabVIEW™. This information is only relevant for troubleshooting purposes when the streamed data is explicitly called for.

In order to extract the individual values of each byte in the 1-D string to process the information, the 1-D string must be converted to 1-D array of decimal values and subsequently converted into 1-D *string array* that contains hexadecimal values. The net effect of this process is conversion of the data from 1-D string to 1-D *string array*. The conversion into 1-D array of decimal values both facilitates the 1-D string to 1-D *string array* conversion and provides a format with which to conduct pre-data processing steps. Only after the bytes have been converted back into hexadecimal format (*string array*) can the individual values of each byte be extracted and processed to generate the necessary energy and count information. The data must be in *string array* to be processed.

Ideally, every 1-D string would begin with the identifier, */FF*, and contain only contiguous 3-byte packets of data. However, because URSA-II streams each individual byte and not whole packets, split packets are not uncommon. (Technically, the bytes are combined into 3-byte packets only by programming technique to process necessary data.) Split packets occur when LabVIEW™ queries the buffer before URSA-II has transferred all 3 bytes of any given packet. This results in only a partial packet transferring to LabVIEW™ in the 1-D string and the remaining byte(s) of the partial packet streaming to the buffer for the next query. Therefore, instead of ending with */FF/ab/cd*, a 1-D string could end */FF/ab* or just */FF*. This poses two problems. First, count and/or energy information are/is lost and subsequently, the counting data and spectrum become inherently erroneous. Second, the remaining byte(s) of the packet is(are) begin(s) the next 1-D string, such that the next line begins with */cd* or *ab/cd*. Also, unrelated to query-generated split packets, software-modified packets occur when an individual byte is occasionally, but rarely, appended or removed from a contiguous 3-byte packet. These erroneous packets taken on the form */FF/ab/cd/ef*, */FF/ab*,or */FF/cd*. Information lost in query-generated split packets can be recovered. Information hidden or deleted in software-modified packets cannot be recovered.

Condition 0, Condition 1, and Condition 2

A string may contain no split packets, a split packet at either the beginning or end of the string, or a split packet at both ends of the string. Assume the current string to be processed is *string n*. A local variable, called *Condition*, was created that holds a value—

either *0, 1,* or *2*—and indicates certain conditions—*Condition 0*, Condition 1, or *Condition 2*, respectively—that characterizes the end of *string n*. By definition, the condition characterizes only the end of *string n*; however, by doing so, it inherently characterizes the beginning of *string n+1*. *Condition 0* indicates that the end of *string n* is a whole 3-byte packet and inherently indicates that the beginning of *string n+1* is a whole 3-byte packet; *Condition 1* indicates that the end of *string n* is the first byte of a 3-byte packet and inherently indicates that the beginning of *string n+1* is the last 2 bytes that complete the 3-byte packet begun at the end of *string n*; *Condition 2* indicates that the end of *string n* is the first two bytes of a 3-byte packet and inherently indicates that the beginning of *string n+1* is the last byte that completes the 3-byte packet begun at the end of *string n*.

Pre-Extraction Step 1: Reading the Condition of *string n-1*

Assuming that *string n* is not the first string of data for a given acquisition, some condition was true about *string n-1* and the appropriate value was written to the local variable. (The process of determining the condition of any given string and writing the appropriate value to the local variable is explained below.) Before the data from *string n* is analyzed in any way, LabVIEW™ automatically reads the value of the local variable that reflects the condition of *string n-1* and places that value in a short-term RAM-type of memory.

Pre-Extraction Step 2: Determining the Condition of *string n*

Identifying the condition of *string n* occurs once the data has been converted from a 1-D string to a 1-D array of decimal values, but before it has been converted to 1-D array of string. Assume that *string n* is converted to *decimal array n* where byte *x* of *string n* becomes *element x* of *decimal array n*. This step determines which part of a 3-byte packet ends *string n* and accordingly alters the end of *decimal array n*. Three possible conditions exist regarding the end of *string n*: a complete 3-byte packet ended *string n*, the last byte of a 3-byte packet ended *string n*, or the last 2 bytes of a 3-byte packet ended *string n*. To determine which condition is true regarding *string n* is a multi-step process.

First, the number of elements in *decimal array n* is determined. Then it is tested if the second-to-last or last element of the *decimal array n* contains a value of *255*. (The second-to-last and last elements of any given array are positions *n-2* and *n-1*, respectively, where *n* is number of elements in the array because position *0* always contains the first value of the array.) If the second-to-last or last element of *decimal array n* array contains *255*, a packet has been split between the end of *string n* and *string n+1*. If the second-to-last or last element of the *decimal array n* does not contain *255*, *Condition 0* is true. If *Condition 0* is true, the last element of *decimal array n* is not altered and *decimal array n* is converted to *string array n*. Simultaneously, a value of *0* is written to the local variable. Programming for this case is displayed in Figure A.1(a).

There are two possibilities why the last element of *decimal array n* might contain *255*. First, if the channel number of the processed pulse can be reduced to $k \times 256 + 255$

where *k* is an integer, then */FF* would take the place of */cd* in the standard format of 3-byte packets. If this is the case, *Condition 0* is true because *string n* ended with a whole 3-byte packet. Programming for this case is shown in Figure A.1(b). Second, the *255* may be the identifier for the two bytes that will begin *string n+1* and *Condition 1* is true. To determine if *Condition 0* or *Condition 1* holds true when the last element of *decimal array n* contains *255*, it is determined if elements in positions *n-3* and *n-6* of *decimal array n* contain *255*. If these elements contain *255*, then the end of *string n* would be in the following format: $\overset{n-6}{FF}/\overset{n-5}{ab}/\overset{n-4}{cd}/\overset{n-3}{FF}/\overset{n-2}{ab}/\overset{n-1}{FF}$. If this is true, *Condition 0* holds true. If *Condition 0* is true, the end of *decimal array n* is not altered and is converted to *string array n* and a value of *0* is written to the local variable. Otherwise, *Condition 1* holds true. If *Condition 1* is true, *decimal sub-array n* is created that includes all but the last element (*/FF*) of *decimal array n* and is converted to *string array n*. Simultaneously, a value of *1* is written to the local variable. Programming for this case is displayed in Figure A.1(c).

Condition 2 holds true if *Condition 0* and *Condition 1* do not hold true. If *Condition 2* is true, *decimal sub-array n* is created from *decimal array n* that includes all but the last two dimensions and is converted to *string array n* and a value of *2* is written to the local variable. The second-to-last element of *decimal array n* is assumed to contain *255* and is deleted. Programming for this case is displayed in Figure A.1(d). The contents of the last element of *decimal array n* are retained with a shift register, and along with *255*, will be appended to the beginning of *string array n+1*. The appending process is explained below.

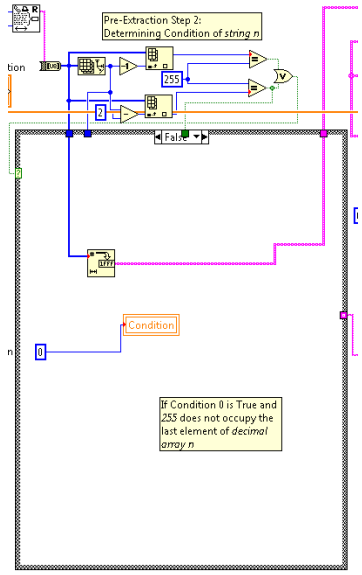

(a)

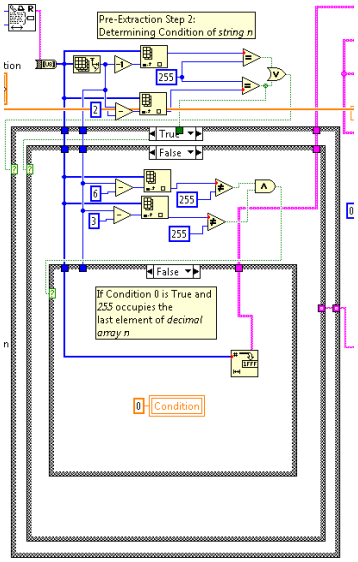

(b)

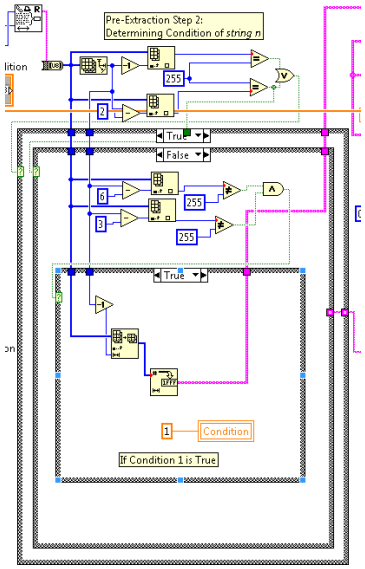

(c)

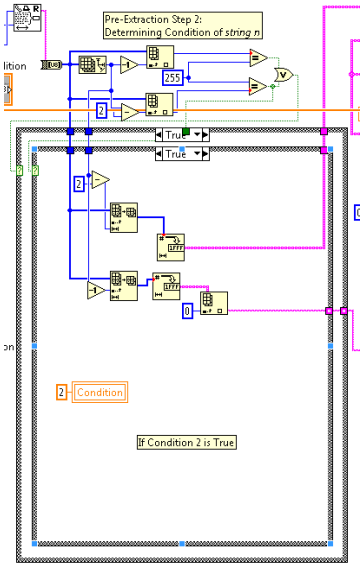

(d)

Figure A.1: Programming for Pre-Extraction Step 2. (a) If *Condition 0* when *255* does not occupy the last element of *decimal array n*. (b) If *Condition 0* when *255* occupies the last element of *decimal array n*. (c) If *Condition 1*. (d) If *Condition 2*.

Pre-Extraction Step 3: Recombining Split Packets

Recombination of split packets occurs after *decimal array n* has been converted to *string array n*. This step determines which part of a 3-byte packet begins *string n* and accordingly alters the beginning of *string array n*. LabVIEW™ accesses the value that was placed in short-term RAM memory that reflects the condition of *string n-1*. If the condition of *string n-1* was *0* (i.e. if the value placed in short-term memory before any analysis of *string n* was *0*), then the beginning of *string array n* is not modified because *string n-1* ended with a whole 3-byte packet, which implies that *string n* began with a whole 3-byte packet. Programming for this case is displayed in Figure A.2(a). If the condition of *string n-1* was *1* (i.e. if the value placed in short-term memory before any analysis of *string n* was *1*), then */FF* is appended to the beginning of *string array n* by inserting */FF* before the first element of *string array n*. Programming for this case is displayed in Figure A.2(b). If the condition of *string n-1* was *2* (i.e. if the value placed in short-term memory before any analysis of *string n* was *2*), then */FF* and the byte that was retained with the shift register from *string n-1* is appended to the beginning of *string array n*. The byte from *string n-1* that is appended to *string array n is* actually taken from the content of a local variable, *Condition 2 Byte*, which is populated with the value that was retained with the shift register from *string n-1*. Programming for this case is displayed in Figure A.2(c).

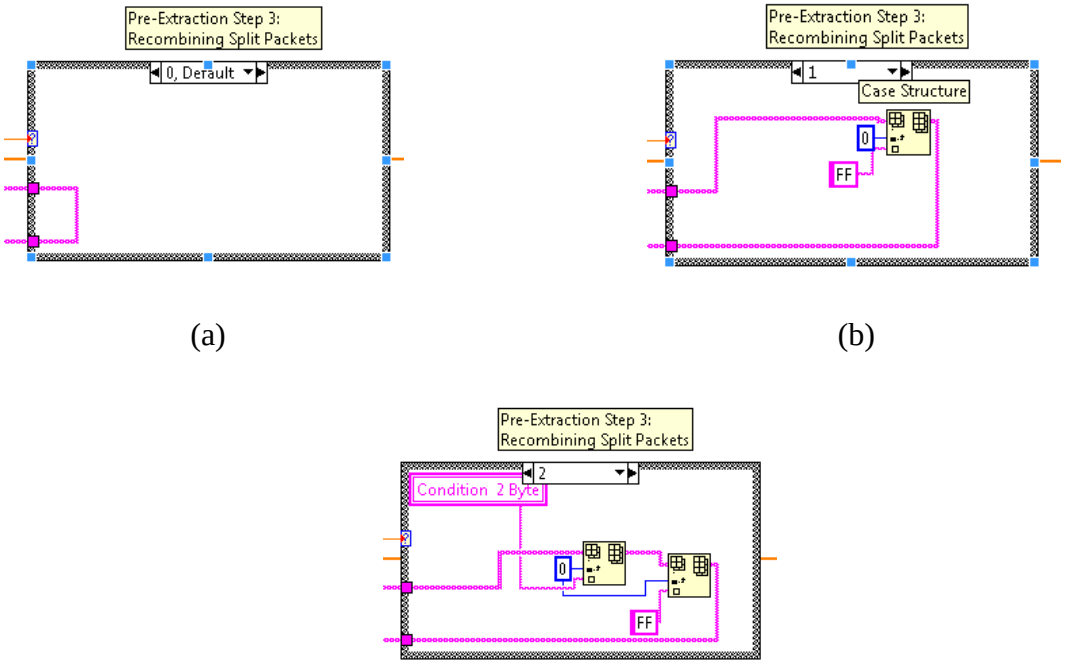

Figure A.2: Programming for Pre-Extraction Step 3. (a) If *string n-1* was *Condition 0*. (b) If *string n-1* was *Condition 1*. (c) If *string n-1* was *Condition 2*.

Extraction Step 1: Searching for a Whole 3-Byte Packet

Once the end of *decimal array n* has been modified according to the condition of *string n* and the beginning of *string array n* has been modified according to the condition of *string n-1*, the process to extract data from *string array n* is conducted. First, the number of elements of *string array n* is determined. This value is divided by 3 to yield the number of packets to be processed. *String array n* is transferred into a For loop that iterates according to the number of packets to be processed. The function of this For loop is to find all 3-byte packets and extract all count and energy information from each packet. S*tring array n* is converted to *decimal array n*. For the first iteration, a search of

decimal array n is conducted to find the first element that contains *255* beginning with *element 0.* Assume the first element that contains *255* is *element y.* (This should be *element 0*). Then, the value of *element y+3* is determined, which should also be *255.* It is assumed that if *element y* and *element y+3* both contain 255, then *element y, element y+1,* and *element y+2* comprise a 3-byte packet. If this is the case, then the contents of *element y+1* and *element y+2* are processed according to the format described previously. Programming for this case is displayed in Figure A.3(a). Specifics regarding the method of processing are described later.

If *element y+3* does not contain *255,* then it is assumed that the packet beginning with *element y* is not a 3-byte packet. A non-3-byte packet is erroneous and cannot be processed. In order to find the first 3-byte packet, iterative searches of *decimal array n* are conducted until *element y+i* and *element y+i+3* both contain *255,* where *i* represents the number of iterations. Each of the iterative searches begin with *element y+i.* Programming for this case is displayed in Figure A.3(b). Once a 3-byte packet is found, *y+i+1* and *y+i+2* are processed according to the format described above.

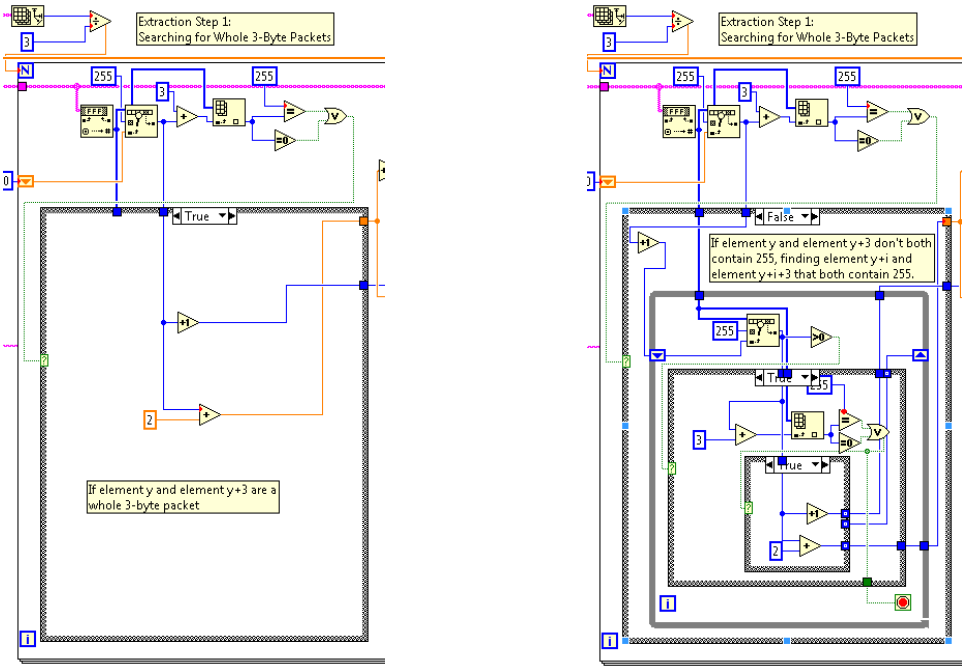

(a) (b)

Figure A.3: Programming for Extraction Step 1. (a) If *element y* and *element y+3* both contain *255*. (b) If *element y* and *element y+3* don't both contain *255*, searching for *element y+i* and *element y+i+3* that both contain *255*.

Extraction Step 2: Extracting Count and Energy Information

It is tested if *element y+1* (or *element y+i+1* if necessary) contains 1 or 2 values. If it contains only 1 value, then the value represents the number of counts with which to increment the channel number and indicates that *0* is the first value of the hexadecimal number that represents the channel number. If it contains 2 values, the first and second values are separated. The first value will be the value with which to increment the channel number. The second value, still a hexadecimal value, is converted to a decimal value with a string to number converting function. If the hexadecimal value is between *1* and *9*, the converting function converts the hexadecimal value to the corresponding

decimal value. However, if the hexadecimal value is between *A-F*, the converting function returns *0* because the string to number converting function only recognizes decimal values. If the function returns *0*, the hexadecimal value that falls between *A-F* is manually converted to *10-15*, respectively. Because this value is the first of a 3-digit hexadecimal value, this decimal value is multiplied by *256*. Similarly, it is tested if *element y+2* (or *element y+i+2* if necessary) contains 1 or 2 values. If it contains only one value, that value is the second byte of the third byte and the first value of the third byte is assumed to be *0*. If it contains two values, the first value of the third byte is translated from hexadecimal format to decimal format and multiplied by *16*. The second value of the third byte is similarly translated and multiplied by *1*. These three values are added to together to yield the channel number of the pulse. The count and energy information are temporarily stored in *element 0* of *count array n* and *element 0* of *energy array n*, respectively. *Count array n* and *energy array n* are products of the For loop and store count and energy information until the For loop has extracted all the information from *string n*. The programming for Extraction Step 2 is displayed in Figure A.4.

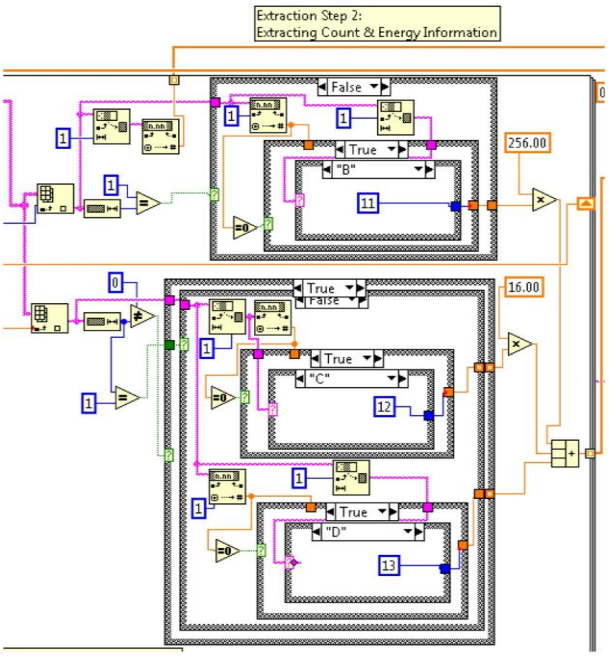

Figure A.4: Programming for Extraction Step 2

Once the information from the first whole 3-byte packet of *string array n* has been extracted, the next 3-byte packet is found by searching *decimal array n* for the first element that contains *255*, beginning with *element y+3* (or *element y+i+3* if necessary). Assume that this element that contains *255* is the new *element y*. Following the process described above, the next whole 3-byte packet is found when the new *element y* and the new *element y+3* or the new *element y+i* and the new *element y+i+3* (if new *element y* and new *element y+3* don't both contain *255*) both contain *255*. Information from the second and third bytes of the packet is extracted using the identical method for extracting data as described above. Count and energy information are stored in *element 1* of *count array n* and *element 1* of *energy array n*.

Iterations of Extraction Steps 1 & 2

This entire process of searching for a 3-byte packet and extracting the information of that packet is repeated for the number of packets in *string array n*. The count and energy information from each packet are stored in corresponding elements of *count array n* and *energy array n*, respectively, such that *element k* of *count array n* corresponds to *element k* of *energy array n*. The number of elements in these arrays is determined by the number of whole packets found in *string array n*.

Spectrum Generation

These two arrays are transferred into another For loop. Also transferred into this For loop is *master array*. For each acquisition, a *master array* with 4096 elements, each containing values of *0*, is created, where each element represents a channel number. This For loop iterates according to the number of elements in *energy array n* using a property called Auto-indexing, which allows the For loop to process the elements of *energy array n* one element at a time. The function of this For loop is, for each iteration, to increment the appropriate element (channel number) of *master array* by the appropriate number of counts. For the k^{th} iteration of this For loop, the value of the k^{th} element of *energy array n* is incremented by the value of the k^{th} element of *count array n* (i.e. if the k^{th} element of *energy array n* contains a value of *557* and the k^{th} element of *count array n* contains a value of *2*, then *element 557* of *master array* will be incremented by a value of *2*). Once all channel numbers have been incremented by the appropriate value, *master array* is retained with a shift register and the entire process beginning with querying the buffer is

repeated until the acquisition is stopped. The programming for Spectrum Generation is displayed in Figure A.5.

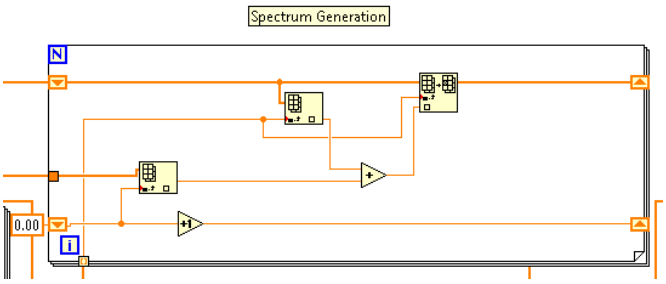

Figure A.5: Programming for Spectrum Generation

High Voltage

High Voltage is written to URSA-II in the format *Vxy* where *x* and *y* are ASCII characters in string format. These ASCII characters are determined by the following method. The desired voltage is multiplied by 65532 and divided by 2000. This decimal value is rounded to the nearest integer, which is then converted to a 4-value hexadecimal number, *h*, in string format. The first two values of *h* are extracted and converted to a decimal number, which is converted ASCII characters in string format, which is *x*. The last two values of *h* are extracted and converted to a decimal number, which is converted to ASCII characters in string format, which is *y*. The command is comprised of a string containing the character *V* that is concatenated with the two strings containing the ASCII characters in the order *Vxy*. The programming for High Voltage is displayed in Figure A.6.

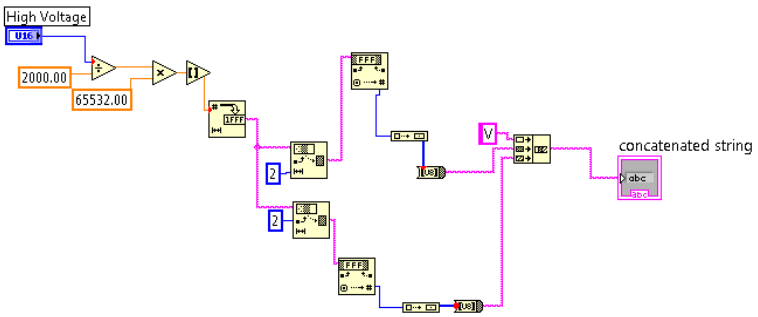

Figure A.6: Programming for High Voltage

Threshold

Threshold is written to URSA-II in the format *Txyz* where *x*, *y*, and *z* are ASCII characters in string format. *x*, *y*, and *z* are determined by the following method. The desired threshold value is multiplied by two and converted to a 12-number Boolean number, *tb*, which stands for threshold Boolean. A value called Offset is concurrently written to URSA-II with the Threshold. The Offset value is equal to the desired threshold, unless the desired threshold is less than 180. The offset value is always greater than 180. The offset value is also converted to a 12-character Boolean number, *ob*, which stands for offset Boolean. From these two 12-character Boolean numbers, 3 8-character Boolean numbers are created. The first of these three Boolean numbers consists of the first 8 values of *tb*. This Boolean number is converted to a decimal number, which is then converted to ASCII characters in string format, which is *x*. The second of the three Boolean numbers consists of the last 4 values of *tb* and the first 4 values of *ob*. Similarly, this Boolean number is ultimately converted to ASCII characters in string format, which is *y*. The third of the three Boolean numbers consists of the last 8 values of *ob*, and is

ultimately converted to ASCII characters in string format. The command is comprised of a string containing the character *T* that is concatenated with the three strings containing the ASCII characters in the order *Txyz*.

Assume *tb* was written *tb1 tb2 tb3 tb4 tb5 tb6 tb7 tb8 tb9 tb10 tb11 tb12* and *ob* was written *ob1 ob2 ob3 ob4 ob5 ob6 ob7 ob8 ob9 ob10 ob11 ob12*, where each value is Boolean. Then the first of the three Boolean numbers is *tb1 tb2 tb3 tb4 tb5 tb6 tb7 tb8*; the second is *tb9 tb10 tb11 tb12 ob1 ob2 ob3 ob4*; the third is *ob5 ob6 ob7 ob8 ob9 ob10 ob11 ob12*. Programming for Threshold is displayed in Figure A.7.

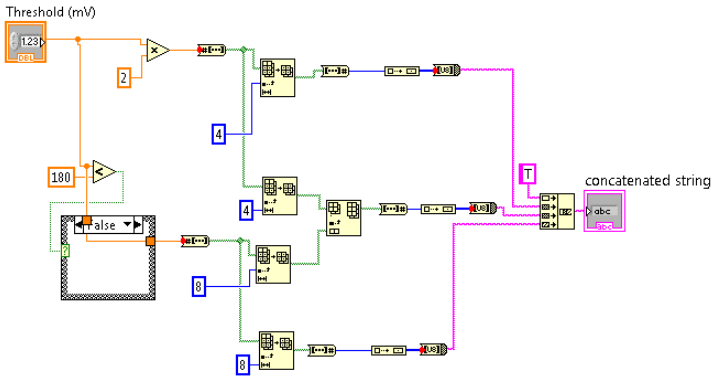

Figure A.7: Programming for Threshold

Appendix B

Motor Controller Programming Guide

Tips for Understanding Motor Controller Programming Guide

- A notated block diagram of motor controller programming is located on the CD accompanying this thesis. The file is called 'Block Diagram Example.vi'. The notes are written in Case 1 of the motor controller Case structure.
- Preliminary steps that are necessary prior to using the motor controllers (found in sequence steps 0 & 1 of the primary sequence structure) are explained in detail in the notated block diagram. Instructions included in this guide expound on steps (sequence step 2 of the primary sequence structure) that are only labeled in the block diagram.
- Wires that "disappear" behind other structures or icons can easily be located and followed by clicking on the visible part of the wire. The entire wire, including the hidden portions, will be highlighted.
- Context Help is an invaluable tool for understanding the functions of certain icons and their role in the grand scheme of URSA-II programming. Context Help can be accessed by clicking on Help → Show Context Help or pressing Ctrl + H. When the mouse hovers over an icon, Context Help displays a summary of the icon's function and a detailed diagram of its inputs and outputs.
- Motor position 0 is determined by the position of the motor when the motor controller is turned on.

Rotary Table Specifics

- The speed of rotary table is set to 1,500 steps/sec.
- There are 14,400 steps in one complete rotation of the rotary table.
- There are 1,800 steps and 900 steps between positions for a table with 8 positions and 16 positions, respectively.

Rotating Shaft Specifics

- Speed of rotary table is set to 40 step/sec.
- There are 400 steps in one complete rotation of the rotating shaft.
- There are 50 steps between each position.

BiSlide™ Specifics

- The speed of the BiSlide™ is set to 500 step/sec. If the speed is set any higher, the motor will whine and the carriage will not move.
- There are 182,800 steps on the BiSlide™.
- There are 12,192 steps between each position.

Fundamental Concept

The fundamental concept is that the current position of the motor-driven assembly is represented by some motor position and the desired position of the motor-driven assembly is also represented by some motor position. The difference between those two motor positions is the number of steps through which the motor needs to advance to place the motor-driven assembly at the desired position.

For the BiSlide™, this is relatively simple because there are finite bounds for the movement of the BiSlide™. Therefore, every position on the BiSlide™ is assigned one—and only one—motor position. For example, assuming the zero position of the BiSlide™ is correctly set at the 1-ft. position, the 1-ft. position is only assigned a motor position of 0, the 2-ft. position is only assigned a motor position of 12,192, etc…

This process is much more difficult for the rotary table and rotating shaft because there are not finite bounds on their motion. Theoretically, they could rotate to negative and positive infinity. If ^{137}Cs is positioned in front of the detector at motor position 0, it will also be in front of the detector at motor position 14,400, motor position 28,800, etc… and motor position -14,400, motor position -28,800, etc… There is no absolute reference motor position for the rotary table or the rotating shaft. Therefore, a system is developed to establish a relative reference motor position in order to non-sequentially advance the motor through the smallest angle necessary to place the desired rotary table position in front of the detector.

The procedures given below are for an 8-position rotary table setup currently at a positive motor position. The procedures can easily be modified for negative motor position, for the rotating shaft, and for the BiSlide™.

Step 1: Obtaining the Correct Format of Motor Position

When the position of the motor controller is first called for, it returns a string of 10 characters in the format ^+xxxxxxx/r, where *xxxxxxx* represents some decimal value that is the motor position and */r* simply represents the ‘Enter’ command. However, for

LabVIEW™ to interpret the string correctly, the string must contain only 9 characters. This step functions to eliminate the first character of the 10-character string so that LabVIEW™ can process the data accordingly.

Step 2: Determining Sign of Motor Position

It is determined if the current motor position is positive or negative by testing if the motor position is greater than or equal to zero.

Step 3: Determining the Relative Reference Motor Position

It is imperative to understand that rotary table position and motor position do not refer to the same thing. The rotary table position refers to one of the eight positions on the rotary table. The motor position refers to position of the motor itself, represented by positive or negative steps. The relative reference motor position is the motor position that would place position 0 in front of the detector while requiring the rotary table to travel through the smallest angle possible from the current position. This motor position is represented by *k*14,400* where *k* represents the nearest whole number of rotations from motor position 0 to the current motor position. For example, if the rotary table has rotated 7.75 times, *k=8*; if the rotary table has rotated 3.125 times, *k=3*. The method to determine the value of *k* is described below.

Once it has been determined that the motor position is positive, the motor position is divided by 14,400. This yields a decimal value, *y.yyy*, that represents the number of rotations (not necessarily an integer) that the current motor position is from motor

position 0. *y.yyy* is then rounded to the nearest integer. It is important to note that the function that rounds a decimal value to the nearest integer in LabVIEW™ rounds *y.5* to the nearest even integer, regardless whether the nearest even integer is *y* or *y+1*. For example, 1.5 and 2.5 both round to 2 and 3.5 and 4.5 both round to 4. It is necessary for programming purposes that *y.5* ultimately be rounded round either up or down. It was arbitrarily decided by the programmer that programming would be developed to force *y.5* to always round down to *y*. So, after LabVIEW™ rounds each decimal value to the nearest integer (*y.5* may still round up or down), it is tested if the difference between *y.yyy* and the rounded value is +0.5. If the difference is equal to +0.5, it indicates that *y.5* was rounded up to *y+1*. Programming then decrements the rounded value by 1, effectively forcing *y.5* to round down to *y*. This rounded value is *k*. For example, if the motor position divided by 14,400 equaled 5.5, LabVIEW™ would round 5.5 up to 6.0. Since it is true that *6.0 – 5.5 = 0.5*, programming would decrement 6.0 by 1, yielding 5.0. The net effect would be that 5.5 would round down to 5.0.

k is then multiplied by 14,400, yielding the relative reference motor position. This is the relative reference motor position because if the rotary table rotated *k* times starting with rotary table position 0 at motor position 0, rotary table position 0 would again be in front of the detector at *k*14,400*.

Step 4: Determining the Distance Between Current and Desired Rotary Table Positions

Each rotary table position is represented by a reference step value, *n*. *n* represents the number of positive steps between rotary table position 0 and each of the other rotary table positions. The reference step values are given in Table B.1.

Table B.1: Rotary Table Positions and Corresponding Reference Step Values

Position	Reference Step Value (*n*)
0	0
1	1800
2	3600
3	5400
4	7200
5	9000
6	10800
7	12600

The motor position that will place the desired rotary table position in front of the detector is *k*14,400 + n*. The vector quantity that represents the distance (number of steps) and direction (forwards or backwards) between the current rotary table position and the desired rotary table position is *k*14,400 + n – mp* = **d**, where *mp* represents the current motor position. However, although ***d*** will place the desired rotary table position in front of the detector, it may not be the shortest distance between the current and desired rotary table positions. It is tested if ***d*** > +7200. If ***d*** > 7200, it indicates that the motor will advance through more than half of a full rotation. If this is the case, ***d*** *– 7200* yields the shortest number of steps between the current and desired rotary table positions.

Step 5: Writing the Command to Rotate

The command to rotate the motor is written by concatenating the string *F,C,I1M* and the string *%d,R*, where *%d* represents the value of ***d***. If the concatenated string is equivalent to *F,C,I1M0,R* then the rotary table is already at the desired position and the table does not rotate.

Programming for the Motor Controller is displayed in Figure B.1.

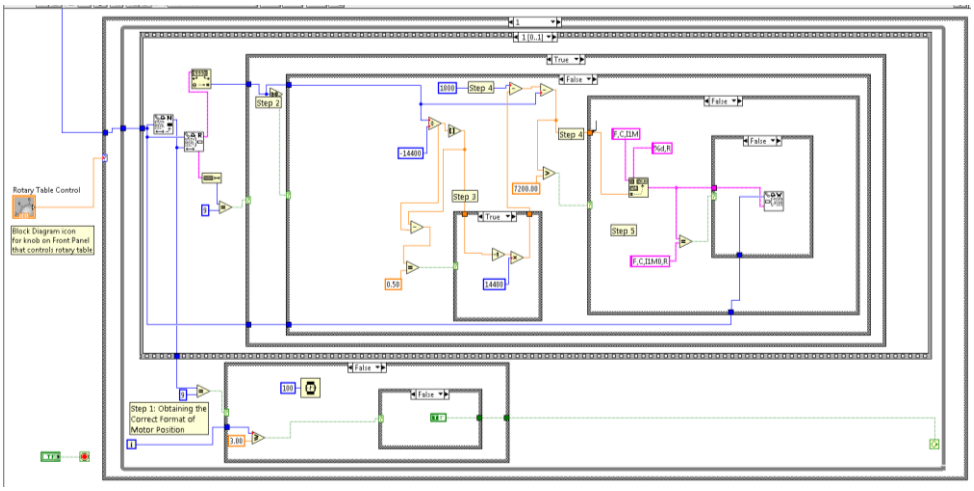

Figure B.1: Programming for the Motor Controller

Appendix C

Instructions for Frequently Used Instrumentation

Inclusion of Appendix C demonstrates, in part, the completion of Objective #4.

Many of the instruments used in this remote laboratory course are used repeatedly in multiple labs. The instructions presented in Appendix C document the frequently-used instruments and are provided to the students at the beginning of the laboratory course as a reference document for each of the labs. These instructions are designed to help the students become familiar with the common instruments, to explain the concepts behind each of the controls and the implications of adjusting each control, and to advise them regarding the proper use of the controls.

Basic Instructions for using LabVIEW™

LabVIEW™ stands for Laboratory Virtual Instrumentation Engineering Workshop and is developed by National Instruments (www.ni.com/labview). LabVIEW is a platform on which computer-controlled instrumentation is developed to remotely control physical instruments. The set of computer-operated controls that operates one or more physical instruments at a time is called the web-based computer instrument.

Each web-based computer interface used for each experiment is different because each experiment that is conducted requires a different set of instruments. Each interface provides the selection all necessary parameters, the control of experimental setups, and the display of graphical, numerical, and visual feedback in real time.

In order to operate the controls on the interface, the interface must be activated. Upon accessing the appropriate interface for an experiment, press the right arrow located near the top left of the screen beneath the Edit menu. When the interface is not activated, the arrow is hollow, displayed in Figure C.1(a). When the interface is activated, the arrow turns solid black, displayed in Figure C.1(b).

(a) (b)

Figure C.1: Button to Activate LabVIEW™ Interface (a) Before interface is activated (b) After interface is activated

URSA-II (Nuclear Electronics) Controls

*To set any of the desired parameters for the URSA-II, the respective buttons to set each parameter must be pressed after the desired parameter is selected with selection tool (drop-down menu, knob, or slide). *Settings must be selected one at a time and may not be changed during acquisition.*

The number that accompanies each of the descriptions in this section and the next two sections (SCA Controls, MCA Controls & Displays) corresponds to the numbered features of Figure C.2.

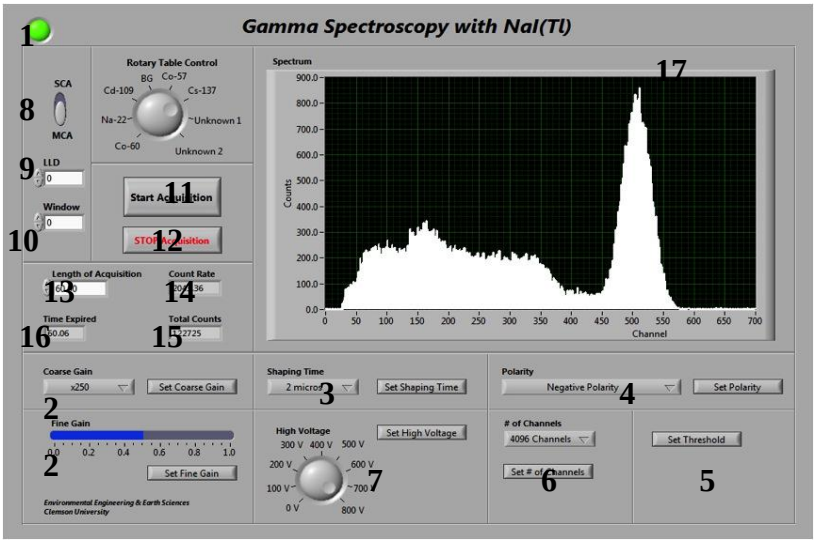

Figure C.2: URSA-II, SCA, & MCA Controls and Displays

- The circular indicator (1) at the top left of each interface indicates whether URSA-II is operating correctly or not. When the interface is initially opened, the indicator is red. However, if URSA-II is operating correctly, the indicator will turn to green almost immediately after the arrow button is pressed at the top left of the LabVIEW™ screen. If it remains red, call Dr. DeVol or the appropriate Clemson personnel.

- **Coarse Gain/Fine Gain** (2) controls the coarse gain and fine gain of the amplifier, respectively. $Gain_{TOT} = Gain_{coarse} \times Gain_{fine}$. This quantity is unitless.

The following coarse gain selections can be made: *x2, x4, x15, x35, x125, x250.* Fine gain can be adjusted in increments of 0.01 between 0.0 and 1.0.

- **Shaping Time** (3) controls the shaping time of the amplifier and determines the integration time of the current pulse. Units are 10^{-6} seconds. The following shaping time selections can be made: *0.25μs, 0.5μs, 1μs, 2μs, 3μs, 4μs, 6μs, 8μs, 10μs*.

- **Polarity** (4) controls the orientation of the pulse that is generated by the amplifier.

- **Threshold** (5) sets the lower limit of energies to be analyzed by the MCA. Units are 10^{-3} volts. Threshold can be set in increments of 1 mV between 0 mV and 2047 mV.

- **# of Channels** (6) sets the total number of channels to be used for spectroscopy. The following number of channels selections can be made: *256, 512, 1024, 2048, 4096*.

- **High Voltage** (7) controls the voltage supplied to the detector. Units are in volts. Because URSA-II always requires 5 seconds to ramp the voltage (regardless of the voltage differential), wait for 5 seconds after pressing *Set High Voltage* to set any other parameters or to acquire a spectrum. High Voltage can be adjusted in increments of 1 volt and the range of operating voltages is determined by the detector type. *Follow instructions before setting high voltage. DO NOT set high voltage to values higher than instructed.

SCA Controls

- **SCA/MCA Switch** (8) determines whether the acquisition is conducted in SCA Mode or MCA Mode.

- **LLD** (9) sets the lower level discriminator (LLD) of the SCA. Units are Volts.

- **Window** (10) sets the energy range (ΔE) between LLD and ULD. Units are Volts. $ULD = LLD + Window$.

MCA Controls & Displays

- **Start Acquisition** (11) begins active acquisition by the detector. A value greater than 0 must be entered in *Length of Acquisition* to acquire a spectrum. (If URSA-II is working properly, a horizontal line in the middle of the graph indicates that a

value greater than 0 has not been entered in *Length of Acquisition*.) The previous spectrum will automatically be cleared when beginning a new acquisition.

- **STOP Acquisition** (12) stops current acquisition before length of acquisition has been reached. ***DO NOT stop an active acquisition by pressing the red octagon 'stop sign' at the top of the LabVIEW window. Improperly stopping an acquisition causes URSA-II to generate erroneous data, which requires the re-acquisition of the erroneous spectrum.

- **Length of Acquisition** (13) controls desired length of real time for spectrum acquisition and can be adjusted in increments of 1 second. Units are seconds. Acquisition will stop when *Time Expired* is equivalent to *Length of Acquisition*.

- **Count Rate** (14) displays total number of counts divided by real time and updates 20 times per second. Units are counts per second.

- **Total Counts** (15) displays total number of counts of current acquisition and updates 10 times every second.

- **Time Expired** (16) displays amount of time elapsed during current acquisition and updates 20 times per second. Units are seconds.

- **Spectrum** (17) is a differential pulse height spectrum and displays the acquired data after it has been analyzed by the MCA. The spectrum updates 20 times per second in real-time. Number of counts is plotted on the ordinate and channel number is plotted on the abscissa. To zoom to a particular feature on the graph, determine the desired upper-bound and lower-bound channel numbers values of the feature. Move the cursor over the upper-most channel number currently displayed on the spectrum (on the *x*-axis). Once the cursor becomes a text selection tool, double-click on the value; the text should now have a black background. Enter the desired upper-bound value and press *Enter* on the keyboard. The upper-bound value should now be the upper-most channel displayed on the spectrum. Repeat with the desired lower-bound value.

MCA Procedures

- If instructed to collect an acquisition for a set amount of time, enter the desired time in *Length of Acquisition* and press *Start Acquisition*.

- If it is necessary to stop an active acquisition prior to the completion of the time entered in *Length of Acquisition*, press *Stop Acquisition.*

Digital Oscilloscope Controls & Display
The number that accompanies each of the descriptions in this section corresponds to the numbered features of Figure C.3.

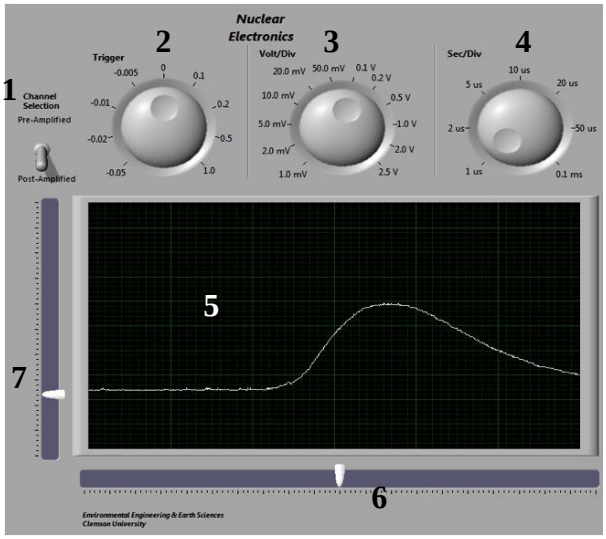

Figure C.3: Digital Oscilloscope Controls & Display

- **Channel Selection** (1) controls which of the two oscilloscope channel inputs is displayed. The pre-amplified signal is displayed when the switch is facing upwards towards *Pre-Amplified* and a post-amplified signal is displayed when the switch is facing downwards towards *Post-Amplified.*

- **Trigger** (2) controls the trigger level when either the pre-amp or post-amp signal is displayed and can be used during active display. Units can be selected over a range of 2 decades between 10^{-3} volts and 10^{-1} volts

- **Volt/Division** (3) controls the amplitude of the pulse when either signal is displayed and can be used during active display. The following amplitude pulse scale selections can be made: *1.0mV, 2.0mV, 5.0mV, 10.0mV, 20.0mV, 50.0mV, 0.1V, 0.2V, 0.5V, 1.0V, 2.0V, 2.5V.*

- **Sec/Division** (4) controls the time base of the pulse when either signal is displayed and can be used during active display. The following time base scale selections can be made: *1μs, 2μs, 5μs, 10μs, 20μs, 50μs, 0.1ms.*

- **Display** (5) displays the signal that is as selected with *Channel Selection.* The display is a standard oscilloscope display with pulse amplitude plotted on the ordinate and time plotted on the abscissa.

- **Horizontal Slide** (6) and **Vertical Slide** (7) (located on abscissa and ordinate of the display, respectively) control the horizontal and vertical signal placement on the display, respectively, when either signal is displayed and can be used during active display.

Appendix D

Procedures for Nuclear Electronics

Inclusion of Appendix D demonstrates, in part, the completion of Objective #4.

Nuclear Electronics

Objectives

1. To become familiar with National Instruments LabVIEW™,
2. To become familiar with the operating characteristics of basic nuclear pulse counting instrumentation,
3. To become familiar with the use and operation of the digital oscilloscope, and
4. To become familiar with nuclear spectroscopy software packages.

Access to Lab Interface

Access the lab interface by connecting to the IP address with the username and password provided for the Nuclear Electronics Lab. Open the file located in Desktop → EE&S611 ONLINE → 1. Nuclear Electronics → Nuclear Electronics Interface. The interface should be identical to Figure D.1. Refer to Appendix C for detailed instructions on interface functionality.

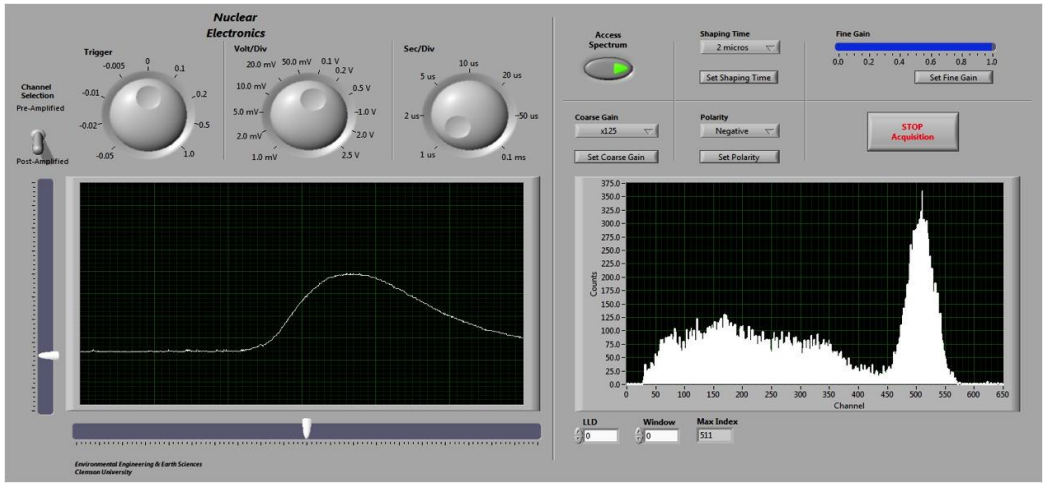

Figure D.1: Interface for Nuclear Electronics Lab

Acquisition and Counting Electronics

- **Access Spectrum** determines whether the oscilloscope (left display) or the MCA (right display) is actively updating. By default, the oscilloscope display is actively updating. When *Access Spectrum* is depressed, the oscilloscope display pauses and the spectrum generated by the MCA is displayed in real time. The previous spectrum will automatically be cleared when beginning a new acquisition. *Access Spectrum* is a one-way switch. The only method by which to stop the acquisition is to press *Stop Acquisition*.

- **Max Index** displays the channel number that contains the highest number of counts within the selected energy range.

Lab Procedure

Introduction
URSA-II, displayed in Figure D.2, is used to control all of the necessary nuclear electronics parameters and provide multichannel analysis for all of the labs in this course.

Figure D.2: URSA-II

The setup for this lab's counting system consists of a preamplifier, amplifier, counter/timer, single channel analyzer (SCA) and multichannel analyzer (MCA) as displayed in Figure D.3. URSA-II contains all the equipment within the dotted line.

Voltage pulses from a radiation detector are simulated using a tail pulse generator (pulser). The digital oscilloscope has two input channels and is used to observe pulses.

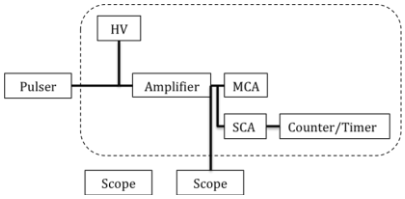

Figure D.3: Counting System for Nuclear Electronics Lab

1. **Oscilloscope**
   The oscilloscope used in this lab is shown in Figure D.4. It has two input channels which are connected to two output channels of URSA-II, which enables the display of pre-amplified and post-amplified signals.

Figure D.4: Digital Oscilloscope

2. **Tail Pulse Generator**
   a. The pulser used in this lab is ORTEC 480 Pulser, displayed in Figure D.5. Figure D.6 displays a screen capture of the pulser when connected directly to the oscilloscope.

Figure D.5: ORTEC 480 Pulser

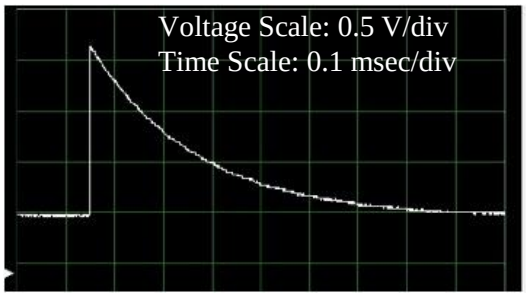

Figure D.6: Tail Pulse Generator Signal

b. Refer to Figure D.6. Note the pulse polarity. If the voltage scale is 0.5 V/div, what is the height of the pulse? If the time base is 0.1 msec/div, what is the frequency and with what does the frequency correspond?
c. Become familiar with the oscilloscope instrumentation by reading the Oscilloscope section under Instructions for Frequently Used Instrumentation.

3. Preamplifier

a. Switch *Channel Selection* to *Pre-Amplified*. The signal now displayed on the oscilloscope display is the pre-amplified pulse. An ORTEC 113 Preamplifier used at Clemson University is displayed in Figure D.7.

Figure D.7: ORTEC 113 Preamplifier

b. Sketch the waveform, noting the pulse polarity, height, and width. How has the preamplifier changed the original pulser signal shape?

4. Amplifier

a. Switch *Channel Selection* to *Post-Amplified*. A typical amplifier used at Clemson University is displayed in Figure D.8.

Figure D.8: ORTEC 570 Amplifier

b. Set the polarity to correspond to the polarity of the pre-amplified signal. *Don't forget to press *Set Polarity* after selecting the appropriate polarity from the drop-down menu.
c. Select a small value (between 0.2 and 0.6) on the fine gain gauge and press *Set Fine Gain*. Observe the change in the amplified signal on the oscilloscope display.
d. Set fine gain to various levels and observe the change in the oscilloscope display again. What happens? Is this what you expected?
e. With the fine gain at a fixed value (e.g. 1), vary the coarse gain. Record and plot the pulse amplitude as a function of the coarse gain for each coarse gain selection between *x15* and *x250*.

5. Single Channel Analyzer (SCA)

a. Set the window to 0.5 V and the LLD to 1.0 V. Determine the minimum and the maximum pulse heights (signal going into the oscilloscope) for the SCA output to occur. Adjust the pulse height using the amplifier coarse gain and fine gain. Repeat for LLD of 2.0 and 4.0.

.

LLD	Minimum Pulse Height	Maximum Pulse Height
1.0		
2.0		
4.0		

6. Multi Channel Analysis (MCA)

a. Set Coarse Gain to *x125*. Set Fine Gain to *0.3*.
b. Press *Access Spectrum* to begin acquiring a spectrum produced by the MCA. Is the spectrum you observe what you expect?
c. Sketch the spectrum, labeling important features.
d. Record and plot the peak channel number and signal voltage (pulse amplitude) as a function of fine gain. What is the relationship between the fine gain and the peak channel number? Peak Channel No. is displayed next to the LLD and Window. How does the spectrum vary when the fine gain is changed? **Remember to press *Stop Acquisition* each time while adjusting fine gain.

Fine Gain Level	Voltage of Signal on Oscilloscope	Peak Channel Number

7. Equipment and Instruments Used

a. Digital Oscilloscope (NI USB-5132)
b. Tail Pulse Generator (ORTEC 480)
c. URSA-II (SE Int'l. Inc.)

Appendix E

Procedures for Gamma-ray Spectroscopy with Scintillation Detectors

Inclusion of Appendix E demonstrates, in part, the completion of Objective #4.

Gamma-ray Spectroscopy with Scintillation Detectors

Objectives:

1. To identify gamma-ray interaction mechanisms using a NaI(Tl) detector,
2. To perform an energy calibration and efficiency calibration of the gamma-ray detector,
3. To identify an unknown source by gamma-ray spectroscopy, and
4. To quantify differences between different sctintillator materials.

Access to Lab Interface

Access the lab interface by connecting to the IP address with the username and password provided for the Gamma-ray Spectroscopy with Scintillation Detectors. Open the file located in Desktop → EE&S611 ONLINE → 2. Gamma Spectroscopy with Scintillation Detectors → Gamma Spectroscopy with Scintillation Detectors Interface. The interface should be identical to Figure E.1. Refer to Appendix C for detailed instructions on interface functionality.

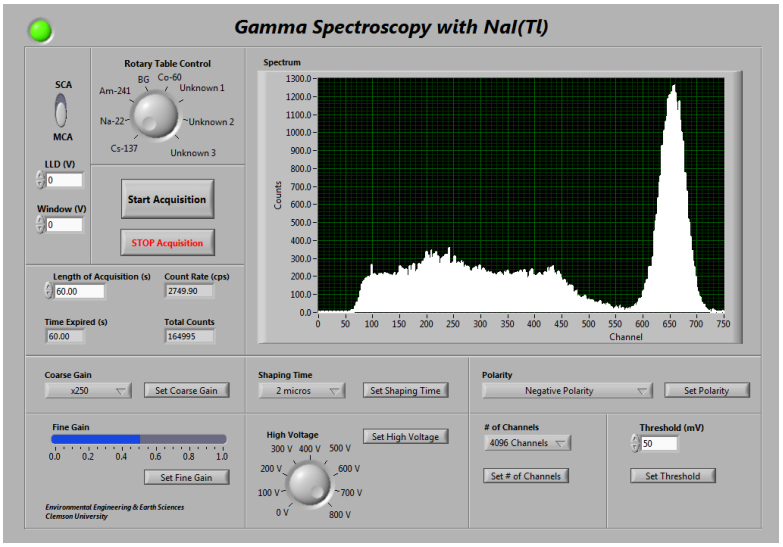

Figure E.1: Interface for Gamma-ray Spectroscopy with Scintillation Detector

Rotary table

- **Rotary Table Control** operates a rotary table that rotates gamma-ray sources to the counting position, which is centered directly above a 2″ x 2″ NaI(Tl) detector. The rotary table will rotate once the knob has been rotated to the appropriate position. Follow the procedures to select appropriate sources at the proper time.

- Streaming images of the rotary table can be viewed by selecting Start → All Programs → Logitech → Logitech Webcam Software → Quick Capture

SCA/MCA

- **SCA/MCA Switch** determines whether a spectrum is acquired in Single Channel Analyzer (SCA) mode or MCA mode. Follow the procedures to determine when to use the SCA or the MCA.

Lab Procedures

1. Lab Setup

This lab utilizes a 17″ diameter clear plastic circular plate mounted on a central rotating mechanism, shown in Figure E.2. Seven 1″ diameter sealed gamma-ray sources are placed at 45° increments around the circumference of the circular plate. ^{137}Cs is in the counting position in Figure E.2

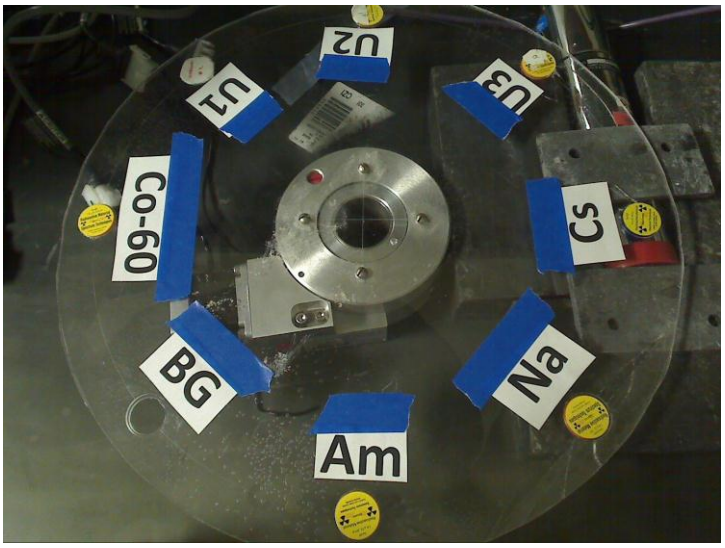

Figure E.2: Rotary Table Setup

2. Spectroscopy Setup

a. Activate the interface by pressing the right arrow located at the top left of the screen. *Confirm that URSA-II is operating correctly.*
b. Set Coarse Gain to *x125* and set Fine Gain to *0.5.*
c. Set Shaping Time to *2 μs*.
d. Set *Negative* Polarity
e. Set # of Channels to *2048*.
f. Set High Voltage to *800 V.*

3. Single Channel Analyzer (SCA)

a. The spectroscopy system for analyzing the pulse height distribution from a 2″ x 2″ NaI(Tl) detector using a single channel analyzer is displayed in Figure E.3. The URSA-II contains all the electronics within the dotted line.

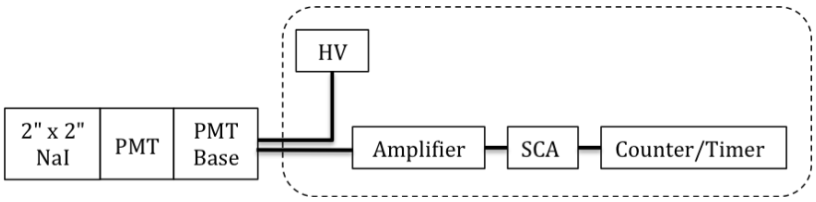

Figure E.3: SCA Spectroscopy System

b. Select *SCA* with the SCA/MCA switch.
c. Select *Background* with *Rotary Table Control* and observe the rotary table rotate until the designated location for background on the rotary table is directly in front of the detector. Take a 100-second background count. Note the number of background counts compared to acquisitions with previous detectors. (In SCA mode, only counts updates; the graph does not update.)
d. Select ^{137}Cs with *Rotary Table Control* and observe the rotary table rotate until the source is directly in front of the detector. Take a 100-second count.
e. Set the LLD to 5.0 V and set the energy window to 0.05 V.
f. Take a 100-second count and record the count rate.
g. Set the LLD to 0.0 V and set the energy window to 0.05 V. Take a 100-second count and record the count rate and the associated LLD and energy window.
h. Increment the LLD by 0.05 V and record the count rate and the associated LLD.
i. Repeat step (h) until the count rate for an energy window is roughly equivalent to the count rate of acquisition taken in Step (e).

4. **Multichannel Analyzer (MCA)**
   a. The spectroscopy system for analyzing the pulse height distribution from a 2″ x 2″ NaI(Tl) detector using a multichannel analyzer is displayed in Figure E.4. URSA-II contains all the electronics within the dotted line.

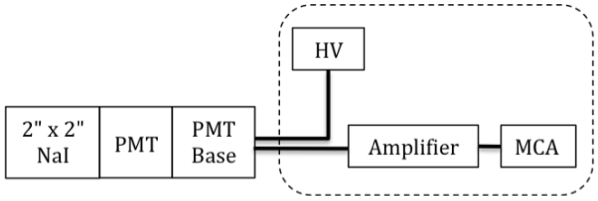

Figure E.4: MCA Spectroscopy System

   b. Select *Background* with *Rotary Table Control*. Take a 10-minute background count. Save the spectrum to your personal folder.
   c. Select ^{137}Cs with *Rotary Table Control*.
   d. After determining the count rate for ^{137}Cs, count the source for a sufficient time to achieve good counting statistics. Save the spectrum to your personal folder.
   e. Record the channel number of all distinguishing features of the spectrum. Record the FWHM and net peak area.
   f. Repeat steps (d) and (e) for ^{60}Co.
   g. Repeat steps (d) and (e) for ^{22}Na.
   h. Repeat steps (d) and (e) for ^{241}Am.
   i. Repeat steps (d) and (e) for *Unknown #1*, *Unknown #2*, and *Unknown #3*.

5. **Comparison with Different Scintillation Detectors**
   a. Contact Dr. DeVol to request that he replace the 2″ x 2″ NaI(Tl) detector with the 1.5″ x 1.5″ $LaBr_3$(Ce) detector.
   b. Count ^{137}Cs for the same amount of time that it was counted in Step 4 (d). Save the spectrum to your personal folder.

6. **Equipment Used**
   a. Rotary Table (Velmex B4836TS), motor (Vexta PK266-03A-P1), and motor controller (Velmex VXM-1)
   b. 2″ x 2″ NaI(Tl) detector (Bicron 2M2/2)
   c. 1.5″ x 1.5″ $LaBr_3$(Ce) detector (SGC BrilLanCe B380)
   d. URSA-II (SE Int'l. Inc.)

7. **Values**
   a. ^{137}Cs: 1μCi calibrated 07/2003
   b. ^{60}Co: 1μCi calibrated 07/2003
   c. ^{22}Na: 1μCi calibrated 07/2003

d. ^{241}Am: 1 μCi calibrated 07/1967
e. Distance between source and detector: 2″
f. Dimension of sources: point source

8. Questions

1. Single Channel Analyzer
    a. Make a careful plot of count rate (cps) vs. pulse height (volts).
    b. Label all distinguishing features in the spectrum.
    c. Determine the detector resolution at 662 keV.
    d. Compare the spectra obtained with the SCA set-up and the MCA for ^{137}Cs.
2. Multichannel Analyzer
    a. Determine the detector resolution at 662 keV (^{137}Cs) and 1.33 MeV (^{60}Co).
    b. Make an energy calibration plot (energy vs. Channel number) using the known photopeak energies.
    c. Display the following information in a table: radionuclide, spectrum features (e. g., backscatter peak, full energy peak, Compton edge, X-ray peak, annihilation peak), channel number, experimental energy, expected energy.
    d. Using the energy calibration, determine the energies from the unknown sources. Identify the unknown based on the gamma-ray energies and any other information that is available.
    e. Determine the activity of the ^{137}Cs source.
3. Compare the energy resolution and detection efficiency (at 662 keV) of the 2″ x 2″ NaI(Tl) and 1.5″ x 1.5″ $LaBr_3$(Ce) detectors. Do you get the expected result? Comment.

Appendix F

Procedures for Gamma-ray Attenuation and External Dosimetry

Inclusion of Appendix D demonstrates, in part, the completion of Objective #4.

Gamma-ray Attenuation and External Dosimetry

Objectives:

1. To determine the attenuation coefficient of gamma rays in two absorber materials,
2. To demonstrate that gamma rays undergo attenuation and not energy absorption,
3. To verify the functional relationship between dose and distance for a point source, and
4. To verify the functional relationship between dose and distance for a line source

Access to Lab Interface

This lab utilizes two interfaces. Access the lab interfaces by connecting to the IP address with the username and password provided for the External Dosimetry & Gamma-ray Attenuation lab. Open the file located in Desktop → EE&S611 ONLINE → 3. External Dosimetry & Gamma Attenuation → External Dosimetry Interface and →Gamma Attenuation Interface. The interfaces should be identical to Figures 1 and 2, respectively. Refer to Appendix C for detailed instructions on interface functionality.

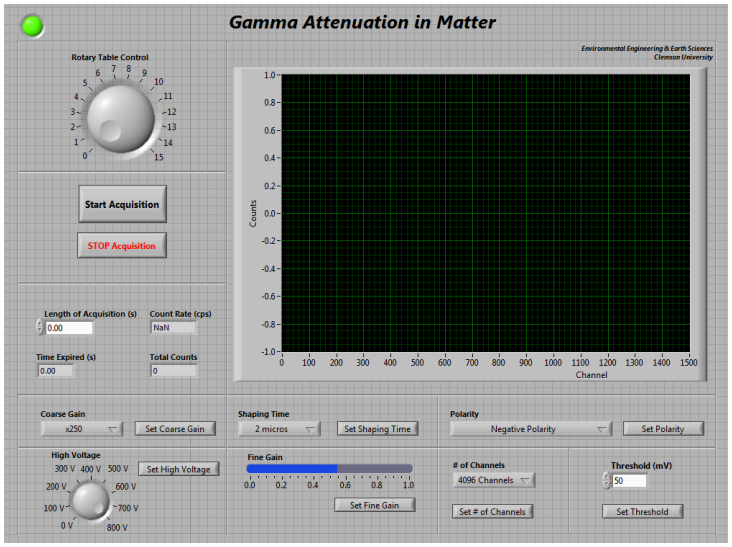

Figure F.1: Interface for Gamma-ray Attenuation Procedures

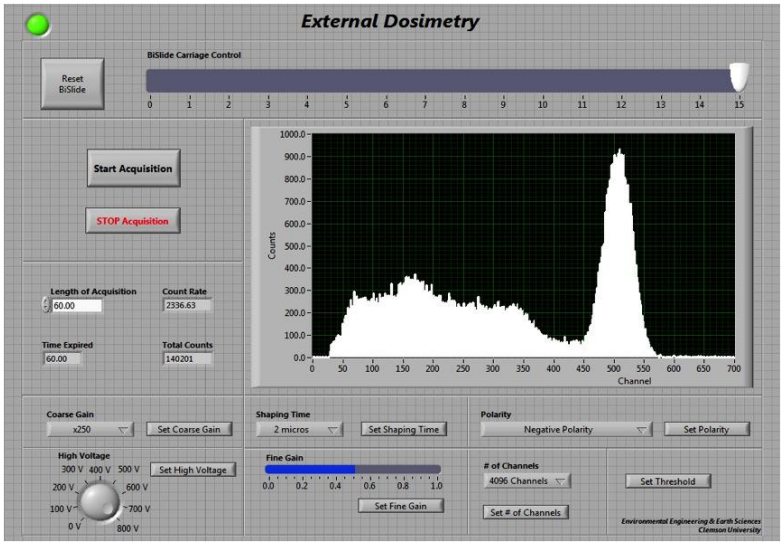

Figure F.2: Interface for External Dosimetry Procedures

BiSlide™

- **BiSlide™ Carriage Control** operates a 15 ft. slide actuator, called a BiSlide™, that varies the distance between the source and the detector. The source is mounted on a carriage that is attached to a belt that travels the entire length of the BiSlide™; the detector is mounted on one end of the BiSlide™. The carriage will begin to move as soon as the pointer on *BiSlide™ Control* is placed at the desired source-detector distance. Source-detector selections can be made in 1-ft. increments between 1 and 16 ft. Follow the procedures to select the appropriate distances at the proper time.

  The BiSlide™ can process only one command at a time and the carriage travels very slowly (30 sec/ft). The carriage will travel the complete distance to any selected source-detector distance before processing the command to travel to a second consecutively selected source-detector distance. For example, assume the pointer is initially at 3 ft. and the carriage is stationary at that source-detector distance. If the pointer is moved to 12 ft., the BiSlide™ will begin traveling to that source-detector distance. Then, if at any time during the carriage's travel to 12 ft., the pointer is moved to 4 ft., the carriage will travel to 12 ft. before it will immediately reverse direction and travel to a source-detector distance of 4 ft.

- If a situation occurs in which it desired to reset the destination of the carriage while it is still in motion without having to wait for the carriage to complete its first command, use **Reset BiSlide™.** *Reset BiSlide™* cancels the current motion of the carriage and resets the destination of the carriage to the most recent source-detector distance selection. Press *Reset BiSlide™* after the pointer has been placed on the new desired source-detector distance and confirm that the carriage has

responded appropriately by observing its motion with the webcam. In the example above, if, after the pointer was moved to 4 ft., *Reset BiSlide*™ was pressed, the BiSlide™ would immediately begin traveling to a source-detector distance of 4 ft.—no matter how far it had traveled towards 12 ft.

- Streaming images of the BiSlide™ can be viewed by selecting Start → All Programs → Logitech → Logitech Webcam Software → Quick Capture

Rotary table

- **Rotary Table Control** operates a rotary table that rotates absorber thicknesses to a position in-between a stationary source and a stationary vertical 2″ x 2″ NaI(Tl) detector. The rotary table will rotate once the knob has been rotated to the appropriate position. Follow the procedures to select appropriate absorber thicknesses at the proper time.

- Streaming images of the rotary table can be viewed by selecting Start → All Programs → Logitech → Logitech Webcam Software → Quick Capture

Lab Procedures

1. Lab Setup

This lab utilizes two different setups.

The setup used to conduct the gamma-ray attenuation procedures of this lab utilizes a 17″ diameter clear plastic circular plate mounted on a central rotating mechanism, shown in Figure F.3. Fifteen absorber thicknesses are placed at 45° increments around the circumference of the circular plate.

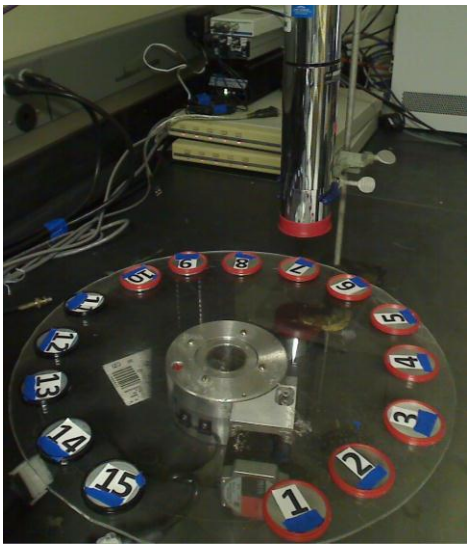

Figure F.3: Rotary Table Setup for Gamma-ray Attenuation Procedures

The setup used to conduct the external dosimetry procedures of this lab utilizes the 15 ft. BiSlide™. Figure F.4 shows the full 15-ft. length of the BiSlide™ mounted on the wall at Clemson University. A close-up of the carriage mounted on the belt of the BiSlide™ is shown in Figure F.5.

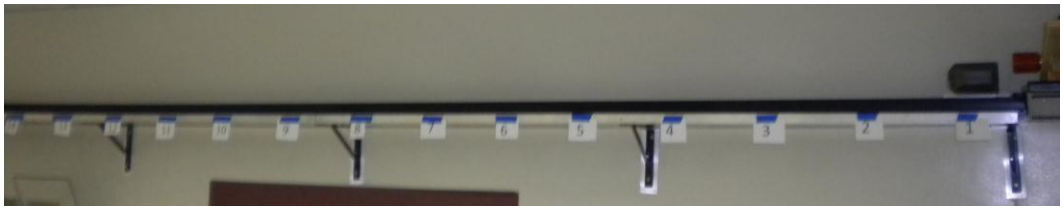

Figure F.4: BiSlide™ Setup for External Dosimetry Procedures

Figure F.5: Carriage Mounted on BiSlide™ Belt

2. Counting Setup

Both setups use the same counting setup, displayed in Figure F.6, with a 2″ x 2″ NaI(Tl) detector.

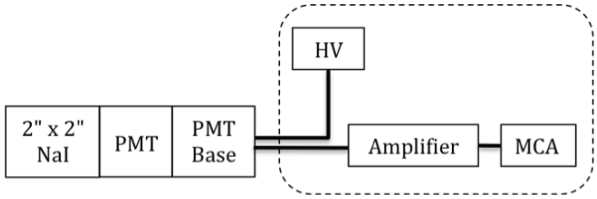

Figure F.6: Counting Setup for Gamma-ray Attenuation and External Dosimetry Procedures

a. Activate the interface by pressing the right arrow located at the top left of the screen beneath the Edit menu. *Confirm that URSA-II is operating correctly.*
b. Set Coarse Gain to *x125* and set Fine Gain to *0.5*
c. Set Shaping Time to *2 μs*.
d. Set *Negative* Polarity
e. Set # of Channels to *2048*.
f. Set High Voltage to *800 V*.

3. Gamma-ray Attenuation & Attenuation Coefficients

a. Numbers 0-15 on the *Rotary Table Control* knob correspond to 15 absorber thicknesses. The numbers, the thicknesses they represent, and the material of the thicknesses are listed in Table F.1.

Table F.1: Absorber Thicknesses and Corresponding *Rotary Control Knob* Numbers

Rotary Control Knob Number	Absorber Thicknesses (mg/cm^2)[1]	Absorber Material
0	None	--
1	549.2	Al
2	619.6	Al
3	687.5	Al
4	858.7	Al
5	960.5	Al
6	974.4	Pb
7	1082.4	Al
8	1224.7	Al
9	1373.4	Al
10	1498.3	Al
11	1602.3	Al
12	1824.2	Pb
13	2650.6	Pb
14	4450.8	Pb
15	7193.6	Pb

1. Absorber Set Model AB-23 from Atomic Accessories, Inc.

b. Select *0* with *Rotary Table Control* so that there is not any attenuation of the source in the counting system. This represents the value I_o. Observe the motion of rotary table and confirm that there are no absorbers positioned in-between the source and the detector.
c. Count the ^{57}Co source for sufficient time to achieve 1% counting statistics. Save the spectrum to your personal folder.
d. Select *1* with *Rotary Table Control*. Acquire the spectrum for the same amount of time as in the previous step. Save the spectrum to your personal folder.
e. Repeat step (d) for absorber thicknesses *2 – 15*.

4. External Dosimetry

a. Contact Dr. DeVol to confirm that there is no source on the BiSlide™ carriage.
b. Collect a 5-minute background count. Save the spectrum to your personal folder.
c. Contact Dr. DeVol and request that he place the point source on the BiSlide™ carriage.
d. Slide the pointer on *BiSlide™ Carriage Control* to 1 ft. Confirm that the carriage traveled to appropriate position.
e. Take a 10-minute count. Save the spectrum to your personal folder.

f. Slide the pointer to 2 ft. so that the source is 2 ft. away from the detector. Confirm that the carriage traveled to the appropriate position.
g. Take a 10-minute count. Save the spectrum to your personal folder.
h. Increase the source-detector distance by 1-ft. increments up to and including a source-detector distance of 16 ft. Repeat step (g) for each 1-ft. increment.
i. Repeat steps (c) – (h) for the line source.

5. Equipment and Instruments Used

a. BiSlide™ (Velmex MB10-1800-M10-33), motor (Vexta 296B2A-SG10), and motor controller (Velmex VXM-1)
b. Rotary Table (Velmex B4836TS), motor (Vexta PK266-03A-P1), and motor controller (Velmex VXM-1)
c. 2″ x 2″ NaI(Tl) detector (Bicron 2M2/2)
d. URSA-II (SE Int'l. Inc.)

6. Values

a. Point Source for External Dosimetry Procedures: 0.1 Ci ^{137}Cs calibrated
b. Line Source for External Dosimetry Procedures: 876 Bq/cm ^{137}Cs calibrated 3/26/2005
c. Source for Attenuation Procedures: 5μCi ^{57}Co calibrated 07/2003
d. Distance between source and top of rotary table: 2″
e. Distance between top of rotary table and detector (without absorbers): 3″
f. Dimension of source for gamma-ray attenuation: point source

7. Questions

a. Gamma-ray Attenuation
    i. Determine the thickness of each absorber by using the density of each material.
    ii. Graph count rate as a function of material thickness for Aluminum and Lead.
    iii. Determine the mass attenuation coefficient of each material. Fit an exponential trendline to the graph created in Step ii and note the value of μ in the following equation: $I = I_O e^{-\mu x}$. Compare your experimental value to published values. Make sure you note the energy of the source.
    iv. Determine the linear attenuation coefficient of each material and compare to published values.
    v. Comment on comparison of peak energy levels for each spectrum.
b. External Dosimetry
    i. Using the data from the external dosimetry procedures, calculate the dose rate for the measured spectra from each source-detector distance. Graph the calculated Net Dose Rate as a function of distance for the point source. Plot the theoretical dose rate on the

same graph. Comment on the relationship between the data and theory.

ii. Repeat Step (i) for the line source.

Appendix G

Procedures for Alpha Spectroscopy and Absorption in Air

Inclusion of Appendix D demonstrates, in part, the completion of Objective #4.

Alpha Spectroscopy and Absorption in Air

Objectives:

- To perform an energy and efficiency calibration of the alpha spectrometer,
- To determine the range of alpha particles in air,
- To investigate the loss of alpha particle energy as it travels through different density thicknesses of air, and
- To identify and quantify unknown alpha sources.

Access to Lab Interface

Access the lab interface by connecting to the IP address with the username and password provided for the Alpha Spectroscopy lab. Open the file located in Desktop → EE&S611 ONLINE → 4. Alpha Spectroscopy → Alpha Spectroscopy Interface. The interface should be identical to Figure G.1. Refer to Appendix C for detailed instructions on interface functionality.

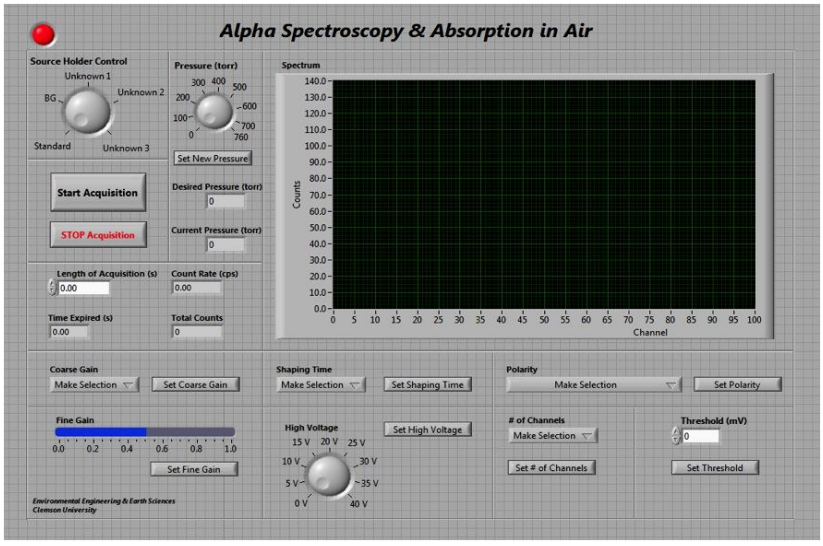

Figure G.1: Interface for Alpha Spectroscopy and Absorption in Air Lab

Source Holder

- **Source Holder Control** operates a source holder that rotates alpha sources to the counting position, which is centered directly beneath a passivated implanted planar silicon (PIPS) detector. The shaft will rotate once the knob has been rotated to the appropriate position. Follow the procedures to select appropriate sources at the proper time.

Digital Vacuum Regulator (DVR)
The digital vacuum regulator is a pressure regulating system that controls the pressure level in the vacuum chamber. The DVR is controlled by a pressure transducer that regulates pressure by automatically operating a valve that separates the vacuum source from the system being evacuated and can regulate the pressure to within 1 torr of the desired pressure. A needle valve stabilizes the pressure fluctuations inherently introduced by the DVR. A vacuum pump provides evacuation to the system.

Follow instructions closely when setting pressure levels. There is not an automated method to purge the vacuum chamber. At the beginning of the lab, the vacuum chamber is at ambient pressure. The procedures are written in such a way that the pressure level in the chamber only decreases as the lab continues. There should be no reason to need to increase the pressure in the vacuum chamber. Increasing the pressure in the vacuum chamber requires personnel at Clemson University to manually purge the system.

- **Pressure** sets the desired pressure of the vacuum chamber that contains the alpha sources. *Set New Pressure* must be pressed to apply the desired pressure. *Do not change during active acquisition.*

- **Desired Pressure** displays the desired pressure as selected with *Pressure* knob.

- **Current Pressure Level** displays the current pressure of the vacuum chamber. The pressure level will fluctuate slightly around the desired pressure level.

Lab Procedures

1. **Lab Setup**
   An octagon is placed in the vacuum chamber, rigidly attached to an aluminum shaft at the center of the octagon. The shaft penetrates the rear wall of the vacuum chamber and is connected to the shaft of the motor with a coupling. An oil seal is fitted to the penetration site to maintain the integrity of the vacuum levels during the experiments. Alpha sources are secured to the 1″ square edges of the octagon. A schematic of the evacuation system is shown in Figure G.2 and the source holder is shown in Figure G.3.

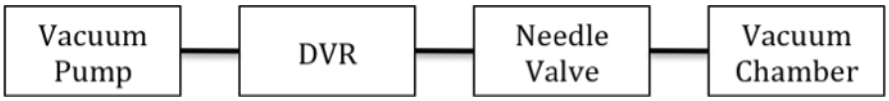

Figure G.2: Schematic of Evacuation System

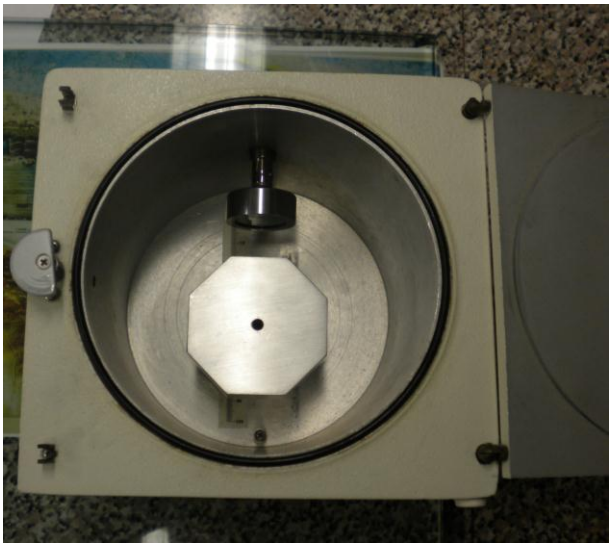

Figure G.3: Alpha Source Holder in Vacuum Chamber

2. Counting Setup

a. The counting system is displayed in Figure G.4. URSA-II contains all the electronics within the dotted line.

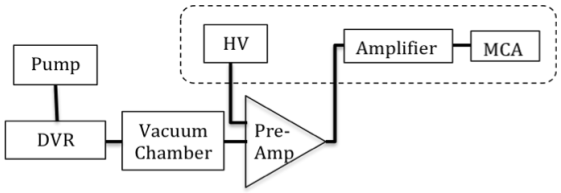

Figure G.4: Counting System for Alpha Spectroscopy and Absorption in Air

b. Activate the interface by pressing the right arrow located at the top left of the screen beneath the Edit menu. *Confirm that URSA-II is operating correctly.*
c. Set Coarse Gain to *x125* and set Fine Gain to *0.5.*
d. Set Shaping Time to *2 μs.*
e. Set *Negative* Polarity
f. Set # of Channels to 2048.
g. Set High Voltage to *40 V.*

h. Set DVR to *760 torr*.

3. Alpha Particle Energy Loss in Air

a. Select *Unknown #1* with *Source Holder Control* knob. Begin with DVR at 700 torr.
b. Determine the count rate.
c. Count in the alpha spectrometer for an appropriate time to achieve 1% counting statistics. Save the spectrum to your personal folder, recording the peak channel number, gross peak area, and energy resolution.
d. Repeat steps (a) – (c) for Unknown #2.
e. Decrease the DVR pressure by increments of 50 torr and repeat steps (b) - (d) until 0 torr. (Although the DVR will not achieve 0 torr, it will come very close. Assume that the lowest pressure level at which the DVR stabilizes is a complete vacuum.) Make sure to continue reporting the significant characteristics of each acquisition as a function of pressure. Maintain 1% counting statistics for as many acquisitions as reasonably possible. Otherwise, maintain 3% counting statistics for as many acquisitions reasonably possible.
f. The following table is provided to supplement steps (a) – (e).

Pressure (torr)	Source	Length of Acquisition	Counts	Filename of Saved Spectra
700	Unknown #1			
	Unknown #2			
650	Unknown #1			
	Unknown #2			
600	Unknown #1			
	Unknown #2			
550	Unknown #1			
	Unknown #2			
500	Unknown #1			
	Unknown #2			
450	Unknown #1			
	Unknown #2			
400	Unknown #1			
	Unknown #2			
350	Unknown #1			
	Unknown #2			
300	Unknown #1			
	Unknown #2			
250	Unknown #1			
	Unknown #2			
200	Unknown #1			
	Unknown #2			
150	Unknown #1			
	Unknown #2			
100	Unknown #1			
	Unknown #2			
50	Unknown #1			
	Unknown #2			
0	Unknown #1			
	Unknown #2			

g. Go to http://www.wyff4.com to record the pressure in Anderson, SC. Record the temperature from the thermometer shown on the webcam image.

4. **Energy Resolution**
    a. Determine the energy resolution of the pulser peak if the pulser peak area is _____, the peak channel is _____, and the FWHM is _____.

5. **Energy & Efficiency Calibrations**
    a. Maintain full vacuum in the vacuum chamber.
    b. Select *BG* from *Source Holder Control* knob. Take a 10-minute count of the background. Note the total number of counts. Save spectrum to your personal folder.
    c. Select *Standard* from *Source Holder Control*. Take a 10-minute count. Refer to the alpha standard spec sheet for known energies and activities. Record the gross counts in each peak. Save the spectrum to your personal folder.

6. **Unknown Source Identification**
    a. Maintain full vacuum in the vacuum chamber
    b. After acquiring spectra for the known alpha sources in a complete vacuum, select *Unknown #1* from *Source Holder Control* knob.
    c. Count the unknown in the alpha spectrometer for a sufficient time to have defined peaks. Save the spectrum to your personal folder and record the peak channel number, gross peak area, and energy resolution of all peaks.
    d. Repeat step (c) for *Unknown #2* and *Unknown #3.*

7. **Equipment Used**
    a. Motor (Vexta PK245-01AA) and motor controller (Velmex VXM-1)
    b. Digital Vacuum Regulator (J-KEM Model 200) and needle valve (J-KEM DVR PNV)
    c. Vacuum Pump (Welch DuoSeal 1399B-01)
    d. PIPS detector in Vacuum Chamber (Canberra 7400A)
    e. Preamplifier (Canberra 2004 DM)

8. **Values**
    a. Source Dimension: point source
    b. Detector dimension: 29/32″ diameter
    c. Distance from source to detector: 2″

9. **Questions**

1. Energy and Efficiency calibration of the Alpha Spectrometer
    a. Plot the energy calibration curve.
    b. Calculate the absolute detection efficiency using the alpha standard. Plot the efficiency calibration curve.
    c. Calculate the energy resolution (FWHM) in units of percent and energy. How does the energy resolution obtained pulser compare with that from

source? Also compare with the gas-flow proportional detector from a previous lab.

2. Alpha Range in Air
    a. Plot the ratio of the intrinsic detection efficiency at each vacuum level to the intrinsic detection efficiency as a function of absorber (air) thickness. Determine the mean range in *cm* and compare with values in the *Radiological Health Handbook,* Cember, or Knoll. The published range values will need to be corrected to the laboratory temperature and barometric pressure at the time of the experiment.
    b. Include the data point that was obtained at complete evacuation.
3. Unknown Source Identification by Range in Air
    a. After determining the ranges in air for the Unknown #1 and Unknown #2, identify the alpha energies that correspond to the energies.
    b. Identify the unknowns based on their ranges in air.
4. Unknown Source Identification by Energy Calibration
    a. Using the energy calibration, calculate the energy of any observed peaks.
    b. Identify the most likely radionuclides based on alpha peak energy.
    c. Comment on the similarities/differences of the isotopes selected for the unknowns based on range in air and energy calibration.
5. Unknown Source Activity
    a. Calculate the activity of Unknown #1 and Unknown #2 based on the radionuclides selected by Energy Calibration.

Appendix H

Original Procedures from EE&S 611

Nuclear Electronics

Objective:

To become familiar with the operating characteristics of basic nuclear pulse counting instrumentation.

Procedure / Results:

Set up a pulse counting system consisting of a preamplifier, amplifier, counter/timer, single channel analyzer (SCA), and multichannel analyzer (MCA). Voltage pulses from a radiation detector will be simulated using a tail pulse generator (pulser). An oscilloscope will be used to observe these pulses as they are processed through the system.

1. **Oscilloscope**
   a. Determine the position of the oscilloscope ground trace. Reposition the ground trace if necessary.
   b. Verify the calibration of the oscilloscope by connecting the internal calibrator to channel one.
   c. Vary the time base and the amplitude to display the calibration pulse.
   d. Sketch below the calibration waveform, note the pulse polarity, height, and width.

2. **Tail Pulse Generator**
   a. Connect the pulser output to channel 1 of the scope.
   b. Vary any of the controls on the pulser to determine their operation. Specify the changes made and what happened to the signal
   c. Record then plot the pulse amplitude as a function of pulser amplitude dial setting. Is there a correlation between the dial setting and pulse amplitude?

Dial Setting	Amplitude
1.0	
2.0	
3.0	
4.0	
5.0	
6.0	
7.0	
8.0	
9.0	
10.0	

d. Sketch the pulser waveform, noting the pulse polarity, height and width. What does the frequency correspond with?

3. Preamplifier

a. Connect the pulser output into the TEST input of the preamplifier.
b. Connect the preamplifier output to the scope.
c. Sketch the preamplifier output waveform, noting the pulse polarity, height and width. How has the preamplifier changed the pulse shape
d.

4. Amplifier

a. Set the pulser amplitude to a small value.
b. Connect the preamplifier output to the input of the amplifier. Set the input polarity to correspond with the output polarity of the preamplifier signal. Connect the amplifier output to the scope.
c. Vary the fine gain. What happens? Is it what you expect?
d. With the fine gain fixed, vary the course gain. Record and plot the pulse amplitude as function of the course gain.

Course Gain	Pulse Amplitude

e. Sketch the amplifier output waveform, noting the pulse polarity, height and width.

5. Single Channel Analyzer (SCA)

a. Split the output of the amplifier, connect one output to channel 1 of the oscilloscope and the other output to the input of the SCA and connect the output of the SCA to channel 2 of the oscilloscope.

b. Set the ΔE range to 10 V and the window to 10 V (10 on the dial). Set E (lower level discriminator, LLD) to 0. Sketch the SCA output pulse shape, noting the pulse polarity, height and width. How does the pulse shape vary from the previous pulses that have been looked at?

c. Set the ΔE range to 0.5 V and the LLD to 1.0 V. Determine the minimum and maximum pulse heights (signal going into the oscilloscope) for the SCA output to occur. Adjust the pulse height using the pulser. Repeat for LLD of 2.0 and 4.0

LLD	Minimum Pulse Height	Maximum Pulse Height
1.0		
2.0		
4.0		

6. Counter/Timer

a. Connect the SCA output to the counter/timer. Adjust the SCA and pulser until the counter/timer is receiving input.

b. How does the pulser amplitude effect the count rate?

c. How does the count rate compare with the pulser frequency?

7. Multichannel Analyzer (MCA)

a. Become familiar with the operation of the MCA.

b. Connect the amplifier output to the MCA. Observe the pulser spectrum. Is the spectrum tha you observe what you expect? Sketch the spectrum, labeling important features.

c. How does the spectrum vary when the pulser amplitude is changed? Record and plot the peak channel number as a function of pulser amplitude. What is the relationship between the pulse amplitude and the peak channel number?

Pulser Amplitude Amp output pulse (V)	Peak Channel Number

Gamma-ray Interactions and Gamma-ray Spectroscopy with Scintillation Detectors

OBJECTIVES:

1. To identify gamma-ray interaction mechanisms using a NaI(Tl) detector.
2. To calibrate an gamma-ray spectrometer
3. To identify an unknown source by gamma-ray spectroscopy.

PROCEDURE:

1. **Set the MCA to 2048 channels**

2. **Single Channel Analyzer (SCA)**
   a. Set-up a spectroscopy system for analyzing the pulse height distribution from a 2" x 2" right circular cylinder of NaI(Tl) using a single channel analyzer.
   b. Take a 100-second background count with a wide energy window.
   c. Position the ^{137}Cs source 10-cm from the front face of the detector.
   d. Set the SCA window of 0.05 volts.
   e. Set the LLD to 0.05 volts. Record the counts in a 100-second time interval.
   f. Increment LLD by 0.05 Vand determine the count rate.
   g. Repeat step f until the background count rate is at background

3. **Multichannel Analyzer (MCA)**
   a. Set-up a spectroscopy system for analyzing the pulse height distribution from a 2" x 2" right circular cylinder of NaI(Tl) using a multichannel analyzer.
   b. Take a 10-minute spectrum. Save spectrum.
   c. Position the source 10 cm away from the front face of the detector.
   d. Obtain a spectrum for ^{137}Cs. Save spectrum. Record the peak channel number of all distinguishing features of the spectrum, including the FWHM and net peak area.
   e. Repeat (d) for ^{60}Co.
   f. Repeat (d) for ^{241}Am.
   g. Repeat (d) for unknown sources.

4. **Comparison of Detector size**
   a. Set-up a spectroscopy system for analyzing the pulse height distribution from either a 3" x 3" or 5" x 5" right circular cylinder of NaI(Tl) using a multichannel analyzer.
   b. Take a 10-minute background spectrum.
   c. Position the source 10 cm away from the front face of the detector.
   d. Obtain a spectrum for ^{137}Cs. Record the peak channel number of all distinguishing features of the spectrum, including the FWHM and net peak area.

RESULTS:

1. **Single Channel Analyzer**
   a. Make a careful plot of count rate (cps) vs. pulse height (volts).
   b. Label all distinguishing features in the spectrum.
   c. Determine the detector resolution at 662 keV.
   d. Compare the spectra obtained with the SCA set-up and the MCA for ^{137}Cs.

2. **Multichannel Analyzer**
   a. Determine the detector resolution at 662 keV (^{137}Cs) and 1.33 MeV (^{60}Co).
   b. Make an energy calibration plot (energy vs. Channel number) using the known photopeak energies.
   c. Display the following information in a table: radionuclide, spectrum features (e. g., backscatter peak, full energy peak, Compton edge, X-ray peak, annihilation peak), channel number, experimental energy, expected energy.
   d. Using the energy calibration, determine the energies from the unknown sources. Identify the unknown based on the gamma-ray energies and any other information that is available.
   e. Determine the activity of the Cs-137 source.

3. **Compare the energy resolution** (at 662 keV) of the 2" x 2" and the 3" x 3" or 5" x 5" NaI(Tl) detectors. Do you get the expected result? Comment.

External Dose Experiment

OBJECTIVES:

1. To verify the functional relationship between dose and distance for different geometries
2. Calculate the build-up factors for different geometries
3. Calculate the count rate to dose for a gamma-ray spectrometer

PROCEDURE:

1. Set-up a counting system consisting of the 2" x 2" NaI(Tl) scintillation detector, amplifier, and MCA.
2. Collect a background spectrum in the laboratory.
3. Collect spectra at several distances from a ^{137}Cs point source. Make at least 5 measurements.
4. Repeat Step 3 while increasing the amount of Pb shielding. Use shielding at three different thicknesses.
5. Repeat Step 3 while increasing the amount of Cu shielding. Use shielding at three different thicknesses.
6. Repeat Steps 3 and 4 with a ^{137}Cs line source.
7. Repeat Step 3 with a ring source.

CALCULATIONS and RESULTS:

1. Using the data from the gamma-ray spectrometer, calculate the dose rate for the measured spectra. Graph the calculated Net Dose Rate as a function of distance for the unshielded point source. Plot the theoretical dose rate on the same graph. Comment on the relationship between the data and theory.
2. Graph the calculated Net Dose Rate as a function of distance for the shielded point source. Plot the theoretical dose rate (both with and without the theoretical build-up factor) on the same graph. Comment on the relationship between the data and theory.
3. Comment on the comparison between the experimental and theoretical build-up factor for the point and line sources.
4. Repeat Steps 1 and 2 (immediately above) for the line source.
5. Repeat Step 1 (immediately above) for the ring source.
6. Compare the experimental ^{137}Cs peak count rate for the point source (shielded and unshielded) at different distances with those obtained with the SuperSynth/MCNP computer simulations.

Alpha Spectroscopy and Absorption in Air

OBJECTIVE:

1. To learn how to calibrate an alpha spectrometer to energy and efficiency.
2. To measure the range of alpha particles in air
3. To identify and quantify unknown sources.

PROCEDURE:

1. Energy and Efficiency calibration of the alpha spectrometer

a. Receive instructions on the operation of the alpha spectrometer. Set the MCA to 2048 channels Note: NEVER OPEN THE ALPHA SPECTROMETER WHEN THE DETECTOR IS BIASED
b. Collect a 600-s spectrum of the background. Note the total count rate. Save the spectrum.
c. Connect the pulser to the test input of the alpha spectrometer. Collect a 600-s spectrum. Measure the energy resolution of the pulser peak.
d. Obtain alpha sources from the instructor. Note: DO NOT TOUCH THE SURFACE OF THE ALPHA SOURCES
e. Count alpha standard #1 at a defined location (~2-3 cm from the detector) in the spectrometer for 600s while under vacuum. Save the spectrum. Record the peak channel number, gross peak area and energy resolution.
f. Repeat step d with alpha standard #2.
g. Note the diameter of the detector and the source to detector distance.

2. Alpha Range in Air (Note PIPS detector dead layer < 50 nm Si)

a. Determine the count time so that the count rate has an uncertainty of less than 1%.
b. Place the source as close to the detector as practical. Observe the differential pulse height spectrum with the MCA. Save the spectrum. Record the peak channel number, gross peak area and energy resolution.
c. Move the source away from the detector in defined increments, recording the peak channel number, gross peak area and energy resolution as a function of position. Be sure to maintain at least 3% uncertainty to the extent practical.
d. Continue to move the source away from the detector until the count rate is down to background. Now apply a vacuum to the chamber and measure the count rate. Do you get what you expect?
e. Repeat with another alpha source.
f. Record laboratory temperature and barometric pressure.

3. **Identify two unknown alpha sources**
    a. Obtain an unknown alpha source from your lab instructor
    b. Prepare and count the source at a defined location in the alpha spectrometer for a sufficient time to have defined peaks.
    c. Save the spectrum. Record the peak channel number, gross peak area and energy resolution of any observed peaks.
    d. Collect background spectra for the same length of time as the unknown samples.

RESULTS:

1. **Energy and Efficiency calibration of the Alpha Spectrometer**
    a. Plot the energy calibration curve.
    b. Calculate the absolute detection efficiency of the two alpha standards. Plot the efficiency calibration curve.
    c. Calculate the energy resolution (FWHM) in units of percent and energy. How does the energy resolution obtained pulser compare with that from source. Also compare with the gas-flow proportional detector from a previous lab.

2. **Alpha Range in Air**
    a. Plot the ratio of the intrinsic detection efficiency at each separation distance to the intrinsic detection efficiency as a function of absorber (air) thickness. Determine the mean range in *cm* and compare with values in the *Radiological Health Handbook*, Cember, or Knoll. The published range values will need to be corrected to the laboratory temperature and barometric pressure at the time of the experiment.
    b. Include the data point that was obtained when the vacuum was pulled.

3. **Source Identification**
    a. Using your energy calibration, calculate the energy of any observed peaks.
    b. Identify the most likely radionuclides based on alpha peak energy.
    c. Calculate the activity of the radionuclides.

Appendix I

Calibration Sheet for Alpha Standard Used in Alpha Spectroscopy

Eckert & Ziegler
Analytics

1380 Seaboard Industrial Blvd.
Atlanta, Georgia 30318
Tel 404•352•8677
Fax 404•352•2837
www.analyticsinc.com

CERTIFICATE OF CALIBRATION
Standard Radionuclide Source

78189-383

24.1 mm Diameter x 0.65 mm Thick Stainless Steel Disk

Customer: Clemson University/Dept. of Environmental Health & Safety
P.O. No.: 0919-08-1073, Item 1

This standard radionuclide source was prepared by electrodeposition of a mixture of alpha emitters onto a stainless steel disk. Total alpha activity was determined with a ZnS scintillation detector. Radionuclide activities were calculated from the total activity and the fraction of activity for each radionuclide determined by alpha spectroscopy.

Analytics maintains traceability to the National Institute of Standards and Technology through Measurements Assurance Programs as described in USNRC Regulatory Guide 4.15, Rev. 1.

CALIBRATION DATE: August 6, 2008 12:00 EST

TOTAL ACTIVITY (dpm): 416
EXPANDED UNCERTAINTY (dpm [k=2]): 9
ENERGY RANGE (keV): 3700-7950

ISOTOPE	*ACTIVITY (dpm)*	*EXPANDED UNCERTAINTY ([k=2)(Bq)*	*HALF-LIFE*	*ENERGY RANGE (keV)*
U-238	*105.4*	*2.4*	*4.468 E9 y*	*3900-4290*
U-234	*103.9*	*2.3*	*2.455 E5 y*	*4580-4860*
Pu-239	*102.7*	*2.3*	*2.41 E4 y*	*4950-5240*
Am-241	*99.2*	*2.2*	*4.322 E2 y*	*5275-5590*

Impurities: U-235 ≈4.6 dpm

Diameter of active area: 24.1 mm

CAUTION: Active material deposited on the unmarked surface. Handle carefully to prevent scratching or damaging the active surface of this source (i.e., use Teflon coated forceps). Store in the container provided when not in use.

Source Calibrated By: _____
D. M. Montgomery, QA Manager

QA Approved: _____ Date: 09-05-08
D. M. Montgomery, QA Manager

End of Certificate

REFERENCES

Abu-Mulaweh, H. I. (2009). Development of a bench-top air-to-water heat pump experimental apparatus. *International Journal of Engineering , 3* (3), 359-369.

American Nuclear Society (ANS), (2004). *Maintaining a Viable Nuclear Industry Workforce* (Position Statement 29, rev. June 2004). Retrieved from www.ans.org/pi/ps/docs/ps29.pdf

American Physical Society (APS), (2008). *Readiness of the U.S. nuclear workforce for 21st century challenges* (A Report from the APS Panel of Public Affairs Committee on Energy and Environment). Retrieved from http://www.aps.org/policy/reports/popa-reports/upload/Nuclear-Readiness-Report-FINAL-2.pdf

Anido, L.; Llamas, M.; Fernandez, M.J. (2001). Internet-based learning by doing. *IEEE Transactions on Education*, 44, 18-37. doi: 10.1109/13.925839

Arthur, J.H., & Sexton, M.R. (2002). LabVIEW application: energy laboratory upgrade. *Proceedings of the 2002 American Society for Engineering Education Annual Conference & Exhibition,* (Session 3233, pp. 1-7). Montreal, Quebec, Canada.

Bitter, R, Mohiuddin, T. & Nawrocki, M. (2001). *LabVIEW Advanced Programming Techniques.* Boca Raton, FL: CRC Press.

Bhargava, P., Antonakakis, J., Cunningham, C., & Zehnder, A. T. (2006). Web-based virtual torsion laboratory. *Computer Applications in Engineering Education*, 14, 1-8. doi: 10.1002/cae.20061

Bogdanov, M. V., Ofengeim, D. K., Kulik, A. V., Zimina, D. V., Ramm, M. S., & Zhmakin, A. I. (2006). Industrial strength software in computer based engineering education (CBEE): a case study. *ArXiv Physics e-prints*, 1-15.

Budhu, M. (2001). Enhancing instructions using interactive multimedia simulations. *Simulation, 76*, 222-231. doi: 10.1177/003754970107600406

Calvo, I., Marcus, M., Orive, D., & Sarachaga, I. (2010). Building complex remote learning laboratories. *Computer Applications in Engineering Education, 18,* 53-66. doi: 10.1002/cae.20239

Cember, H. & Johnson, T. (2009). *Introduction to Health Physics.* New York: McGraw-Hill Medical.

Charting the course for American nuclear technology: evaluating the Department of Energy's Nuclear energy research and development roadmap: Hearing before the House Committee on Science and Technology, 111th Cong. (testimony of Mark Peters). Retrieved from http://democrats.science.house.gov/Media/file/Commdocs/ hearings/2010/ Full/19may/Peters_Testimony.pdf

Chetty, M., & Dabke, K. P. (2000). Towards a web-based control engineering laboratory. *International Journal of Electrical Engineering Education , 37* (1), 38-47.

Cockrum, R. H., & Koutras, A. E. (2001, September). *Collaborations between a university and industry over the Internet*. Paper session presented at the meeting of the 2nd International Conference on New Horizons in Industry and Education, Milos Island, Greece.

Cooper, D., & Dougherty, D. (1999). Enhancing process control education with the control station training simulator. *Computer Applications in Engineering Education, 7* (4), 203-212.

Cornford, J., & Pollock, N. (2003). *Putting the University Online.* Bury St Edmunds: Open University Press.

Depcik, C., & Assanis, D. N. (2005). Graphical User Interfaces in an engineering educational environment. *Computer Applications in Engineering Education, 13*, 48-59. doi: 10.1002/cae.20029

Elgamal, A., Fraser, M., & Pagni, C. (2002). Internet live shake-table testing for education in earthquake engineering. *Proceedings of the 2002 International Conference on Engineering Education,* (Session O045, pp. 1-8). Manchester, England.

Ellis, W. H., & He, Q. (1993). Computer-based nuclear radiation detection and instrumentation teaching laboratory system. *IEEE Transaction on Nuclear Science, 40* (4), 675-679.

Faw, R.E. & Shultis, J.K. (1999). *Radiological Assessment: Sources and Exposures*. La Grange Park, IL: American Nuclear Society.

Gao, Y., Yang, G., Spencer, J. B., & Lee, G. C. (2005). Java-powered virtual laboratories for earthquake engineering education. *Computer Applications in Engineering Education, 13*, 200-212. doi: 10.1002/cae.20050

Globig, J., An interdisciplinary, LabVIEW based, data acquisition and measurements course. *Proceedings of the 2003 American Society for Engineering Education Annual Conference & Exposition,* (Session 2147, pp. 1-16). Nashville, Tennessee

Good, T. L., & Brophy, J. E. (1990). *Educational Psychology: A Realistic Approach.* New York: Longman.

Hall, J. T. (2002). EET Laboratory courses: from the classroom to the web--from research to practice. *Proceedings of the 2002 American Society for Engineering Education Annual Conference & Exposition,* (Session 2248, pp. 1-12). Montreal, Quebec, Canada.

Health Physics Society (HPS), (2008). *Human Capital Crisis in Radiation Safety* (Position Statement 15-2, rev. October 2008). Retrieved from www.hps.org/documents/humancapital_ps015-2.pdf

Health Physics Society (HPS), Health Physics Society Human Capital Crisis Task Force (2004). Human Capital Crisis Task Force Report. Retrieved from www.hps.org/documents/ManpowerTaskForceReport.pdf

Huang, S. H., Su, Q., Samant, N., & Khan, I. (2001). Development of a web-based integrated manufacturing laboratory. *Computer Applications in Engineering, 9*, 228-237. doi: 10.1002/cae.10006

Jiang, H., Kurama, Y. C., & Fanella, D. A. (2002). WWW-based virtual laboratories for reinforced concrete education. *Computer Applications in Engineering Education, 10* (1), 1-16.

Kiritsis, Nikos, Hugan, Yi-Wei, & Ayrapetyan, David (2003). A multi-purpose vibration experiment using LabVIEW™. *Proceedings of the 2003 American Society for Engineering Education Annual Conference & Exposition*, (Session 1426, pp. 1-10). Nashville, TN.

Knight, C. V., & McDonald, G. H. (1998). Modernization of a mechanical engineering laboratory using data acquisition with LabVIEW. *Proceedings of the 1998 American Society for Engineering Education Annual Conference & Exposition*, (Session 2266, pp. 1-13). Seattle, WA.

Knoll, G.F. (2000). *Radiation Detection and Measurement*. New York: Wiley.

Kucuk, S., & Bingul, Z. (2010). An Off-Line Robot Simulation Toolbox. *Computer Applications in Engineering Education, 18*, 41-52. doi: 10.1002/cae.20236

Kypuros, J. A., & Connolly, T. J. (2007). Animating virtual dnyamic systems using MATLAB/Simulink®. *Proceedings of the 2007 ASEE Gulf-Southwest Annual Conference*, (pp. 1-10). Edinburg, TX.

Lamar, J. E., Cronin, K. C., & Scott, L. E. (2005). Virtual Laboratory Enabling Collaborative Research in Applied Vehicle Technologies. *Proceedings from RTO/AVT-123 Symposium on Flow Induced Unsteady Loads and the Impact on Military Applications*, (pp. Keynote 2-1 - 2-18).

Li, Shu-Guang, & Liu, Q. (2003). Interactive Groundwater (IGW): An innovative digital laboratory for groundwater education and research. *Computer Applications in Engineering Education, 11*, 179-202. doi: 10.1002/cae. 20236

Li, Y., LeBoef, E. J., Basu, P. K., & Hampton, I. L. (2003). Development of a web-based mass transfer processes laboratory: system development and implementation. *Computer Applications in Engineering Education, 11*, 25-39. doi: 10.1002/cae. 10036

Ma, J., & Nickerson, J. V. (2006). Hands-on, simulated, and remote laboratories: a comparative literature review. *ACM Computing Surveys, 38*, 1-24. doi: 10.1145/ 1132960.1132961

Magin, D. & Kanapathipillai, S. (2000). Engineering students' understanding of the role of experimentation. *European Journal of Engineering Education, 25*, 351-358. doi: 10.1080/03043790050200395

Manseur, R. (2005). Virtual reality in science and engineering education. *Proceedings of the 35th ASEE/IEEE Frontiers in Education Conference*, (pp. F2E1-6). Indianapolis, IN.

Mendes, D., Marongoni, C., Meneguelo, A. P., Machado, R. A., & Bolzan, A. (2010). Educational simulator for multicomponent distillation research and teaching in chemical engineering. *Computer Applications in Engineering Education, 18*, 175-182. doi: 10.1002/cae.20134

National Nuclear Security Administration (NNSA), New Mexico State University (2010). National Security Preparedness project (Report No. DOE/NA/28084-SF311). Retrieved from http://www.osti.gov/bridge/servlets/purl/974324-QNO3fT/974324.pdf

Nedic, Z., Machotka, J., & Nafalski, A. (2003). Remote laboratories versus virtual and real laboratories. *Proceedings of the 2003 33rd Annual Frontiers in Education Conference.*, (pp. T3E1-6). Boulder, CO.

Neitzel, I., & Lenzi, M. K. (2000). A simple real time process control experiment using serial communication. *Acta Scientiarum, 22* (5), 1167-1171.

Nickerson, J. V., Corter, J. E., Esche, S. K., & Chassapis, C. (2007). A model for evaluating the effectiveness of remote engineering laboratories and simulations in education. *Computers & Education, 49*, 708-725. doi: 10.1016/j.compedu.2005.11.019

NNSA (2010, February 23). NNSA Launches Innovative Mentoring System [Press Release]. NNSA Press Releases: http://nnsa.energy.gov/mediaroom/pressreleases/02.23.10b

Nuclear Energy Institue (NEI) (2007, November 6). Nuclear Renaissance Presents Significant Employment Opportunities, NEI Tells Senate Panel [News Release]. NEI News Releases: http://www.nei.org/newsandevents/newsreleases/berrigansenaterelease

Orabi, I. (2002). Application of LabVIEW for Undergraduate Lab Experiments On Materials Testing. *Proceedings of 2002 American Society of Engineering Education Annual Conference & Exposition*, (Session 2168, pp. 1-8). Montreal, Quebec, Canada.

Powell, R. M., Anderson, H., Van der Spiegel, J., & Pope, D. P. (2002). Using web-based technology in laboratory instruction to reduce costs. *Computer Applications in Engineering Education, 10*, 204-214. doi: 10.1002/cae.10029

Scanlon, E., Colwell, C., Cooper, M., & Di Paolo, T. (2004). Remote experiments, re-versioning and re-thinking science learning. *Computers & Education , 42*, 153-163. doi: 10.1016/j.compedu.2003.12.010

Shen, Q., Chung, J. K., Challis, D., & Cheung, R. C. (2007). A comparative study of student performance in traditional mode and online mode of learning. *Computer Applications in Engineering Education, 15*, 30-40. doi: 10.1002/cae.20092

Shin, Young-Suk (2002). Virtual reality simulations in web-based science education. *Computer Applications in Engineering Education, 10*, 18-25. doi: 10.1002/cae. 10014

Soh, C.K., & Gupta, A. (2000). Intelligent interactive tutoring system for engineering mechanics. *Journal of Professional Issues in Engineering Education and Practice, 126* (4), 166-173.

Swain, N., Anderson, J. A., Singh, A., Swain, M., Fulton, M., Garrett, J. et al. (2003). Remote data acquisition, control and analysis using LabVIEW front panel and real time engine. *Proceedings of the IEEE SoutheastCon, 2003*, (pp. 1-6). Ochos Rios, Jamaica.

Uran, S., & Safaric, R. (2009). Web based control teaching. In S. G. Tzafestas (Ed.), *Web-Based Control and Robotics Education* (pp. 61-82). Dordrecht: Springer.

Vasquez, D. C. (2009). *The design, use and implementation of digital radiation detection and measurement equipment for the purpose of distance instruction* (Master's thesis). Retrieved from http://ir.library.oregonstate.edu/jspui/bitstream/1957/15291/1/VasquezDavidC2010.pdf

Whelan, Paul F., (1997). Remote access to continuing engineering education (RACeE). *Engineering Science and Education Journal, 6* (5), 205-211.

Yao, Yingxue, Li, Jianguang, & Liu, Changqing (2007). A virtual machining based training system for Numerically Controlled machining. *Computer Applications, 15,* 64-72. doi: 10.1002/cae.20097

Yarbrough, S.E. & Gilbert, R.B. (1999). Development, implementation, and preliminary assessment of virtual laboratory. *Journal of Professional Issues in Engineering Education and Practice, 125* (4), 147-151.